PLASMACYTOID DENDRITIC CELLS AND NEUTROPHILS – UNDERESTIMATED CELL POPULATIONS DURING THE ONSET OF ATHEROSCLEROSIS

VON DER FAKULTÄT FÜR MATHEMATIK, INFORMATIK UND NATURWISSENSCHAFTEN DER RWTH AACHEN UNIVERSITY ZUR ERLANGUNG DES AKADEMISCHEN GRADES EINER DOKTORIN DER NATURWISSENSCHAFTEN GENEHMIGTE DISSERTATION

VORGELEGT VON

MASTER OF SCIENE

YVONNE DÖRING

AUS LAUTERBACH IN HESSEN, DEUTSCHLAND

BERICHTER:

UNIVERSITÄTSPROFESSOR DR. MED. CHRISTIAN WEBER

UNIVERSITÄTSPROFESSOR DR. RER. NAT. MARTIN ZENKE

TAG DER MÜNDLICHEN PRÜFUNG: 07.07.2011

THE RESULTS OF THIS WORK WILL BE PARTLY PUBLISHED IN:

Döring, Y.*, Soehnlein, O.*, Drechsler, M., Meiler, S., Shagdarsuren, E., Hartwig, H., Hieronymus, T., Hristov, M., Koenen, R.R., Zenke, M., Weber, C., and Zernecke, A., *Chronic myelogenous leukemia-like disease due to hematopoietic IRF8-deficiency fuels atherosclerosis in mice*. Circulation Research, **2011** (in revision).

Döring, Y., Manthey, H., Drechsler, M., Lievens, D., Manca, M., Hartwig, H., Busch, M., Koenen, R.R., Soehnlein, O., Zenke, M., Daemen, M.J., Weber, C., Lutgens, E., and Zernecke, A., *Autoantigenic protein-DNA complexes stimulate plasmacytoid dendritic cells to promote atherosclerosis*. Circulation, **2011** (in revision).

TABLE OF CONTENTS

ABBREVIATIONS

Ab	antibody
AD	atopic dermatitis
Ag	antigen
APCs	antigen presenting cells
Apoe	Apolipoprotein E
BM	bone marrow
BMDCs	bone-marrow derived DCs
BSA	bovine serum albumin
CAD	coronary artery disease
CD	cluster of differentiation
cDC	conventional DC
cDNA	copy DNA
CFSE	carboxyfluorescein succinimidyl ester
Cy3	cyanine 3
DAPI	4',6-Diamidino-2-phenylindol
DC	dendritic cell
Di	1,1`-dioctadecyl-3,3,3`,3`-tetramethylindocarbo-cyanine perchlorate
DMSO	dimethylsulfoxide
DNA	desoxyribonucleic acid
dsDNA	double stranded DNA
EDTA	ethylenediaminetetraacetic acid
e.g.	for example (from Latin: exempli gratia)
ELISA	enzyme-linked immunosorbent assay
FACS	Fluorescent avtivated cell sorting
FCS	fetal calf serum
FITC	fluorescein isothiocyannate
FMO	fluorescence minus one
GAGs	glycosaminoglycans
GAPDH	glyseraldehyde-3-phosphate dehydrogenase
GM-CSF	granulocyte–macrophage colony stimulating factor
CpG	Cytidine – phosphate – Guanosine –rich DNA
h	hours
HFD	high fat diet
HBSS	Hanks' balanced salt solution
HRP	horse radish peroxidase
HSP	heat shock proteins
IFN	interferon
IgG	Immunglobulin G
IL	interleukin
LDL	low-density-lipoprotein
LFA-1	lymphocyte function-associated antigen-1
LN	lymph node
mAb	monoclonal Ab
MFI	mean fluorescence intensity
MHC	major histocompatibility complex
min	minute
MMP-9	Matrixmetalloproteinase-9
MPO	Myeloperoxidase

NC	normal chow diet
o.n.	overnight
OVA	ovalbumin
oxLDL	oxidized LDL
pAb	polyclonal Ab
PBS	phosphate buffered saline
PCR	polymerase chain reaction
pDC	plasmacytoid DC
PDCA-1	pDC antigen-1
PFA	paraformaldehyde
PMA	phorbol-12-myristate-13-acetate
RNA	ribonucleotid acid
RT	room temperature
SD	standard deviation
SDS	sodium-dodecylsulfate
SEM	standard error of mean
SMC	smooth muscle cell
SSC	saline-sodium citrate
STAT	signal transducer and activator of transcription
TCR	T cell receptor
Th	T helper
Treg	regulatory T cells
TNF	tumor necrosis factor
wt	wild-type

1 INTRODUCTION

A comparison between the average life span of German people today and roughly 100 years ago would reveal something very obvious: The life span has increased by more than a 100% from 37 years in 1880 to 78 years in 2004* due to improved living conditions. However, this change comes at the cost of side effects, *e.g.* age-related disorders such as coronary artery disease (CAD). Atherosclerosis is the underlying cause of most CAD and this group of diseases is the main cause of death in the Western world today.[1] Therefore understanding how atherosclerosis develops and which immune mechanisms are involved represents one way of fighting its consequences. The following introduction will give a short overview on how our immune system is built up, how different cell types influence the immune response – highlighting the role of neutrophils and plasmacytoid dendritic cells – and how atherosclerosis develops.

1.1 THE IMMUNE SYSTEM

Constant exposure to harmful omnipresent pathogens in our environment is one of the greatest challenges for all living organisms. To prevent pathogen invasion every organism has its natural barriers which have to be constantly monitored. To keep these borders protected an immune system has evolved, which is able to rapidly eliminate invading pathogens. To fulfill this task, the immune system of vertebrates offers two ways of response: **Innate** and **Adaptive**immunity.[2] **Innate** immunity detects distinct molecular patterns of pathogens (PAMPs: pathogen-associated molecular patterns) with various pattern recognition receptors (PRR), such as Toll-like receptors (TLRs). Among the cells that express PRRs are macrophages, dendritic cells (DCs), mast cells, neutrophils, eosinophils, and NK cells. Pathogen exposure activates these cells, which in turn induce a rapid inflammatory response to eliminate the intruder.[3] However, if the innate immune system is unable toclear the infection, activation of an **adaptive** immune response becomes necessary. Adaptive immune responses are initiated by specialized antigen-presenting cells, most importantly by DCs, via presentation of pathogen derived peptides (antigens) to B- and T-cells. This leads to an activation of B- and T-cells, which have the unique ability to express receptors that are not encoded in the germ line, but can be generated *de novo* from rearranged gene segments. This mechanism allows a great variability in adaptive immune recognition by offering an almost unlimited repertoire of antigen receptors which enables the immune system to create a

* Average of men and women together, source: www.zdwa.de

specific immune response to virtually any pathogen present. Activated T cells release specific sets of cytokines inducing a cell-mediated immune response, while activated B cells produce antibodies as part of a humoral immune response.[4,5] However, adaptive immunity requires the innate arm to orchestrate its response to guarantee an optimal host defense, emphasizing that two players are needed to build up a working team.

1.2 CELLS OF THE IMMUNE SYSTEM

Innate as well as adaptive immunity relies on leukocytes (white blood cells) which originate from hematopoietic stem cells (HSC) located in the bone marrow. These HSCs differentiate further into common myeloid (CMP) and lymphoid progenitors (CLP).[6] Among others CMPs are the precursors of macrophages, granulocytes (including neutrophils), dendritic cells, and megakaryocytes which are all part of the innate immune system. Instead CLPs give rise to B cells and T cells, which build up adaptive immunity. As an exception CMPs and CLPs can both develop into dendritic cells, which may underline their important relevance at the border of innate and adaptive immunity (Figure 1-1).[7,8]

1.2.1 NEUTROPHILS

Neutrophils belong to a group of white blood cells referred to as granulocytes also including eosinophils and basophils. The discovery of granulocytes dates back to the German Nobel laureate Paul Ehrlich, who already realized in 1900 the functional potential of the granule contents in the inflammatory process: "… it is likely that the leukocyte granulations are in fact secretory products, which the cell dissolves and spreads to the environment as needed".[9] Hence, PMN are characterized by granules in their cytoplasm and multilobed nuclei, the reason why they are as well called polymorphnuclear leukocytes (PMN). Of note, PMN may also abbreviate for polymorphnuclear neutrophil, which is used as a synonym for the term "neutrophil" throughout this work. Neutrophils are the most abundant cell type in humans making up to 70% of the normal leukocyte blood count. In contrast mice only show up to 25% PMNs in leukocyte counts of normal peripheral blood.[10,11] It is not clear how this difference can be explained and neutrophils seem to cover the same functions in both organisms.[12] PMNs are professional phagocytes that are able to take up and destroy infectious agents (mostly bacteria) by releasing the contents of their granules into the phagosome accompanied by the production of reactive oxygen species (ROS). In addition to the phagocytic activity, PMN are capable of forming neutrophil extracellular traps (NETs).

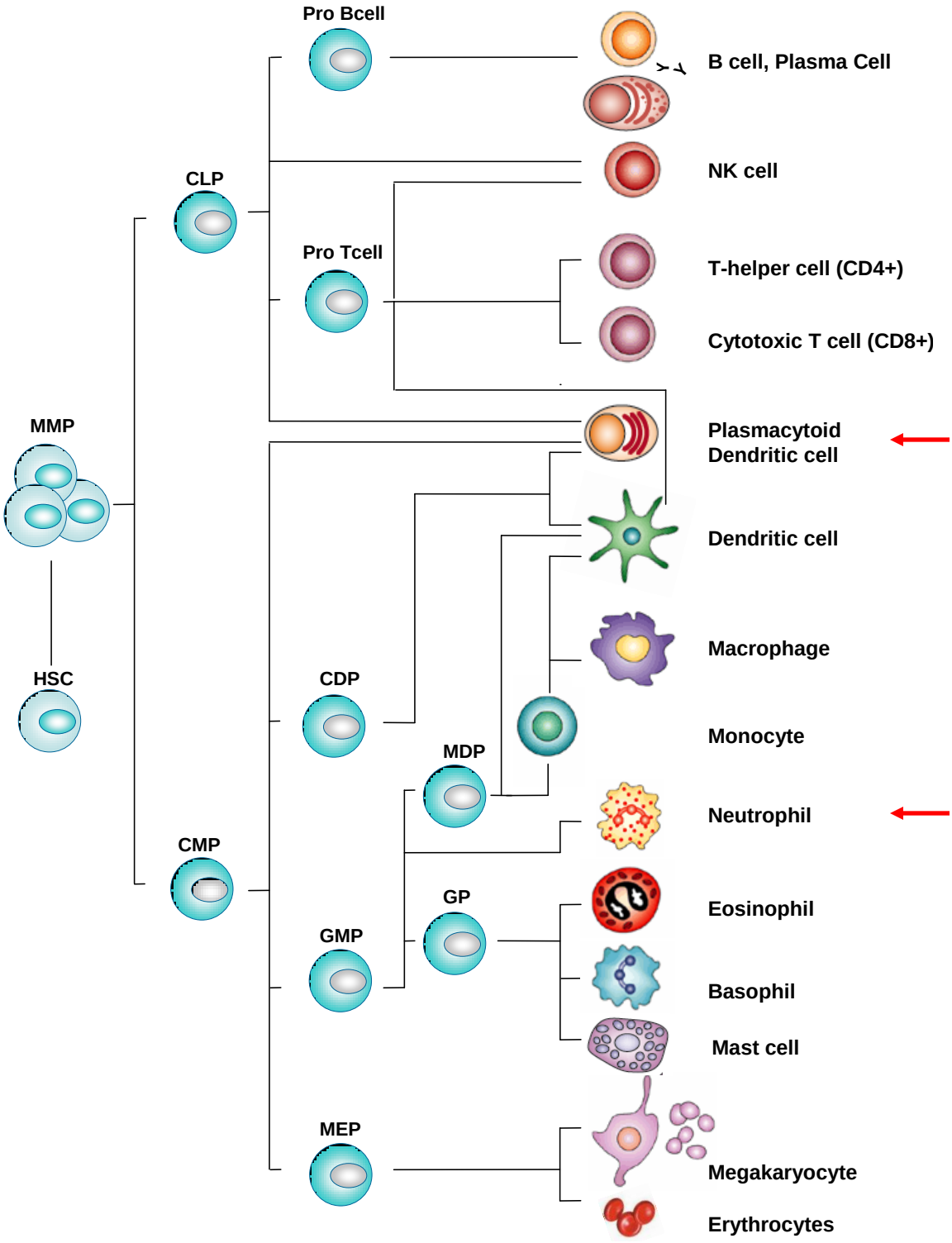

Figure1-1. Hematopoieses. Tree diagram, showing the development of different blood cells from HSCs via different progenitors into mature cells. Cells, which are important throughout this study, are marked by a red arrow. Abbreviations: CDP, common DC progenitor; CMP, common myeloid progenitor; CLP, common lymphoid progenitor; GMP, granulocyte and macrophage progenitor; GP, granulocyte progenitor, HSC, hematopoietic stem cell; MDP, macrophage and DC progenitor; MEP, megakaryocyte and erythrocyte progenitor; MPP, multipotent progenitors.

These NETs are composed of neutrophil nuclear contents and *e.g.* serine proteases, which are one reason why NETs are able to kill bacteria extracellulary.[13,14] Moreover PMN do also have the ability to generate chemokines (e.g. MIP-1α, IL-8)[15,16] and proinflammatory cytokines (TNFα, IFNγ)[17,18]. However, neutrophil-mediated immune responses do not only have a beneficial impact but can also lead to tissue damage.[19,20] Maturation of PMNs occurs in the bone marrow in about two weeks, a process in which the myeloid-specific growth factors G-CSF and GM-CSF play an important role.[10] Maturated neutrophils are stored in the bone marrow and have a high turnover once they enter the circulation (6-12 hours) until they migrate to tissue or undergo apoptosis. In general their life span does not exceed seven days.[11] Retention of neutrophils from the bone marrow is tightly controlled by the stromal derived factor–1 (SDF-1) and its chemokine receptor CXCR4, whereas G-CSF induces neutrophil release from the bone marrow, in major part, by disrupting stromal derived factor-1/CXCR4 signaling.[21,22] Transcription of genes facilitating PMN development is controlled by PU.1 together with C/EBP(CCAAT/enhancer-binding protein)-α to the level of GMPs, while C/EBPε guides maturation along the granulocytic lineage (Figure 1-1). Instead, among others, interferon regulatory factor 8 (IRF8, also known as Interferon consensus sequence binding protein, ICSBP) is essential in directing monocyte and macrophage differentiation and represses genes promoting granulocytic differentiation and maturation.[23] Human PMN can be distinguished from other leukocytes by their surface expression of CD177[24] and CD15[25], mouse neutrophils can be discriminated with antibodies against Ly6G (part of Gr1)[26] and the exclusion of monocytes with an antibody against CD115.[27] Additionally, both, human and mouse PMN appear very high in the sideward scatter if examined with flow cytometry, due to their high granularity.

1.2.1.1 NEUTROPHIL GRANULE PROTEINS

Granule proteins are key effectors in the immune response initiated by PMN and are released upon activation of the cell. Their subsets can be classified as primary, secondary, and tertiary granules, as well as secretory vesicles. This classification is based on the analysis of marker proteins, which differ between granule classes.

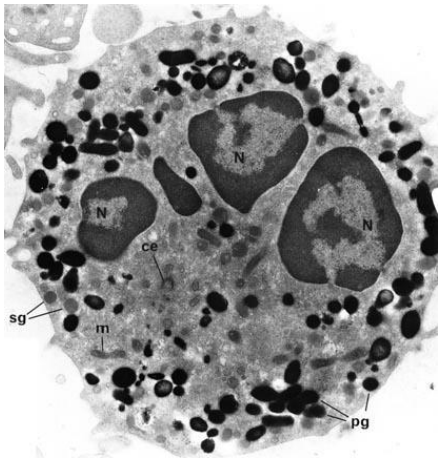

Figure 1-2. Electron microscopy showing the various intra-cytoplasmic granules of a resting neutrophil. Peroxidase-positive granules are primary granules, (*pg*), which appear as large dark granules. Secondary granules(*sg*) are smaller in size. Nucleus (*N*); centriole (*ce*); mitochondria (*m*), (adapted from Witko-Sarsa *et al.*)[28]

Granule biogenesis proceeds sequentially during granulopoiesis and proteins are formed according to their numerical order (primary, secondary…).Instead, neutrophils on their way from blood to sites of infection release their granules in a hierarchical order (Figure 1-2)[29-31]: Secretory vesicles are characterized by their immediate release when contact is established between the PMN and the endothelium. Once a neutrophil transmigrates tertiary granules are mobilized, whereas secondary and primary granules are liberated at the site of inflammation. Thus granule proteins cover multiple tasks of neutrophil action, *e.g.* enabling PMN to extravasate tissue, kill microorganisms or affect surrounding inflammatory cells by deposition of granule proteins in extravascular spaces. Several constituents of neutrophil granules (underlined red in Figure 1-3) were found to be of essential importance during the course of the experimental progress of this thesis. Therefore, a brief summary of these granule proteins will follow:

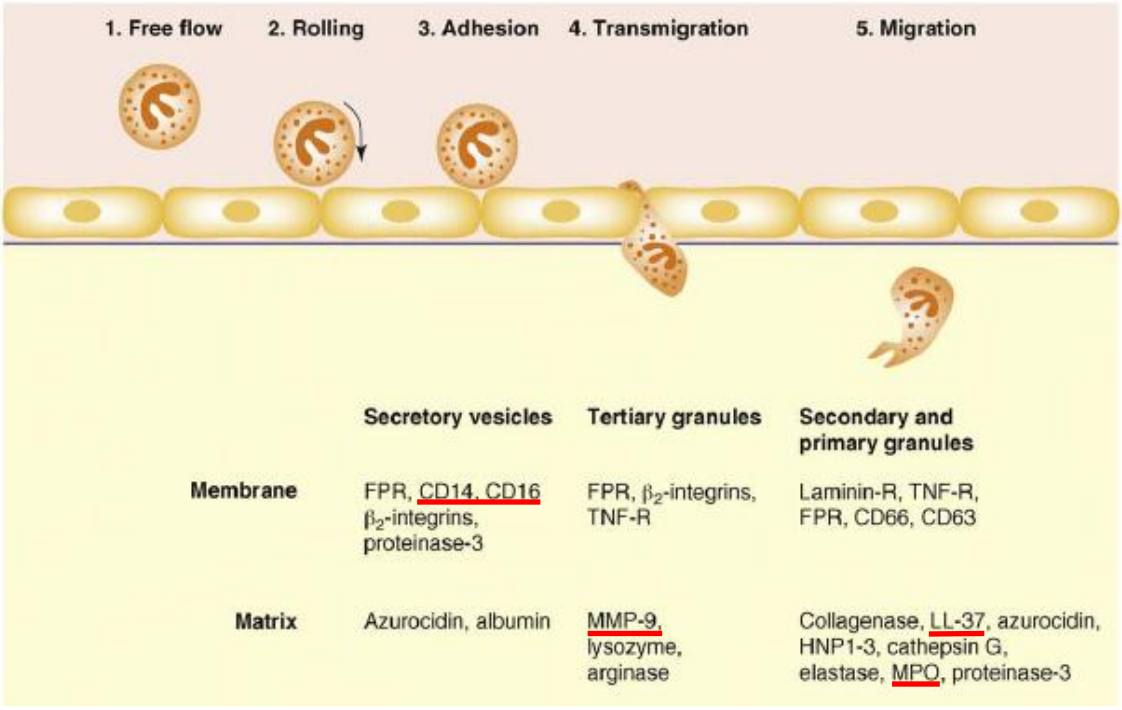

Figure 1-3. Granule subsets are released at different stages of PMN extravasation. PMNs migrate from the vasculature through a coordinated series of cell-cell and cell-matrix interactions. Granule subsets are thought to be released at distinct steps of PMN extravasation, thereby releasing granule proteins into the surroundings or presenting membrane-bound granule proteins on the PMN cell surface. Release of secretory vesicles following PMN adhesion leads to the deposition of azurocidin and proteinase-3 on the endothelial cell surface and incorporation of receptors (CD14, CD16, β2-integrins) into the PMN cell surface. Transmigrating PMNs release tertiary granules, which contain proteases to help penetration of the basement membrane. The migrated PMNs deposit antimicrobial polypeptides (*e.g.* LL-37, azurocidin, HNPs) and proteases (*e.g*. cathepsin G, elastase) in the extravascular tissue, leading to interaction with nearby cells. Abbreviations: FPR, formyl peptide receptor; HNP, human neutrophil peptide;MMP-9, matrix metalloproteinase 9; MPO, myeloperoxidase; TNF-R, tumor necrosis factor receptor (adapted from Soehnlein *et al.*).[32]

LL-37 or CRAMP: LL-37/hCAP-18 is the only cathelicidin present in humans[33], its proform is termed hCAP-18 and to be found in secondary granules (Figure 1-3) of PMN, LL-37 is the biological active C-terminal cleavage product of hCAP-18.[34] Cathelin-related antimicrobial peptide (CRAMP) is the homologues molecule of LL-37 in mice showing very similar functions as its human counterpart.[35] Besides the broad antimicrobial activity of LL-37/CRAMP against bacteria[36], LL-37/CRAMP has gained attention for its immunomodulating properties[37]. Among others, LL-37 has been shown to be involved in chemoattraction of immune cells[38,39], activation of Th-1 cytokine release by DCs[40], and modulation of immune responses on monocytes and DCs to TLR-ligands[41-43].

Matrix Metalloproteinase-9: Matrix metalloproteinase-9 (MMP-9; gelatinase B) is a member of the MMP enzyme family, which is widely expressed in many tissues and cell types. Like other MMPs, MMP-9 mainly degrades components of the extracellular matrix, *e.g.* to enhance neutrophil attraction to chemokines.[44,45] Furthermore, studies about its enzyme activity identified MMP-9 as an important target in inflammatory and vascular diseases.[46] In PMN MMP-9 is stored in tertiary granules and exocytosis of these granules is initiated upon neutrophil transendothelial migration (Figure 1-3).[32]

Myeloperoxidase: Myeloperoxidase (MPO) is a protein present in primary and secondary PMN granules (Figure 1-3). Once the PMN is activated MPO is released into the phagosome to amplify the toxic potential of H_2O_2. This amplification is mediated through the production of reactive intermediates of H_2O_2, such as hypochlorous acid, which is a potent oxidant of electron-rich substrates. These MPO-derived oxidants are also part of the respiratory burst, in which various reactive oxygen species are generated. Implications of MPO-derived oxidants are known for various inflammatory processes, also unrelated to host defense.[47]

CD14/CD16: Cluster of Differentiation 14 (**CD14**) is a receptor of bacterial lipopolysaccharide (LPS) and described as a glycosylphosphatidylinositol (GPI)-anchored protein lacking transmembrane and intracellular domains; therefore the mechanisms by which CD14 mediates signaling are still not fully understood.[48] **CD16** belongs to the family of Fcγ receptors found in mice and humans on all cells of hematopoietic origin. It is also referred to as FcγRIII. CD16 is a multichain receptor involved in phagocytosis by macrophages and PMN and specifically recognizes the heavy chain of IgG antibodies.[49] Binding to both, CD14 and CD16 leads to the activation of PMN accompanied by the release of granule proteins and both are part of secretory vesicles (Figure 1-3).

Reactive oxygen species: Reactive oxygen species (ROS) include compounds generated by incomplete oxygen reduction, such as superoxide anion ($O2^-$), hydrogen peroxide (H_2O_2) and

thehydroxyl radical (HO•). ROS are crucial for antimicrobial activity, function as signaling molecules, but can also damage host tissue. They are not present in neutrophilic granules but do form in phagolysosoms and can be released by PMN.[50-52]

1.2.2 PLASMACYTOID DENDRITIC CELLS

DCs are professional antigen presenting cells equipped with high phagocytic activity, which take up, process and present antigen to T cells. However, they are a very heterogeneous cell population with various subtypes differing in location, migratory pathways and detailed immunological functions.[53,54] In addition, DCs can rise from CLPs and CMPs, which is a unique feature among cells of haematopoietic origin (Figure 1-1).[55]

One subpopulation of DCs are plasmacytoid dendritic cells (pDCs), which have first been described by Lennert und Remmele in 1958[56], but were for a long time referred to as plasmacytoid T cells or plasmacytoid monocytes in humans.[57,58] Not until the late nineties of the last century it was agreed that this cell population carries dendritic cell characteristics and is identical with a cell population which had been termed “natural type I interferon-producing cell” (IPC).[58-61] This conclusion promptly led to the identification of a pDC counterpart in mouse.[62-64] In contrast to other DC populations pDC development is influenced by transcription factors (Spi-B[65], ID2 and ID3[66]) only known to be important for lymphocyte formation. In addition pDCs exhibit immunoglobulin H diversity-joining gene rearrangements and expression of markers typical for immature B- and T-cells.[67] These findings together with their lymphoblast-like appearance under steady state conditions (Figure 1-4 a,b) made their lymphoid origin most likely, but was broadened by the finding that pDCs can rise from CLPs and CMPs (Figure 1).[55] Other very recent studies may even support evidence for a distinct developmental pathway just for pDCs.[68-71] PDCs fully evolve within the bone marrow and migrate to lymph nodes, mucosal-associated lymphoid tissues and spleen under steady state conditions with an average turnover of about 2 weeks.[72] Migration is mediated through the expression of L-Selectin, CXCR4 and ChemR23 in response to their corresponding ligands CD34, SDF-1 (CXCL12) and chemerin. Under inflammatory conditions this repertoire is expanded by the expression of CXCR3 (ligands CXCL9/10/11), CCR5 (ligands CCL3/4/5) and CCR7 (ligands CCL19/CCL21). Among the latter chemerin seems to be the most specific and important regulator of pDC trafficking, especially under inflammatory conditions.[73,74] Notably, in contrast to cDCs pDCs have the ability to enter lymphnodes via high endothelial venules (HEV), but do seldomly traffic by afferent lymphatics.[75] One hallmark of DCs is antigen presentation, yet pDCs are less efficient compared to cDCs in presenting exogenous antigens[58], but they are fully capable of presenting endogenous antigens and most likely are

as well able to cross present viral antigens[76,77]. One reason accounting for the weaker presentation of exogenous antigen by pDCs is their inability to accumulate long-lived MHCII-peptide complexes on their cell surface, owing to a different regulation of the master transcription factor of the MHCII presentation machinery, CIITA (MHC class II transactivator).[78]

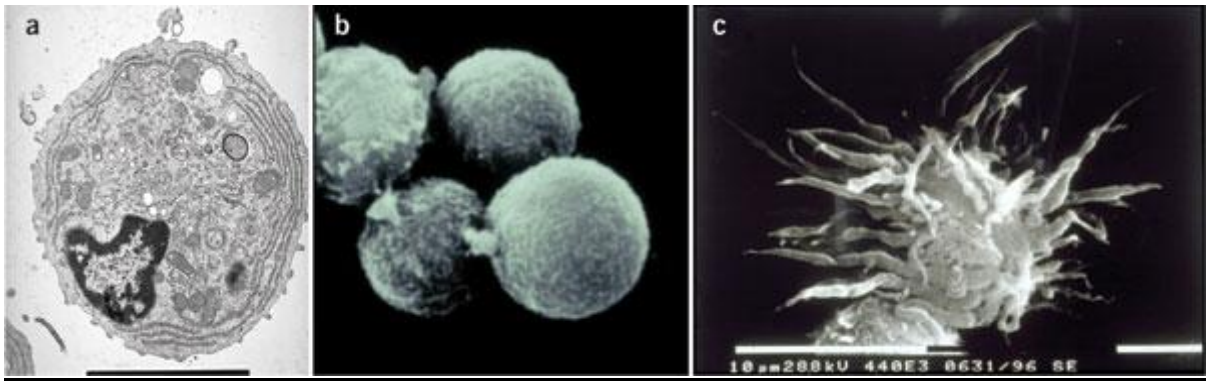

Figure 1-4. Morphology of pDCs. (a) By electron microscopy, pDCs appear as lymphoblasts with a medium-to-large diameter, a slightly eccentric, indented, round or oval nucleus, lightly stained perinuclear areas and well developed rough endoplasmic reticulum. **(b, c)** By scanning electron microscopy, resting pDCs have a spherical shape **(b)**, whereas CD40L-activated pDCs have a dendritic cell–like morphology **(c)**. Original magnifications, ×7,000 (a) and ×3,000 **(b,c)** (adapted from Colonna *et al*.).[79]

Although pDCs are a rare subtype in human and mouse they are the main source of type I interferons (IFN), producing up to 1000-fold higher levels of IFNs in comparison to other cells.[59,80] Hence, during infection pDC numbers increase and can be detected in various tissues, such as lung, vaginal mucosa and skin.[81] Furthermore, pDCs are described in the context of many autoinflammatory diseases, *e.g.* psoriasis[82], systemic lupus erythematosus[83] and multiple sclerosis[84]. Human pDC markers are IL-3 receptor-a chain (CD123)[58] and blood DC antigen 2 and 4 (BDCA-2 and BDCA-4)[85], while mouse pDCs can be identified by sialic-acid-binding immunoglobulin-like lectin H (SiglecH) expression[86] and an antibody named mouse pDC antigen 1 (mPDCA-1)[87].

1.2.2.1 THE TYPE I INTERFERON RESPONSE

pDCs are highly specialized for sensing viral and certain microbial infections, which is based on their selective expression of TLR7 and TLR9 and their capacity to respond to inactivated viral nucleic acids in the absence of viral replication.[88] Upon activation of TLR7 and TLR9 the unique ability of pDCs to produce large amounts of type I IFNs is induced.[89] TLRs are the best known PRRs comprising a family of conserved membrane-spanning molecules that contain an ectodomain of leucin-rich repeats, transmembrane domains and intracellular Toll–interleukin 1

(IL-1) receptor (TIR) domains. TLR7 and TLR9 are solely expressed intracellularly within the endoplasmatic reticulum (ER), endosomes, multivesicular bodies and lysosomes, but their activation seems to be restricted to acidified endolysosomal compartments.[90] The ligand for TLR7 is viral single stranded RNA (ssRNA)[91,92], instead TLR9 recognizes **C**ytidine-**p**hosphate-**G**uanosine (CpG)-rich bacterial (or viral) DNA[93]. In addition both receptors can also be activated by synthetic agonists, *e.g.* imidazoqinoline derivates (TLR7) or synthetic oligonucleotides (TLR9). Recognition of nucleic acids through these receptors leads to initiation of a signaling cascade involving a MyD88-IRAK4-TRAF6-complex that binds to IRF7, the master regulator of type I IFN responses in pDCs or other signaling molecules (Figure 1-5). To provide sufficient IFN production, IRF7 is constitutively expressed by pDCs ensuring a constant and rapid assembly of the signaling described.[94,95] In addition, pDCs are able to retain DNA in early endosomes for prolonged time periods potentially by multimeric DNA complex formation allowing a sustained activation of IRF7.[96] In contrast, monomeric DNA quickly traffics through early endosomes into more acidic late endosomes initiating a different signaling cascade and therefore a different immune response of the cell.[97] Thus, different pathogens may induce distinct answers, depending on which mechanism fits their killing best. IFNs *per se* are widely expressed cytokines that have potent antiviral and growth-inhibitory activity. The IFN family includes two main classes of related cytokines: type I IFNs and type II IFNs, which are named after their ability to 'interfere' with viral infections. Type I IFNs are numerous and all share obvious structural homology and bind to a common receptor (IFN receptor I). Instead, there is only one type II IFN – IFNγ – with its own receptor and no considerable structural homology with type I IFNs.[98] Among the type I IFNs expressed by pDCs are IFNα, IFNβ, IFN$\lambda$and IFNω, hence the quantity of IFNα is much higher relative to all other IFNs produced.[99] Notably IFNα influences several immune responses, *e.g.* maturation of $CD11c^+$ conventional DCs[100], induction of Th1 differentiation[101], or stimulation of B cells to differentiate into antibody secreting plasma cells[102].

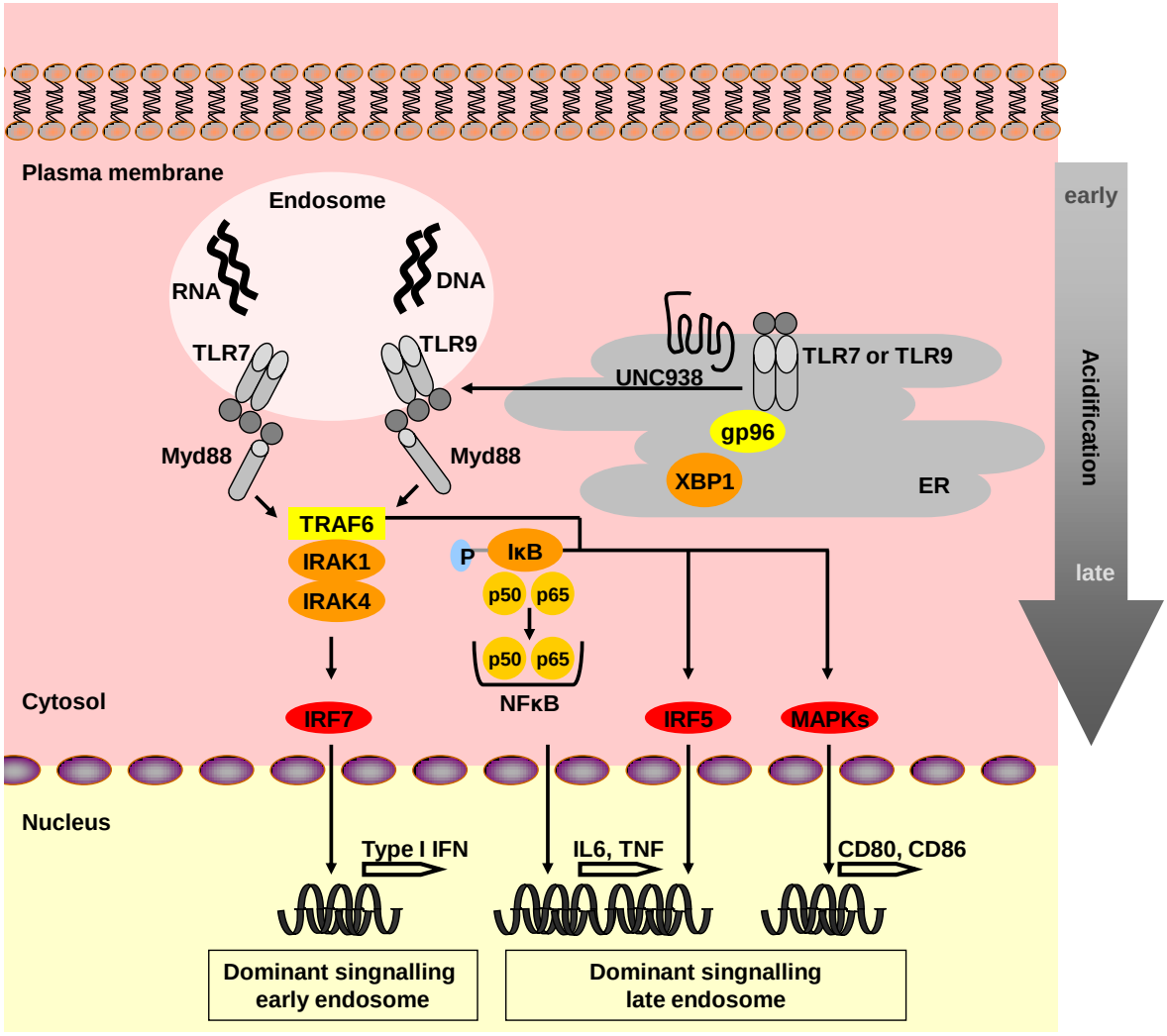

Figure 1-5. TLR7 and TLR9-MyD88 signalling pathway
Resting pDCs predominantly express TLR7 and TLR9, which reside in the endoplasmic reticulum (ER) in association with UNC93B and gp96. Following exposure to virus or nucleic acids, TLR7 and TLR9 relocate from the ER to the endosomes to engage with their RNA or DNA agonists. Conformational changes in the TLRs lead to the activation of MyD88 (myeloid differentiation primary-response gene 88) in the cytosol. MyD88 in turn associates with a signal complex comprised of TRAF6 (tumor-necrosis factor (TNF)-receptor-associated factor 6), BTK (Bruton's tyrosine kinase), IRAK4 (interleukin-1-receptor (IL-1R)-associated kinase 4) and IRAK1, which leads to the activation of IRF7 (interferon-regulatory factor 7), NF-κB (nuclear factor-κB) and MAPKs (mitogen-activated protein kinases). Multimeric DNA binding to TLR9 occurs in the early endosomes, prolonged TLR9 signaling from the early endosome activates MyD88 and importantly IRF7, which promotes strong type I interferon (such as IFNα, IFNβ, IFNλ and IFNω) production. By contrast, monomeric DNA that binds to the TLR9 complex quickly traffics through the early endosomes and into the more acidic late endosome or lysosome. This presumably activates a different set of signal mediators, particularly NF-κB, MAPKs and IRF5, and thereby leads to production of *e.g.* IL-6 and TNF and upregulation of costimulatory molecules by pDC, without high levels of IFN production (modified from Gilliet *et al*.).[97]

1.2.2.2 PLASMACYTOID DENDRITIC CELLS IN AUTOIMMUNITY

A pDC's main task is to sense for nucleic acids of foreign origin without responding to self-nucleic acids of dying host cells. As a critical consequence the expression of TLR7 and TLR9 is restricted to endosomal compartments within a cell, which has been shown to prevent recognition of self nucleic acids, but is not needed for ligand-receptor interactions.[103] However, as already pointed out (1.2.2) pDCs are known to be involved in the pathophysiology of several autoimmune diseases. In patients with systemic lupus erythematosus (SLE) breakdown of innate tolerance occurs through the continuous activation of pDCs by circulating immune complexes, comprised of self DNA and antibodies to DNA or nucleoproteins.[104,105] These pDCs, in turn, permanently produce type I IFNs, which stimulate autoreactive B- and T-cells.[106,107] Mechanistically, complexes of self DNA and DNA-specific antibodies are bound and internalized by low-affinity Fc receptors for IgG (FcγRIIA) and translocated to TLR9-containing endosomal compartments.[108] Interestingly, this mechanism does not only account for pathophysiologic type I IFN levels, but also reduces therapeutic activity of glucocorticoids.[109] Furthermore, in psoriasis, an autoimmune disease of the skin, free self-DNA forms complexes with cationic LL-37, overexpressed and released by neutrophils as well as damaged epithelial cells.[42] These complexes protect self-DNA from nuclease degradation and enter endosomal compartments of pDCs most likely via lipid rafts.[110] Aggregated self-DNA-LL37 complexes are retained within early endosomes and induce robust type I IFN production, as already described (1.2.2.1). In addition, high-mobility group box 1 protein (HMGB1), which is released by dying cells, may also ligate to nucleic acid-protein complexes. HMGB1 binds to RAGE (receptor for advanced glycation end-products) and thereby facilitates the association of DNA with TLR9 in early endosomes.[111]

Of note, although being part of the discussion (ref. to 4.2.3), it may already be pointed out here, that both, SLE and psoriasis are associated with an increased risk of atherosclerosis (ref. to 1.3).[112-114] Therefore, pathogenic mechanisms so far only accounting for one or the other may be important for all three and hence be transferred.

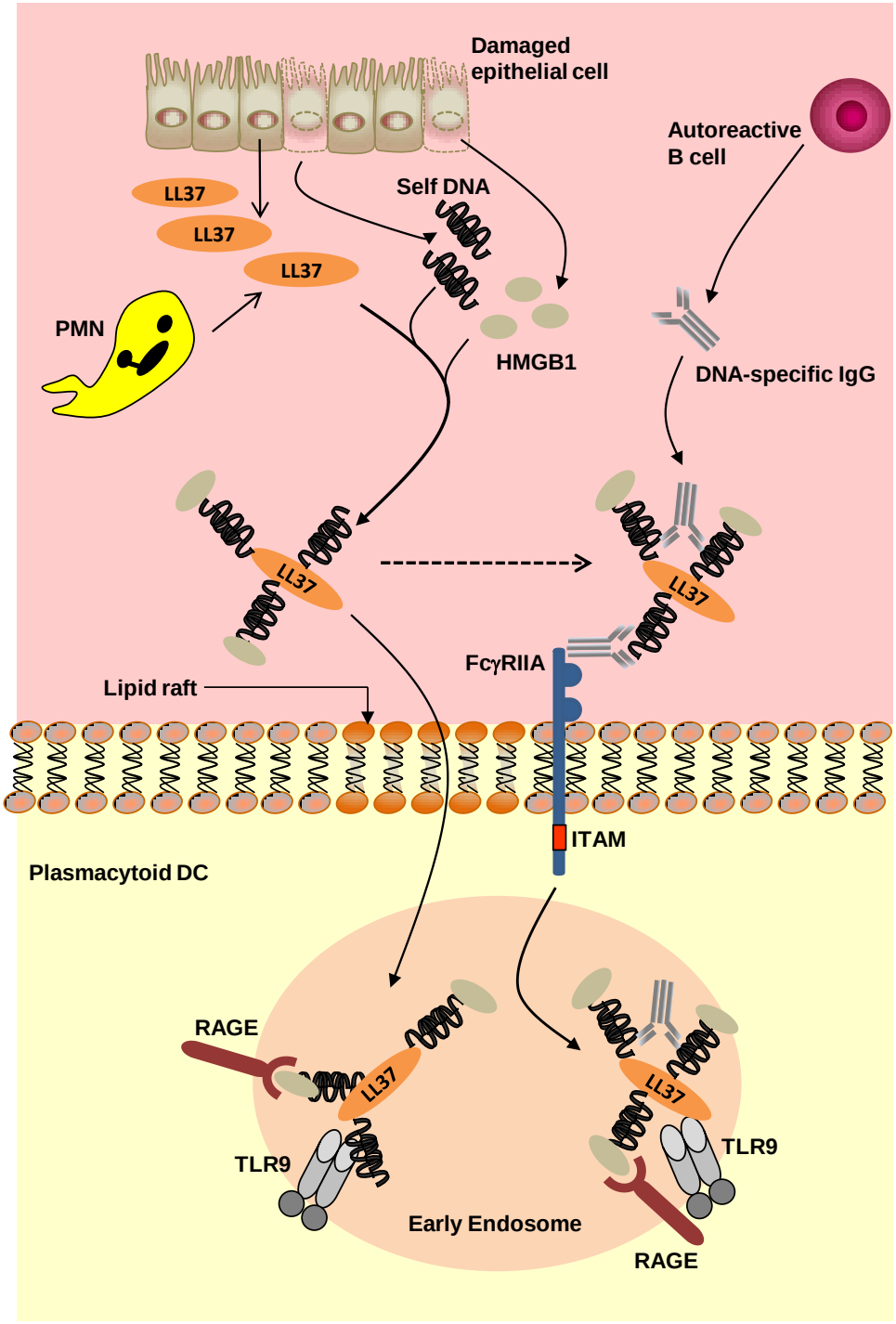

Figure 1-6. A model of pDCs sensing self-DNA. The antimicrobial peptide LL37 is secreted by damaged epithelial cells or deposited by tissue-infiltrating neutrophils. It binds self-DNA fragments released by dying cells to form aggregated and condensed structures that are protected from extracellular nuclease degradation and delivered via lipid rafts from the extracellular environment into the early endosomes of pDCs. Dying cells also release high-mobility group box 1 protein (HMGB1), which binds aggregated self-DNA–LL37 complexes and promotes their association with TLR9 in early endosomes by binding to RAGE (receptor for advanced glycation end-products). In SLE, DNA-specific IgG autoantibodies produced by autoreactive B cells bind self-DNA–LL37–HMGB1 complexes and potently increase their translocation into TLR9-containing endosomes in pDCs through FcγRIIA. ITAM, immunoreceptor tyrosine-based activation motif (adapted from Gilliet *et al.*).[97]

1.2.3 OTHER CELLS

As discussed before, immune responses depend very much on different cell types and their interaction. Thus, PMN and pDCs may be influenced by others, among which are monocytes, macrophages and T cells being described briefly in the following section.

1.2.3.1 MONOCYTES

Monocytes originate from bone marrow, where they do share early progenitors with granulocytes (Figure 1-1). Upon release of monocytes to the peripheral blood they circulate for several days until they enter various tissues to replenish macrophage populations. In human and mice monocytes make up to 5-10% of the total leukocyte population and vary in size and degree of granularity.[115] They are fully equipped effector cells, exhibiting phagocytic activity, migration to sites of inflammation and production of inflammatory cytokines. Under inflammatory conditions monocytes rapidly differentiate to macrophages or inflammatory DCs depending on the surrounding milieu.[53] In human blood, two subsets of monocytes are characterized by their differential expression ofCD14 and CD16: (i) “classical” $CD14^{+}CD16^{-}$ monocytes, typically representing up to 95 % of peripheral monocytes in a healthy individual and (ii) “non-classical” $CD14^{lo}CD16^{+}$ monocytes. These subsets differ phenotypically in their adhesion molecule and chemokine receptor expression.[116] Mouse blood monocyte subtypes are identified by their expression of CD115, CD11band a different expression of granulocyte antigen 1 (Gr1). Mouse monocytes with a high Gr1 expression are also referred to as “inflammatory” monocytes, because of their rapid recruitment to sites of inflammation. Instead monocytes exhibiting a low surface expression of Gr1 are called “resident” monocytes, due to their prolonged persistence in blood and normal tissue.[117]

1.2.3.2 MACROPHAGES

Macrophages were first described by the Russian biologist Elie Metchnikoff in 1882, who recognized the presence of highly mobile mononuclear phagocytes in invertebrates.[118] They are derived from myeloid progenitor cells, which ultimately develop into monocytes that enter the peripheral bloodstream. Circulating monocytes give rise to a variety of heterogeneous tissue-resident macrophages throughout the body, which have an important role in the maintenance of tissue homeostasis by clearance of dead cells and tissue repair after inflammation.[115] Thus, macrophages are professional phagocytes expressing a variety of PRRs, such as the mannose receptor, TLRs and scavenger receptors. Additionally, macrophages are capable to function as an APC including the expression of MHCII and costimulatory molecules to activate an adaptive immune response.[119] Macrophage activation

is thought to underlie two basic mechanisms resulting in two main phenotypes: “Classical” macrophages or M1 macrophages are activated through TLRs and IFNγ resulting in enhanced killing of intracellular pathogens, secretion of high levels of cytokines (*e.g.*interleukin (IL)12, IL-23, IL-6 and TNF) and higher expression of costimulatory molecules. Instead, “alternative” or M2 macrophages differentiate in the presence of IL-4, IL-13, IL-1 or vitamin D3 leading to secretion of IL-10 and the expression of arginase-1 and the mannose receptor CD206.[120-122]

1.2.3.3 T CELLS

T cells are a large group of lymphocytes, originating from one progenitor (Figure 1-1) and are part of the adaptive immune response. They mature in the thymus (therefore called T cells) and can be divided into two main groups in mice and human based on their surface expression of CD4 and CD8. $CD4^+$ T cells carry out “helper” functions and naïve $CD4^+$ T cells differentiate into at least four types of T helper (Th) cells: Th1, Th2, Th17 and regulatory T cells (Treg).[123,124] Th1 cells mediate a cellular immune response while Th2 cells trigger a humoral response. Instead, Th17 cells appear to play an integral role in both tissue inflammation and activation of neutrophils to combat extracellular bacteria. Th1, Th2 and Th17 immune responses influence each other antagonistically and at a time one is dominating a certain pathogen response.[125] $CD8^+$ T cells are called cytotoxic T cells, because of their ability to kill virus-infected and tumor cells. In general both, $CD4^+$ and $CD8^+$ T cell populations carry T cell antigen receptor (TCR)/CD3 complexes and are able to “mature” in the presence of an antigen. $CD4^+$ T cells respond to antigens presented by APCs via MHCII, $CD8^+$ T cells recognize their targets by MHCI.[123,126]

1.3 ATHEROSCLEROSIS

Atherosclerosis, the term has its etymologically roots in the two Greek words ‘athera’ (gruel) and ‘sklerosis’ (induration), is now agreed to be a chronic inflammatory disease of the vessel wall driven by intense immunological activity, of both, innate and adaptive immunity. Moreover atherosclerosis is the most common pathophysiological process leading to CAD and therefore heads the list of death causes in developed countries.[1,127]

Already more than a 180 years ago, in 1829, Jean Lobstein implemented the term ‘atherosclerosis’ followed by his two colleagues Carl von Rokitansky and Rudolf Virchow, who proposed two opposing views on the pathology of atherosclerosis in the middle of the 19th century. Rokitansky assumed that initial injury of the vessel wall due to mechanical trauma led to endothelial dysfunction, whereas Virchow already postulated the critical role of inflammatory cells in the pathology of atherosclerosis.[128] In the early years of the 20th century the correlation of high cholesterol levels in disease progression could be elucidated[129,130], however, detailed insight in the pathogenic mechanisms remained elusive. An extended view of the Rokitansky proposal was established by Ross, who came up with the “response to injury” hypothesis in the 1970ties.[131-133] This hypothesis was further broadened in the nineties by Steinberg and others, who suggested altered lipoproteins as the initial triggers of the disease, primarily oxidized low-density lipoprotein (oxLDL).[134-136]

But, even to date – despite the intensive research in this field, the concordant acceptance of hyperlipidemia as the main risk factor and growing evidence that atherogenesis is strongly regulated by immunological mechanisms – the initial reason unbalancing the system remains vague.[127]

Pathomechanism: Atherosclerotic lesions, also termed plaques, originate from local endothelial dysfunctions under elevated levels of LDL. This leads to an infiltration of blood borne immune cells, mostly leukocytes and anasymmetrical thickening of the intima (most inner layer of the vessel) (Figure 1-7a). Intima swelling is accompanied by the recruitment of monocytes, which turn into lipid-laden macrophages, also known as foam cells. These early lesions, referred to as “fatty streaks”, are typical for younger individuals and asymptomatic, but can progress or disappear with time (Figure 1-7b). Continuous cell influx leads to plaque progression resulting in mature plaques (atheromas), which are more complex.

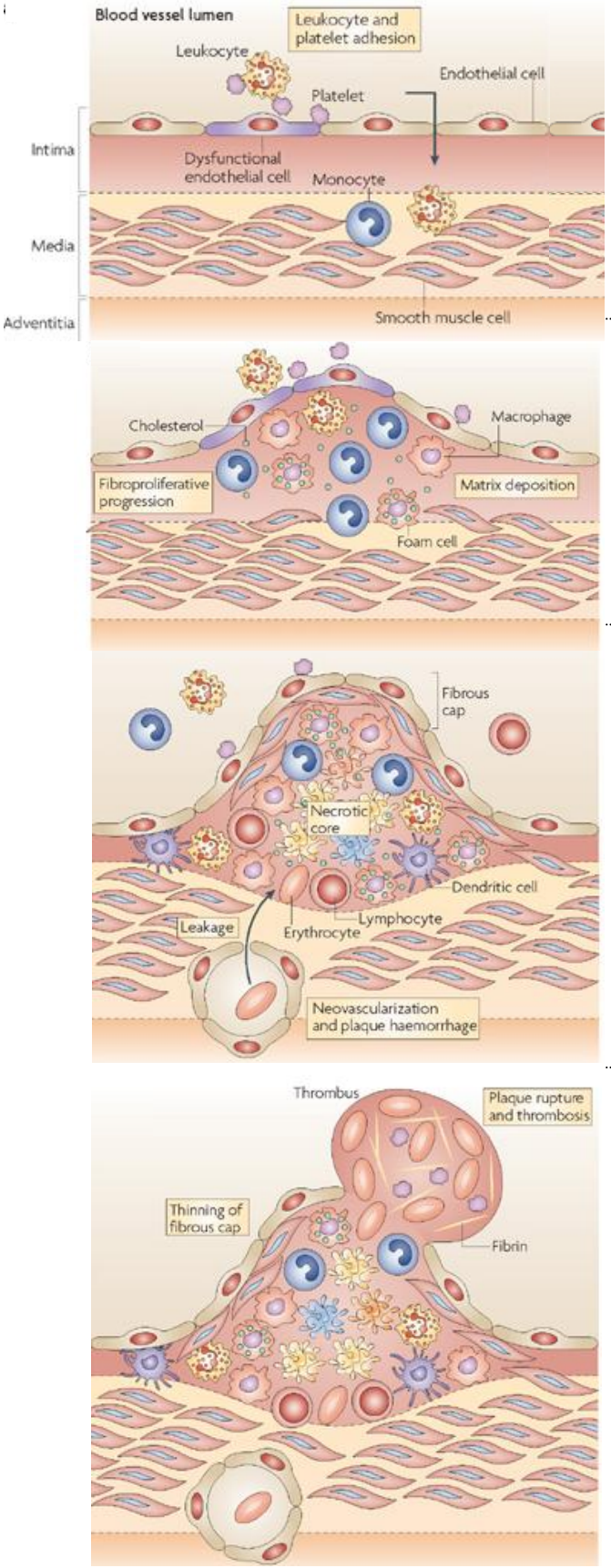

Figure 1-7. Development and progression of atherosclerosis:

a) Endothelial-cell dysfunction and activation under pro-inflammatory conditions of hyper-lipidemia leads to early platelet and leukocyte adhesion and increased permeability of the endothelium.

b) Monocytes that are recruited to the intima and subintima accumulate lipids and transform into macrophages or foam cells, which make up fatty streaks. Continued mononuclear-cell influx, deposition of matrix components and recruitment of smooth muscle cells give rise to the fibroproliferative progression of the plaques.

c) Apoptosis of macrophages and other plaque cells creates a necrotic core, and a fibrous cap that consists of matrix and a smooth-muscle-cell layer forms. Neovascularization can occur within the plaque and from the adventitia, and leakage of fragile vessels can lead to plaque hemorrhage.

d) Thinning and erosion of the fibrous cap in unstable plaques, for example, owing to matrix degradation by proteases, ultimately results in plaque rupture, with release of debris, activation of the coagulation system and plaque thrombosis of the artery. This leads to arterial occlusion and myocardial infarction or stroke (modified from Weber *et al*.).[137]

Atheromas consist of a necrotic core (containing lipids), surrounded by foam cells and other immune cells overall covered by a cap of smooth muscle cells and collagen rich matrix (Figure 1-7c). Finally the release of pro-inflammatory cytokines and proteases reduces collagen formation and thins the collagenous cap, which leads to plaque weakening and may peak in plaque rupture (Figure 1-7d). Rupture results in thrombus formation possibly causing acute ischemia, manifesting as myocardial infarction or stroke.[1,127,135,137-139]

1.3.1 NEUTROPHILS IN ATHEROSCLEROSIS

Although atherosclerosis is a chronic inflammatory disease and neutrophils are thought to be more important for acute and early inflammatory responses, growing evidence underlines their impact in the onset of atherosclerosis.[39,140,141] One reason for their underestimation in atherosclerotic lesions formation so far is most likely due to only low numbers being detectable in plaque regions. Yet, this may be explained by their short life span along with their high turnover. However PMN are detectable in both, human[142] and mice[141] lesions and a correlation of peripheral PMN counts with myocardial infarction in humans has already been shown.[143,144] Additionally, as demonstrated in a murine model of atherosclerosis, neutrophil numbers in blood seem to positively correlate with plaque size, whereas depletion of PMN reduces plaque formation in these mice.[141,145]

Hence, presumably several mechanisms may account for PMN in atherosclerosis overviewed in Figure 1-8. The broad variety of granule proteins released and deposited by PMN will most likely trigger monocytes adhesion and extravasation, finally leading to foam cell formation.[39] In addition macrophages will be activated by these granule constituents and subsequently release proinflammatory cytokines.[146] Furthermore, apoptotic neutrophils eaten up by macrophages might eventually overload the phagocytic capacity of these macrophages, resulting in secondary necrosis and therefore increased inflammation within the lesion.[147] Ultimately, ROS formation and subsequent modification of LDL to oxLDL together with the proteolytic weakening of the fibrous cap by PMN-derived proteases may exacerbate plaque destabilization.[148] In summary, PMN are clearly involved in the pathogenesis of atherosclerosis, but the assumptions made on their contributions to this disease have to be further investigated.

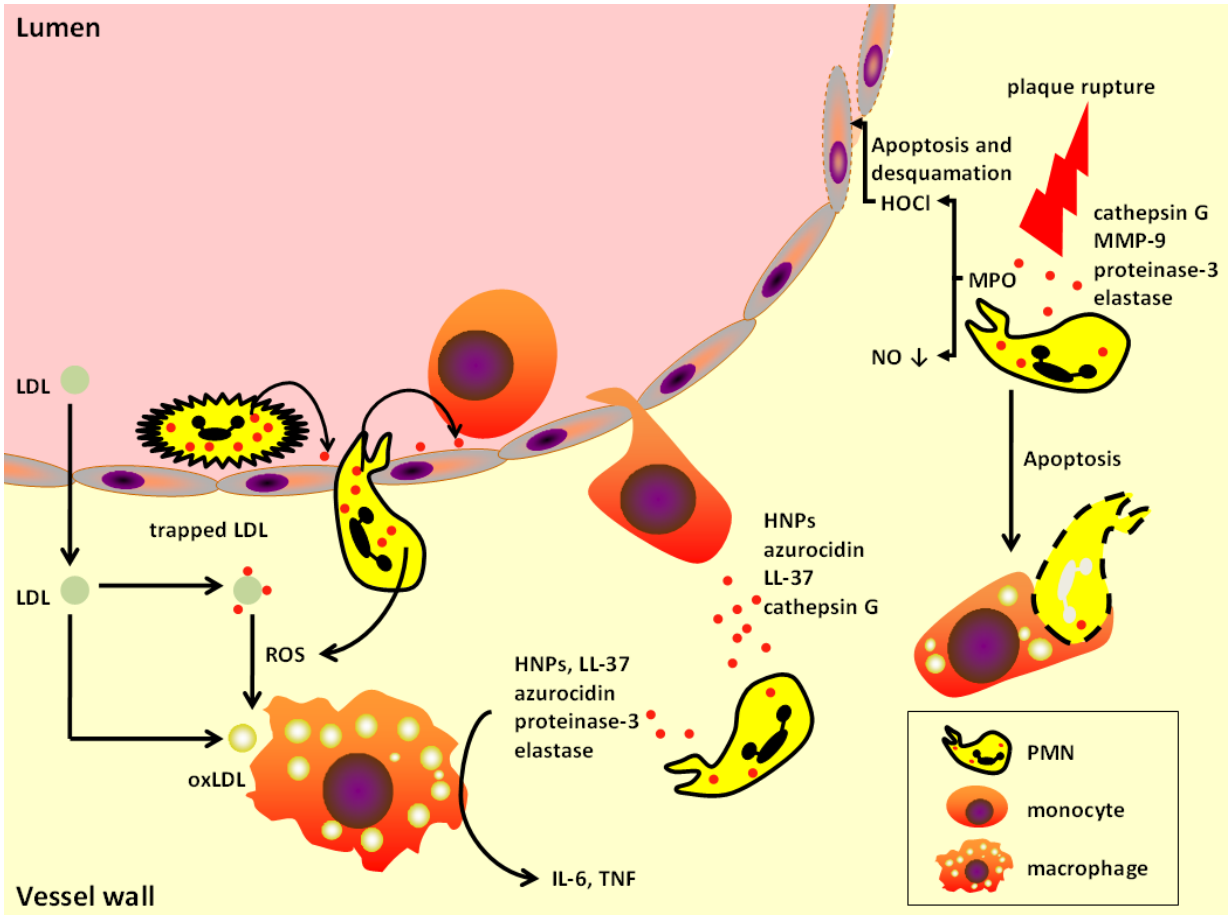

Figure 1-8. Potential role of PMN in atherosclerosis. Although direct proof only exists for the correlation of peripheral PMN count and plaque size, the PMN may be involved in several critical processes in atherosclerosis. Deposition of PMN granule proteins on the endothelium and in the vessel wall may trigger monocyte adhesion and extravasation. There granule components enhance macrophage differentiation and activity resulting in release of pro-inflammatory cytokines. Extravasated LDL may be trapped by binding of PMN-derived HNPs and further modified via ROS, thereby supplying substrate for foam cell development. Proteases released from PMN granules may further weaken the fibrous cap and promote plaque rupture. In addition, MPO reduces the bioavailability of NO and leads to production of HOCl. The latter may induce endothelial cell apoptosis and desquamation, thus resulting in plaque erosion (adapted from Soehnlein and Weber).[148]

1.3.2 PLASMACYTOID DENDRITIC CELLS IN ATHEROSCLEROSIS

Both, cDCs and pDCs are found in atherosclerotic lesions in human[149] and mice[150]. However, since the first description of DCs within the intima of arteries[151] and in atherosclerotic lesions[152] in 1995 the function of DCs within healthy and atherosclerosis-prone arteries needs to be further investigated.[127,141] PDCs are described in the shoulder region of the plaque, where they cluster with cDCs and most likely produce type I IFNs in response to nucleic acids of self and foreign origin.

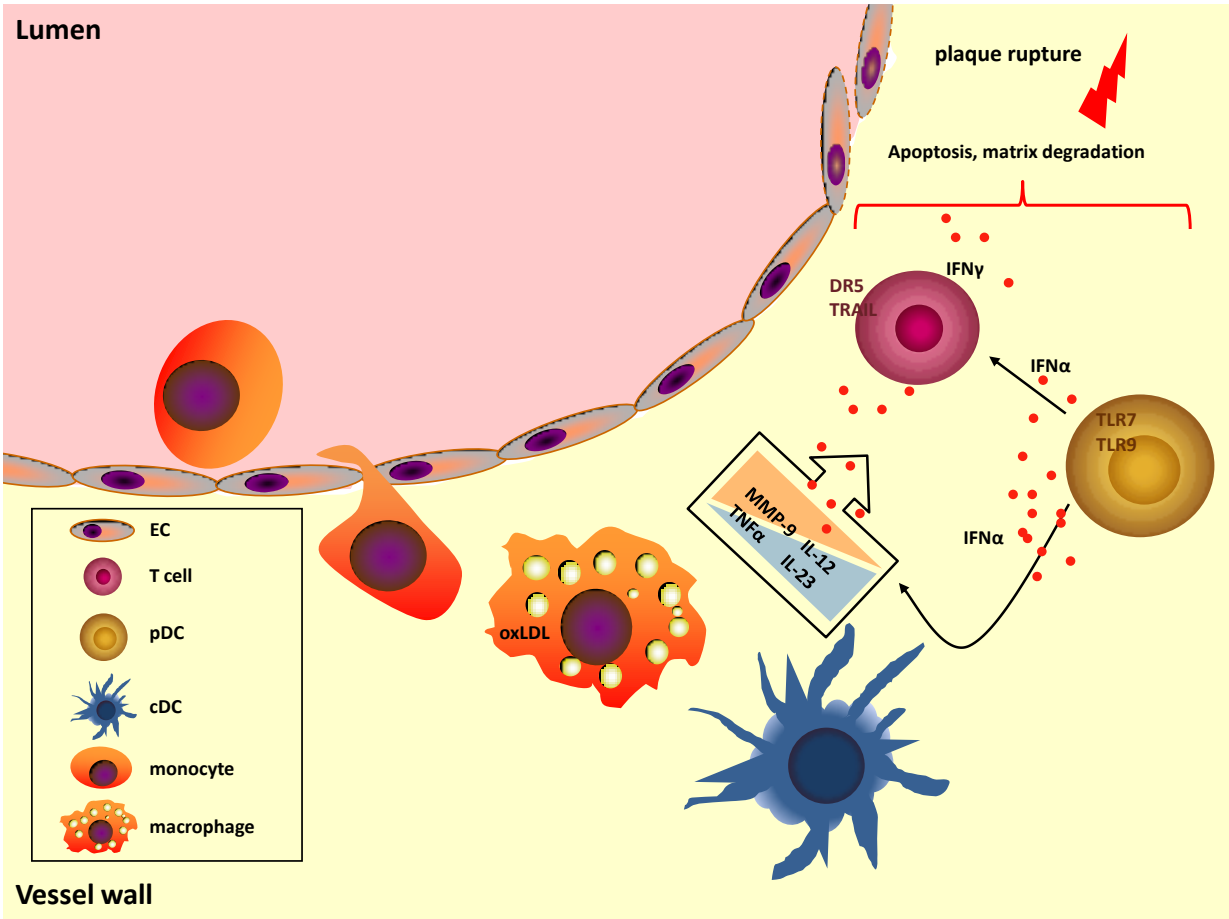

Figure 1-9. Potential role of dendritic cells in the atherosclerotic plaque. Activated cDC and macrophages produce effector molecules such as metalloproteinases degrading the extracellular matrix. Further, they trigger the recruitment of cytotoxic T cells via production of IL-12. PDC are mainly activated by viral antigens binding tointracellular receptors such as TLR7 and TLR9. Activated pDC produce vast amounts of IFN-α. This cytokine enhances the sensitivity of other antigen presenting cells by upregulation of TLR4. Furthermore, it upregulates the expression of the pro-apoptotic molecule TRAIL on T cells thereby multiplying their cytotoxic potential. These TRAIL-expressing T cells have the ability to kill plaque-resident cells such as activated VSMC and EC expressing the death receptor DR5. Abbreviations: EC, endothelial cells, DR5, death receptor 5, TNF-α, tumor necrosis factor-alpha (modified from Niessner *et al.*).[153]

Secretion of IFNα seems to correlate with plaque instability, activating $CD4^+$ T cells, which in turn produce IFNγ and TRAIL (TNF-related apoptosis inducing ligand) in an antigen independent manner leading to apoptosis of vascular smooth muscle cells.[154] In addition IFNα may function as an inflammatory amplifier inducing upregulation of TLR4 on cDCs, resulting in a synergistic effect of different danger signals within the two DC subsets.[155] Another very recent study demonstrates that IFNβ enhances macrophage-endothelial cell adhesion and promotes leukocyte attraction to atherosclerosis-prone sites as well as increased macrophage accumulation within the plaque.[156] In contrast, human and mouse pDC do both have the ability to trigger the development of regulatory T cell responses, *e.g.* inhibiting acute graft-versus

host disease[157] or mediating tolerance to vascularized grafts[158]. Thus, our understanding of how dendritic cells, including pDCs, assign to certain stages of atherosclerosis needs to be further improved, also with regard to clinical applications.[153]

1.4 AIM OF THE STUDY

One of the pressing goals of atherosclerosis research is to understand the participation of the immune system in the pathomechanisms leading to plaque formation and progression. Major aim of this thesis was the systematically examination of the contribution of pDCs and PMN to atherosclerotic lesion formation.

PMN were long underestimated in atherosclerotic lesions formation most likely due to their low numbers in plaque regions and their importance in acute inflammation. However, PMN have recently been implicated in lesion development and an increase of circulating neutrophils positively correlates with plaque sizes. This study aims at the understanding to which extend this contribution influences plaque formation.

- How does atherosclerosis develop in a mouse model with impaired macrophage functions, but increased PMN numbers?
- How far may lesion progression be driven by PMN exclusively?
- Is a myeloproliferative disorder a risk factor in atherosclerosis?

The role of pDCs in atherosclerosis is only poorly understood and studies shading light on this issue are very scarce. Therefore, detailed analysis of how pDCs influence atherosclerosis *per se* is outlined here.

- Does pDC activation or depletion influence disease development?
- Is pDC activity influenced by classical risk factors (*e.g*. oxLDL)?
- Does the implication of pDCs in the pathomechanisms of various autoimmune diseases suggest similar activation patterns in atherosclerosis?

2 MATERIALS AND METHODS

Protocols were adapted from standard protocols[159] if not stated otherwise. All solutions were prepared with double distilled water (Heraeus Destamat, Heraeus, Germany) or Millipore water (Milli-Q Plus ultrapure purification, Millipore,MA). Reagents were from Fluka (Buchs, Switzerland), Sigma-Aldrich (Deisenhofen, Germany), or Roth (Karlsruhe, Germany), if not stated otherwise.

2.1 GENERAL EQUIPMENT

equipment	source
autoclave	Systec 2540EL (Systec, Wettenberg, Germany)
balance	Analytical Plus, (Ohaus, Pine Brook, NJ, USA)
centrifuges	Eppendorf 5417C (Eppendorf, Hamburg, Germany), Heraeus Labofuge 400 and Heraeus Multifuge 3 S-R (Heraeus, Osterode,Germany)
flow cytometers	FACSCantoII, FACSAria (BD Biosciences, San Jose, CA, USA)
fluorescence plate reader	SpectraFluor Plus (Tecan, Crailsheim, Germany)
gel electrophoresis	Mini-sub cell GT (Bio-Rad, Hercules, CA, USA)
laminar flow hood	Herasafe (Heraeus, Osterode, Germany)
microscopes	Olympus IX71 and BX51 (Olympus Optical,Hamburg,Germany), Leica DMLB (Leica, Wetzlar, Germany)
PCR thermocyclers	MyCycler (Bio-Rad, Hercules, CA), DNA Engine Opticon (MJResearch, Hercules, CA, USA)
pH-meter	InoLab level 1 (WTW, Weilheim, Germany)
spectrometer	NanoDrop (Peqlab, Erlangen, Germany)

2.2 MICE

Wild-type (**wt**) C57BL/6, Apolipoprotein E deficient (***Apoe***$^{-/-}$)[160,161] and low-density lipoprotein receptor (LDLR)-deficient mice (***Ldlr***$^{-/-}$)[162] were obtained from the local animal breeding facility or purchased at Charles River, England or Janvier, Belgium. *Apoe*$^{-/-}$ and *Ldlr*$^{-/-}$ mice are established mouse models to study the development and disease progression of atherosclerosis.

OT-II[163] transgenic mice, interferon regulatory factor 8 (formerly known as interferon consensus sequence binding protein, ICSBP) *knock out* mice (***Irf8***$^{-/-}$)[164] and the cathelin-related antimicrobial peptide (CRAMP) *knock out* mice (***Cramp***$^{-/-}$), encoded by the gene *Cnlp* (Camp cathelicidin antimicrobial peptide)[165], were obtained from the local animal breeding facility (University Hospital, Aachen Germany).

OT-II mice express a mouse α-chain and β-chain TCR that pairs with the CD4 co-receptor and is specific for chicken ovalbumin 323-339 (OVA-2) presented by MHC class II molecules. CD4^{+}T cells isolated from these mice exhibit a dose-dependent proliferation in response to OVA-2 peptide. *Irf8*$^{-/-}$ mice have two prominent phenotypes: first is enhanced susceptibility to viral infections and second is a deregulated hematopoiesis manifesting in a syndrome similar to human chronic myeloid leukemia. *Cramp*$^{-/-}$ mice demonstrated no obvious phenotype when housed under aseptic conditions, but are more susceptible to infections of Group A *Streptococcus.*

2.3 CYTOKINES AND RECOMBINANT PROTEINS

name	source
Chemerin	R&D systems (Minneapolis, MN USA)
CRAMP	Innovagen (Lund, Schweden)
murine FLT3-ligand	PeproTech (Rocky Hill, NJ, USA)
murine Interferon alpha	PBL laboratories, Piscataway, USA
murine Interferon alpha	HyCult Biotec, Uden, Netherlands
OVA-2 (323-339)	AnaSpec (San Jose, CA, USA)
Platelet activating factor	Enzo, Life sciences (Plymouth Meeting, USA)
murine TNFα	PeproTech

2.4 MISCELLANEOUS REAGENTS

(Di[†])-oxidized LDL	Intracel (Frederick, MD, USA)
Calcein (cell permeant dye)	Invitrogen (Carlsbad, CA, USA)
Dexamethasone (synthetic glucocorticoid)	Sigma-Aldrich
Annexin V (molecular probe)	BD Biosciences

2.5 TOLL LIKE RECEPTOR STIMULI

CpG ODNs are synthetic oligonucleotides (ODN) that contain unmethylated CpG dinucleotides (CpG motifs).[166] CpG ODNs are recognized by TLR9 leading to strong immunostimulatory effects.[167] Among the stimulatory CpG ODNs three different types have been described: types A, B and C. These three differ in their immune stimulatory activities. Type A CpG ODNs induce high IFN-α production from pDCs, but are weak stimulators of TLR9-dependent NF-κB signaling. Type B CpG ODNs strongly activate B cells but stimulate weakly IFN-α secretion by pDCs. Type C CpG ODNs combine features of both types.[168] All CpG types will finally induce pDC maturation resulting in an upregulation of costimulatory molecules and the ability to function as an antigen presenting dendritic cell. **ODN 1585**[169] (Type A) was used for *in vitro* and *in vivo* stimulation of pDCs (2.8.3) and was purchased from InvivoGen (San Diego, CA, USA).

[†] 1,1`-dioctadecyl-3,3,3`,3`-tetramethylindocarbo-cyanineperchlorate

2.4 ANTIBODIES

2.4.1 PRIMARY ANTIBODIES

Name	mAb	clone	source
anti-SMA	mouse anti-human	1A4	Dako, Glostrup, Denmark
MOMA-2	rat anti-mouse	MCA519	AbD Serotec, Düsseldorf, Germany
CD3	mouse anti-human	PC3/188A	Santa-Cruz Biotechnology, Santa Cruz, CA, USA
Ly6G	rat anti-mouse	1A8	BD Biosciences, San Jose, CA, USA
SiglecH	rat anti-mouse	440c	eBioscience, San Diego,CA, USA
Cramp	rabbit anti mouse		Innovagen
IgG	rabbit anti mouse		Vector Laboratories
Myeloperoxidase	rat anti-mouse	RB-373-AO	Neomarkers Fremont, CA, USA
MMP9	rat anti-mouse	M17	Santa Cruz Biotechnology

2.4.2 DIRECTLY CONJUGATED ANTIBODIES

name	mAB	clone	source
B220-PE-Cy7	rat anti-mouse	RA3-6B2	eBioscience
CD115-PE	rat anti-mouse	AFS98	eBioscience
CD11b-PerCP	rat anti-mouse	M1/70	BD Pharmingen
CD11c-PE-Cy7	rat anti-mouse	N418,	eBioscience
CD14-PE-Cy7	rat anti-mouse	Sa14-2	BioLegend, San Diego, CA,USA
CD16-PE	rat anti-mouse	93	BioLegend
CD19-PerCP	rat anti-mouse	RA3-6B2	eBioscience
CD25-APC or PE	rat anti-mouse	PC61.5	eBioscience
CD36	rat anti-mouse	No.72-1	eBioscience
CD3-PerCP,APC,FITC	rat anti-mouse	145-2C11	eBioscience
CD40-APC	rat anti-mouse	1C10	eBioscience

name	mAB	clone	source
CD45-APC-Cy7	rat anti-mouse	30-F11	BD Pharmingen
CD4-PE,APC, FITC	rat anti-mouse	RM4-5	eBioscience
CD80-APC	rat anti-mouse	16-10A1	eBioscience
CD86-PE	rat anti-mouse	GL1	eBioscience
CD8a-PE or PE-Cy7	rat anti-mouse	53-6.7	eBioscience
F4/80-APC	rat anti-mouse	A3-1	Serotec, Raleigh, NC, USA
FoxP3-APC	rat anti-mouse	FJK-16s	eBioscience
Gr-1-PerCP	rat anti-mouse	RB6-8C5	BD Pharmingen
Ly6G-APC	rat anti-mouse	1A8	BioLegend
MHC-II-APC	rat anti-mouse	M5/114.15.2	BioLegend
MHC-II-PE	rat anti-mouse	2G9	BD Pharmingen
PDCA-1-PE	rat anti-mouse	JF05-1C2.4.1	Miltenyi Biotec
SiglecH-APC	rat anti-mouse	eBio440c	eBioscience

2.4.3 SECONDARY ANTIBODIES

name	AB	source
Rat IgG,Cy3-conjugated	donkey-anti-rat-IgG	Jackson ImmunoResearch, West Grove, PA
Mouse IgG, Cy3 conjugated	donkey-anti-mouse-IgG	Santa-Cruz Biotechnology

2.4.4 DEPLETION ANTIBODIES

name	mAB	clone	source
PDCA-1	rat anti-mouse purified	JF05-1C2.4.1	Miltenyi Biotec
Ly-6G	rat anti-mouse purified	RB6-8C5	BioXCell, West Lebanon, NH
Isotype control	rat IgG2b, purified	LTF-2	BioXCell

2.5 CELL CULTURE

Cell culture was performed under sterile conditions in a laminar flowhood. Cells were maintained in a CO_2-incubator at 37°C and a humidified 5% CO_2 atmosphere. Cells were cultured in growth medium (RPMI 1640) supplemented with 10% (v/v) fetal calf serum (FCS), 2 mM L-glutamine and penicillin (100 U/mL)/streptomycin (100 µg/mL) (PAA, Pasching, Austria) to avoid contamination with bacteria. FCS was incubated at 56°C for 30 min to inactivate the complement system and stored at -20°C until use. All media and solutions used for cell culture were from Gibco if not stated otherwise and purchased sterile or sterilized through a 0.2 µm filter. Cultured cells were regularly tested to be mycoplasma free by the VenorGeM Mycoplasma detection kit (Minerva Biolabs, Berlin, Germany).

2.5.1 PREPARATION OF PRIMARY CELL SUSPENSIONS

For flow cytometric analysis of lymph nodes (brachial, axillary, cervical, popliteal, and inguinal) or spleen organs were digested with collagenase D free of tryptic activity (Sigma-Aldrich) for 30 min at 37°C. Cells isolated from spleen were lysed with red blood cell lysis buffer for 5 min. Single cell suspensions were generated by pressing lymph nodes (LN) or spleen cells through a 70-µM cell strainer. Aortas were excised and digested with 1.8 mg/ml of LPS-free Blendzyme Liberase III (Roche, Mannheim, Germany) diluted 1:20 in RPMI 1640 for 30 min at 37°C. Hanks`complete solution was added, and cells were passed through a 70-µm strainer. Bone marrow (BM) cells were extracted from the tibia and femur with Hank's complete solution using a 1 ml syringe and 23-gauge needle. The single cell suspension was centrifuged and the pellet resuspended in about 1 ml RBC lysis buffer for 5 min. Cells were washed 2-3 times and passed through a cell strainer to remove bone fragments and dead cell clumps. Whole blood obtained from the retro-orbital plexus of mice was EDTA-buffered and subjected to red-cell lysis for 15 min followed by 2 wash steps in Hank's complete solution. Cells were then used for further analysis.

Red blood cell lysis buffer:

0.8 % ammonium chloride, 10 mM potassium hydrogen carbonate (KHCO3), 0.1 mM EDTA, pH 8.0

Hanks´complete solution:

1 x HBSS, 0.1% BSA and 0.3 mM EDTA

2.5.2 ISOLATION OF DCS

PDCs were isolated from spleens of wt mice via depletion of all other cells. For this purpose, the Plasmacytoid Dendritic cell Isolation Kit II (containinga cocktail of biotin-conjugated antibodies as well as anti-biotin MicroBeads) and a separation column (all Miltenyi Biotec, Bergisch-Gladbach, Germany) were used according to the recommended protocol, allowing a negative selection of pDCs. Briefly, the freshly isolated spleen cells were mixed with the cocktail of biotin-conjugated antibodies (Abs) and incubated for 10 min at 4°C. After washing with MACSbuffer, the cells were mixed with magnetic anti-biotin microbeads, incubated for 15 min at 4°C, washed and loaded onto the separation column. The magnetically labeled cells were retained in a separation column placed in a magnetic field, whereas cells were recovered in the eluat and cultured in cell culture medium (2.5) for further analysis.

For the isolation of $CD11c^+$ DCs cells from spleens and LN of wt mice cell suspensions were incubated with CD11c Micro Beads (Miltenyi) for 15 min at 4°C, washed and loaded onto the separation column. The $CD11c^+$ DCs retained in the separation column and could be eluted after the column was removed from the magnetic field. Further analyses were performed in culture medium (2.5).

2.5.3 ISOLATION OF $CD4^+$ T CELLS

$CD4^+$T cells were isolated from secondary lymphoid organs of OT-II mice via depletion of non-$CD4^+$T cells. For this purpose, the $CD4^+$T cell Isolation Kit (containing a cocktail of biotin-conjugated Abs against CD8a, CD45R, CD11b, CD49b and Ter-119, as well as magnetic anti-biotin MicroBeads) and a separation column (all Miltenyi Biotec) were used according to the recommended protocol, allowing a negative selection of $CD4^+$T cells. The isolation procedure is identical to the one already described for the isolation of pDCs (2.5.1).

MACS buffer:

PBS, 0.5 % BSA, 2 mM EDTA

2.5.4CELL SORTING

PDCs: For isolation of pDCs via cell sorting freshly isolated spleen or BM cells of wt mice were mixed with Abs against CD45, B220 (CD45RA) and SiglecH (440c). **Neutrophils:** For isolation of neutrophils via cell sorting freshly isolated blood, bone marrow or air pouch lavage cells were mixed with an Ab cocktail against CD45, Gr1 and Ly6-G. Cells were sorted with a

BD FACSAria (BD Bioscience), and used in RT-PCR, phagocytosis, migration, proliferation and apoptosis assays.

2.5.5 BLOOD SMEAR STAINING AND LIPID ANALYSIS

Mouse peripheral blood smears were prepared and analyzed in the local animal facility (University Hospital, Aachen, Germany). All slights were Wright's stained. This staining enables the discrimination between different types of 'white' blood cells, such as neutrophils, lymphocytes, monocytes, eosinophils and basophiles as well as platelets.
Cholesterol and triglyceride levels were determined by routine laboratory assays (Department of Clinical Chemistry, University Hospital Aachen).

2.6 MOLECULAR METHODS

2.6.1 ISOLATION OF DNA

Genomic DNA for mouse genotyping was isolated from mouse tail cuts with the Bio Sprinter 96 from Qiagen (Hilden, Germany) according to the manufacturer's protocol.

2.6.2 ISOLATION OF RNA

Dependent on cell number, RNA from sorted peripheral cells (2.5.4), aortas or whole lymph nodes and spleens were isolated using either the RNeasy Mini Kit or the RNeasy Micro Kit (both Qiagen, Hilden, Germany) or the ZR RNA MicroPrep RNA isolation kit (Zymo Research) according to manufacturer's protocols. Isolation was followed by digestion of genomic DNA using the RNase-free DNase set (Qiagen, Hilden, Germany) according to the manufacturer's protocol.

2.6.3 QUANTIFICATION OF DNA AND RNA

DNA and RNA concentrations and purity were determined by measuring the absorbance at 260 nm (A_{260}) and 280nm (A_{280}) in a spectrophotometer (Nanodrop). Pure DNA or RNA has an A_{260}/A_{280}ratio of 1.8-2.0 at pH 7.0.

2.6.2 QUANTATIVE REAL-TIME POLYMERASE CHAIN REACTION (PCR)

To determine the gene expression of SiglecH (a specific pDC marker), the cytokine IFNα and the antimicrobial peptide Cramp a real-time PCR was performed using the SYBR Advantage qPCR Kit (Clontech, Saint-Germain-en-Laye, France) and gene specific primers according to

manufacturer's protocol. The real-time PCR technique is based on the specific fluorescence properties of SYBRGreen when bound to double stranded DNA, *i.e.* the increase in double-stranded DNA can be directly detected. Thus, the increase of fluorescence over the reaction time can be associated with the initial mRNA concentration. After determination of the RNA amount (2.6.1), up to 1 µg total RNA was reverse-transcribed into cDNA with the M-MLV RT Kit (Promega, Madison, WI, USA) using oligo-dT or Random Hexamer primers (Sigma-Aldrich) at 37°C for 1 h. 20 ng cDNA were assessed in each *real-time* PCR reaction. The housekeeping gene glyceraldehyde 3-phosphate dehydrogenase (GAPDH) was used as a reference gene.

Reverse transcription: 5 µl 5x reverse transcription buffer
0.5 µl dNTP mix (20 mM each)
1.1 µl 10 µM oligo-dT or Random Hexamer primer
1 µl reverse transcriptase enzyme
up to 2 µg template RNA
H_2O to a final volume of 25 µl

Real time-PCR : 2 µl cDNA or H_2O
13 µl 2x QuantiTect SYBR Green PCR Master Mix
forward primer to a final concentration of 0.5 µM
reverse primer to a final concentration of 0.5 µM
RNase free water to final volume of 25 µl

Real time-PCR Program:

1. Initial activation	95°C, 15 min	
2. Denaturation	94°C, 15 sec	X 45 cycles
3. Annealing	58°C, 30 sec	
4. Extension	72°C, 30 sec	
5. Plate read		

The relative mRNA expression is calculated as follows:
$\Delta C_t = C_t$(target gene) - C_t(reference gene); $\Delta\Delta C_t = \Delta C_t$(sample) - ΔC_t(control sample)
relative mRNA expression: (C_t) $2^{-(\Delta\Delta Ct)}$
C_t: Cycle number at which the fluorescence intensity exceeds a determined threshold

Primers for real-time PCR:

mouse *Cramp*:	for	5'-TCCCAAGTCTGTGAGGTTCC-3',
	rev	5'- CCCATACACTGCTTCACCAC -3',
mouse *IFNα*	for	5'- TCTGATGCAGCAGGTGGG-3'
	rev	5'- AGGGCTCTCCAGACTTCTGCTCTG-3'
mouse *SiglecH*:	for	5'- GCTGGGATGCTGCTGTCCCG-3',
	rev	5'- GGTGGCAGGGCACAAGGACA -3';
mouse *Gapdh*	for	5'-CCATCACCATCTTCCAGGAG-3'
	rev	5'-GTGGTTCACACCCATCACAA-3'

2.7 PROTEIN ASSAYS

2.7.1 FLOW CYTOMETRY

Flow cytometry can be used to analyze cells by their size, granularity and protein expression (by *e.g.* fluorescence-conjugated detection antibodies) or to sort cell populations (FACS, Fluorescent activated cell sorting). In a buffer stream, one cell at a time passes by an argon laser, which excites fluorescently labeled cells. Measurements of the size (forward scatter) and granularity (sideward scatter) are independent from the fluorescence signal. Measurement of fluorescence intensity using fluorescence-labeled antibodies was performed to examine and distinguish different cell populations in lymph nodes and spleen by the expression of different markers on the cell surface. In addition, the maturation status of pDCs was examined using Abs against costimulatory molecules, *e.g.* CD86. To determine the state of neutrophil activation CD11b and CD14 were used. All flow cytometry results were displayed as dot plots showing the logarithmic distribution of the fluorescence intensity or as diagrams demonstrating the change in mean fluorescence intensity (MFI) or percentage (%). For surface receptor expression determination, up to 1×10^6 cells were resuspended in FACS staining buffer with specific fluorescence-conjugated antibodies (1:100) and incubated for 20 min on ice. The cells were washed with Hanks` complete and analyzed immediately in a FACS CantoII (BD Biosciences) and evaluated with FlowJo Software (Treestar, Inc, Ashland, OR, USA), if not stated otherwise. As control the fluorescence minus one (FMO) method was used.

FACS staining buffer:

PBS, 2 % BSA, 2 % mouse serum, 2 % rabbit serum, 2 % human serum

2.7.2 BEAD ARRAY

Cell culture supernatants, mouse sera, air pouch and peritoneal lavage fluid were analyzed for various cytokines using flow cytomix Th1/Th2 10 plex assay (BenderMedSystems, Wien, Austria), sample preparation and analysis was performed according to the manufacturer's protocol.

Principle: The kit allows the simultaneous detection and quantification of soluble murine GM-CSF, IFN-γ, IL-1α, IL-2, IL-4, IL-5, IL-6, IL-10, IL- 17 and TNF-α in a single sample. The bead-based assay follows the same principle as a sandwich immunoassay. Fluorescent polystyrol beads are coupled with antibodies specific to the analytes to be detected. Beads are differentiated by their sizes and distinct spectral signature by flow cytometry. Two sets of beads with different sizes (4 µm and 5 µm) are used in this assay. Each of the two sizes consists of bead populations which are differentiated by varying intensities of an internally fluorescent dye. The dye emits in the far red (690 nm), which is detected in the FL-3/FL-4 channel. The combination of the two different bead sizes and different internal dye intensities makes it possible to distinguish up to 20 bead sets in one fluorescent channel. Streptavidin-phycoerythrin (PE), which binds to the biotin conjugate, emits at 578 nm and is detected in the FL-2 channel and allows the quantification of the analyte. For determination of cytokines released by OT-II T cells, a mix of coupled beads is incubated with the supernatants for 2 h at RT. During the incubation, analytes in the supernatants bind to the antibodies coupled to the beads. At the same time, a biotin-conjugated antibody mix is added, which binds to the analytes bound to the capture antibodies. Afterwards, streptavidin-PE is added for 1 h at RT. Samples were examined by FACS CantoII (BD Bioscience), the results were analyzed using the FlowCytomix Pro 2.2 analysis software. Standard curves based on the MFI of cytokine beads were used for quantifying sample cytokine concentrations.

2.7.3 ENZYME-LINKED IMMUNOSORBENT ASSAY (ELISA)

ELISA is an immunological method to determine the amount of an antigen in biological fluids.

All ELISAs performed were based on the principle of a sandwich immunoassay. Briefly, a purified Ab specific for the antigen of interest is pre-coated onto a microplate. All samples and standards are added, and any antigen present binds to the capture Ab. After washing the detecting Ab is added, and binds to the antigen. The next step is the addition of an enzyme-linked secondary Ab, which binds to the detecting Ab. After adding the substrate the enzyme reaction yields a blue product that turns yellow when the stop solution is included. The intensity of the color measured is in proportion to the amount of antigen bound in the initial

step. The sample values are then read of a standard curve. Cell culture supernatants, mouse sera, air pouch or peritoneal lavage fluids were analyzed for one or more of the following targets: IFNα (VeriKine™ Mouse Interferon-Alpha ELISA Kit, PBL laboratories), IL-10 (Mouse IL-10 Quantikine ELISA Kit, R&D Systems), antinuclear antibodies (ANAs) (Mouse Anti-ANA Kit, Alpha Diagnostic, San Antonio, TX, USA) double stranded DNA (dsDNA) (Mouse anti-dsDNA Kit, Alpha Diagnostic), Single stranded DNA (ssDNA) (mouse anti-ssDNA, Alpha Diagnostic), Chemerin (Mouse Chemerin Quantikine ELISA Kit, R&D Systems) or Flt3L (Mouse Flt3L Quantakine ELISA Kit, R&D Systems).

2.7.4 ANALYSIS OF MPO AND MMP-9 ACTIVITY AND ROS FORMATION

MPO activity within the air pouch lavage fluid was measured by spectrophotometry using enzyme-specific substrates as described.[170] MMP-9 activity was quantified using the SensoLyte MMP-9 assay kit (Anaspec. Fremont, CA, USA), based on the proteolytic cleavage of a specific substrate. The fluorescent product was measured at 520 nm using a spectrophotometer. For the detection of ROS formation, neutrophils from *Irf8*$^{+/+}$ or *Irf8*$^{-/-}$ mice were seeded in 96-well plates and loaded with 2′,7′-dichlorodihydrofluorescein diacetate (H_2DCFDA, Invitrogen) in PBS at a final concentration of 10 µM for 30 min at 37°C. Fluorescence was measured before and every 4 minutes after exposure to TNFα (10 ng/ml), phorbol 12-myristate 13-acetate (PMA; 10 ng/ml), or vehicle (PBS) using a spectrophotometer.

2.7.5 HISTOCHEMISTRY

Hearts and aortas were harvested by *in situ* perfusion fixation with 4% Paraformaldeyd (PFA). The extent of atherosclerosis was assessed in aortic roots and on thoracoabdominal aortas by staining for lipid depositions with 0.5 % oil-red-O (Sigma-Aldrich) for 30 minutes. For roots 5 µm transversal sections (3-6/mouse) were used. Aortas were opened longitudinally along the ventral midline, and lesion areas in *en face* preparation were stained. The percentage of lipid deposition was calculated by dividing the stained area by the total surface and quantified by computerized image analysis (Diskus software, Hilgers, Königswinter) and Leica Qwin Imaging software (Leica Ltd, Cambridge, UK).

4% PFA:

1 liter: 40g PFA, 50g Succrose, 40ml of 500mM EDTA, 100ml 10x PBS

2.7.6 IMMUNOFLUORESCENCE

The relative content of macrophages, T cells, SMCs, and neutrophils was determined by monoclonal Ab (mAb) staining of 5 µm transversal tissue sections of aortic roots for MOMA-2, CD3, smoothelin and Ly6G (2.4.1), respectively. In addition, staining for Myeloperoxidase and MMP-9 (2.4.1) were performed using the specific mAbs as indicated. Stainings were visualized by fluoresceinisothiocyanate- or cyanine-3-conjugated secondary Abs (2.4.3). Appropriate IgG antibodies served as isotype controls. Apoptotic nuclei were detected by terminal deoxynucleotidyl nick-end labeling (TUNEL-kit, Roche). PDCs were detected by staining for Siglec-H (440c, HyCult Biotech). A rabbit anti-Cramp Ab (Innovagen) was used to detect Cramp on acetone fixed fresh frozen sections. Plaque IgG was detected using a biotinylated rabbit anti-mouse IgG (Vector Laboratories) followed by a streptavidin-conjugated Alexafluor-555 (Molecular Probes) on 4% paraformaldehyde-fixed frozen sections. Nuclei were counter- stained by 4',6-Diamidino-2-phenylindol (DAPI). Collagen was stained using Sirius red (Polysciences, Inc., Warrinton, PA, USA). Images were recorded with a Leica DMLB fluorescence microscope and CCD camera.

2.8 FUNCTIONAL ASSAYS

2.8.1 APOPTOSIS AND CELL CYCLE ASSAYS

Peritoneal macrophages or neutrophils sorted from the air pouch lavage, blood and bone marrow were cultured in cell culture medium (2.5). Cells were seeded at 1 x 10^6 cells/ml and analyzed at 0, 12, 36, 60 and 84 hours of culture by staining with Annexin V (BD Bioscience) in the appropriate staining buffer (BD Bioscience) or propidium iodide (10 µg/ml) in PBS buffer containing 0.25 % TritonX-100 and RNase A (4 µg/ml; GenScript, Piscataway,NJ, USA) following fixation with 70 % ethanol. Apoptosis and cell cycle were assessed by FACS analysis using a FACS Calibur (BD Biosciences).

2.8.2 PHAGOCYTOSIS ASSAYS

Peritoneal macrophages harvested after peritonitis (2.9.3) were seeded at 1 x 10^6 cells/ml into 96-well plates and incubated with di-labeled oxLDL (10µg/ml) (Intracel) or calcein- (Invitrogen) labeled apoptotic neutrophils (sorted from bone marrow 2.5.5) (1:1 ratio) for 1 h. Neutrophils were rendered apoptotic by serum deprivation over night and apoptosis was confirmed by Annexin V binding (>95%). Phagocytosis of apoptotic neutrophils and di-oxLDL was analyzed by FACS.

Isolated pDCs (2.5.3) seeded at 1 x 10^5 cells/200µl in flat bottom 96-well plates and incubated with di-labeled oxLDL (10µg/ml) for 12 h and analyzed by FACS.

2.8.3 *IN VITRO* STIMULATION OF PDCS

Isolated pDCs were seeded at 1 x 10^5 cells/200µl into flat bottom 96-well plates in cell culture medium (2.5) supplemented with 25 ng/ml FLT3-L (Peprotech) and were stimulated with 10µg Cramp (1ug/µl, Innovagen), 2 µg DNA (1 ug/µl, Zyagen), 1µg ODN 1585 (1µg/µl, Invivogen), 10µg oxLDL or di-oxLDL (1ug/µl), and 4ul of mouse serum containing high (36 Units/µl) or low (1 Unit/µl) titers of anti-dsDNA antibodies per well for 12 h. For the generation of complexes, 10µg of Cramp was mixed with 2 µg self-DNA in 20 µl of PBS and incubated for 15 min at room temperature asdescribed by Ganguly *et al.*[171]. Apoptotic (dead) PMN used for stimulation purposes were rendered apoptotic by UV-light treatment for 6 min at a concentration of 1 x 10^6 cells/ml in cell culture medium. PMN and pDCs were cocultured at ration of 5:1.

2.9 ANIMAL MODELS

All animal experiments were approved by the local ethical committee and carried out in accordance with the guidelines of the “Landesamt für Natur, Umwelt und Verbraucherschutz” North Rhine-Westphalia.

2.9.1 MOUSE MODELS OF ATHEROSCLEROTIC DISEASE

Female *Apoe*$^{-/-}$ *or Ldlr*$^{-/-}$mice were fed a normal chow or, at 8 weeks of age, an atherogenic diet containing 21% fat and 0.15% cholesterol (Atromin) for 4 to 12 weeks depending on the experimental setup. After sacrificing the mice hearts were harvested by *in situ* perfusion fixation with 4% PFA. The extent of atherosclerosis was assessed in aortic roots and thoracoabdominal aortas by staining for lipid deposition with Oil-red-O (2.7.5). The relative content of macrophages, neutrophils, $CD3^+$T cells and SMCs was determined by immunofluorescence (2.7.6).

2.9.1.1 CELL DEPLETION ASSAYS

PMN depletion in *Ldlr*$^{-/-}$ mice was performed by intaperitoneal injections of mAb RB6-8C5 (100 µg/mouse, BioXCell) over 5 weeks every second day accompanied by atherogenic diet feeding of the mice for 5 weeks. Efficiency and specificity of PMN depletion was confirmed by flow cytometry analysis of blood samples. PDC depletion in *Apoe*$^{-/-}$ mice was performed by *i.v.*

injection of mAB PDCA-1 (500ug/mouse, Miltenyi) at day 1 and day 7 or day 30 and 37 depending on the experimental setup. Mice were put on an atherogenic for 4 or 8 weeks. Efficiency and specificity of pDC depletion was confirmed by flow cytometry analysis of representative lymph nodes.

2.9.1.2 CELL STIMULATION ASSAYS

PDC stimulation in *Apoe*$^{-/-}$ mice was carried out with the *i.v.* injection of the oligodinucleotide CpG1585 (ref. to 2.5) (25ug/mouse, Inovagen) complexed to DOTAP (15ug/mouse, Roche) 3 times a week for 4 or 8 weeks. During injections *Apoe*$^{-/-}$ mice were fed a high fat diet. Efficient pDC stimulation was confirmed by determining the IFNα concentration in serum. Alternatively *Apoe*$^{+/+}$ mice were injected with the same dose, but sacrificed 4, 12 or 24 after injection of CpG complexed to DOTAP. Another set of *Apoe*$^{-/-}$ was injected with murine IFNα (100 000 Units/mouse, HyCult Biotec) twice a week *i.p.* for 4 weeks together with high fat diet feeding.

2.9.2 BONE MARROW TRANSPLANTATION

To assess the contribution of IRF8 and CRAMP to lesion progression, *Apoe*$^{-/-}$ or *Ldlr*$^{-/-}$ mice were lethally irradiated and reconstituted with bone marrow of *Irf8*$^{-/-}$ *and Cramp*$^{-/-}$ mice. For bone marrow transplantations femurs and tibias were aseptically removed from donor *Irf8*$^{-/-}$, and *Cramp*$^{-/-}$or *Apoe*$^{-/-}$ and *Ldlr*$^{-/-}$ control mice. Bone marrow cavities were flushed and single cell suspensions prepared. Donor cells (5×10^6) were administered by tail vein injection into the recipient mice 24 h after an ablative dose of whole-body irradiation (2x6 Grays(Gy)). After recovery for 4 weeks the transplanted mice were fed a HFD over 4-12 weeks depending on the experimental setup. After sacrificing the mice, hearts and thoracoabdominal aortas were harvested and stained for lipid deposition (2.7.5). Additionally blood, lymph nodes, spleen and femur were removed for further analysis of different cell populations in flow cytometry assays (2.7.1).

2.9.3 PERITONITIS

Irf8$^{-/-}$ and *irf8*$^{+/+}$ mice were injected with thioglycollate broth intraperitonealy and peritoneal macrophages were harvested and isolated after 4 days as described.[172] Sterile 3% thioglycollate was prepared by autoclaving and was stored at room temperature in the dark for at least 6 month before use. Mice received *i.p.* injections of 1 ml of thioglycollate broth or PBS as control.

2.9.4 SUBCUTANEOUS AIR POUCH

For recruitment of pDCs and neutrophils to a subcutaneous air pouch[39] mice were injected at day 0 and 4 with 5 ml sterile air subcutaneously in the back. At day 7, 1 ml sterile PBS containing PAF (1µM, Biomol), TNFα (50ng/ml, Peprotech), IFNα (100ng/ml, PBL Laboratories) or PBS alone were injected into the pouch. 4 h or 18 h later the pouch was lavaged with 5 ml of ice-cold HBSS containing 0.3 mM EDTA and 0.1 % BSA. Thereafter, cells in the lavage fluid were counted manually using a Neubauer chamber and processed for FACS analysis as described before (2.7.1).

2.9.5 T CELL PROLIFERATION *IN VIVO*

$CD4^+$ T cells were isolated from spleen and LNs of OT-II mice using the $CD4^+$ T cell isolation kit (Miltenyi Biotec) (2.5.4). $CD4^+$ OT-II cells were labeled with CFSE (Fluka) by incubation with 5 µM CFSE in labeling medium for 10 min. Labeling was stopped by adding one volume of labeling medium, and cells were washed an additional two times. Subsequently, 5×10^6 $CD4^+$ $CFSE^+$ OT-II cells were injected into the tail vein of each wt recipient mouse. One day after T cell injection, *ex vivo* isolated pDCs (2.5.3) were pulsed with 6µg/ml OVA2 peptide for 45 minutes for MHC class II-restricted T cell stimulation. Untreated pDCs were used as control. 1×10^5 pDCs were applied to recipient mice by footpad injection. Three days later, single-cell suspensions of popliteal LNs were prepared and the T cell proliferation was monitored by CFSE dye dilution using flow cytometry.

Labeling medium:
RPMI 1640, 10% FCS

2.10 DATA ILLUSTRATION AND STATISTICAL ANALYSIS

Data are expressed as mean ± SD and analyzed by Student's t-test, ANOVA with Newman-Keuls or Dunnett's multiple comparison test, non-parametric Mann-Whitney test or Kruksal-Wallis test with Dunn's post-hoc test, as appropriate. Data for ROS measurement were analyzed with two-way repeated measures analysis of variance (ANOVA; treatment × time) followed by planned comparisons. Differences of $p<0.05$ were considered to be statistically significant. All data was processed and displayed with GraphPad Prism 5 software.

3. RESULTS

3.1 RESULT OUTLINE

The following section will explain and display the experimental results, which were obtained throughout this thesis.

The first part will describe experiments and subsequent conclusions carried out to unveil the participation of PMN in atherosclerosis. Neutrophils were detected and characterized with the help of different antibodies, which not only enable their discrimination by flow cytometry, but also allow visualization of PMN in tissue sections. Furthermore, in depth analysis of PMN activation and the subsequent examination of their granule proteins in the context of atherosclerosis will reveal a broader view of their contribution to plaque formation. In addition, analysis of apoptosis and proliferation rates as well as systemic PMN depletion will deepen our understanding of their role in atherosclerosis.

The second part illustrates the experimental setup chosen to gain insight in the role of pDCs in lesion development. Specific antibodies allow the identification of pDCs in various organs and their detection in atherosclerotic lesions. Moreover, oligonucleotides facilitate pDC stimulation *in vivo* and thus enable us to analyse the consequences of pDC activation in atherosclerosis. To complement these findings, the effect of pDC depletion on atherosclerotic lesion formation was studied. In this context the potency of pro-atherogenic stimuli such as oxLDL to promote pDCs activation was examined. Ultimately, the mechanisms known to drive pDC activation in autoimmune diseases will be explored in the context of atherosclerosis.

For a better overview of the result section the following flow chart outlines the experimental setup for each of the two projects.

Chronic myelogenous leukemia-like disease due to hematopoietic IRF8-deficiency fuels atherosclerosis in mice	Activated plasmacytoid dendritic cells accelerate early atherosclerotic lesion formation
Does IRF8 influence plaque development?	***Are pDCs present in atherosclerotic lesions?***
Phenotypical analysis of *Apoe*$^{-/-}$ mice transplanted with *Irf8*$^{-/-}$ bone marrow	Immunhistochemistry of aortic roots and FACS analysis *of Apoe*$^{-/-}$ aortas
Evaluation of lesion development and composition in *Irf8*$^{-/-}$►*Apoe*$^{-/-}$ mice	***Does pDC depletion or stimulation change plaque development?***
Are monocyte and macrophage functions impaired?	Evaluation of lesion development and composition in *Apoe*$^{-/-}$ mice with specific pDC depletion or stimulation
Characterization of *Irf8*$^{-/-}$ monocytes and macrophages in an acute (air pouch) and prolonged (peritonitis) inflammation model	***Does oxLDL treatment alter the function of pDCs in vitro and in vivo?***
	Phagocytosis and stimulation assays with oxLDL treated pDCs
Determination of apoptosis and proliferation in peritoneal macrophages of *Irf8*$^{-/-}$ mice	Antigen specific T cell proliferation assay *in vivo*
Do neutrophils function normally?	***Are autoimmune mechanisms involved in pDC stimulation?***
	-Cramp-
Examinaton of neutrophil recruitment to an acute inflammation (air pouch) and determination of apoptosis, proliferation and activation of neutrophils in *Irf8*$^{-/-}$ mice	*in vitro* stimulation of *ex vivo* isolated pDCs with the antimicrobial peptide Cramp in combination with or without DNA
	Evaluation of lesion development in *Ldlr*$^{-/-}$ mice transplanted with *Cramp*$^{-/-}$ bone marrow or in *Apoe*$^{-/-}$ stimulated with Cramp+DNA complexes
Does neutrophil depletion revert the atherosclerotic phenotype?	***-anti-dsDNA-antibodies-***
Evaluation of lesion development and composition *in Irf8*$^{-/-}$ ►*Ldlr*$^{-/-}$ mice in comparison to *Irf8*$^{-/-}$ ►*Ldlr*$^{-/-}$ mice with neutrophil depletion	Measurement of serum anti-dsDNA titer in all treated animals
	In vitro stimulation of pDCs with sera high or low in anti-dsDNA antibody titers

Summary of the experimental setup in order of the questions addressed.

3.2 ROLE OF HEMATOPOIETIC IRF8 IN ATHEROSCLEROTIC LESION FORMATION AND ITS EFFECTS ON MONOCYTE/MACROPHAGE AND PMN FUNCTIONS RELATED TO ATHEROSCLEROSIS

IRF8 is exclusively expressed in hematopoietic cells and critical in lineage determination and development of myeloid cells. Furthermore, it is essential in directing monocyte and macrophage differentiation, but is repressing genes promoting granulocytic differentiation and maturation.[164,173,174] In consequence *Irf8*$^{-/-}$ mice develop a chronic myeloid leukemia (CML)-like syndrome with a striking increase in PMN numbers, while monocytes and macrophage numbers are significantly reduced and functionally compromised.[164,174-176] Therefore we took advantage of the increased number of PMN in *Irf8*$^{-/-}$ mice and reconstituted lethally irradiated *Apoe*$^{-/-}$ mice with bone marrow of *Irf8*$^{-/-}$ mice to study the effect of hematopoietic IRF8 deficiency and the impact of increased PMN counts in atherosclerotic lesion formation.

3.2.1 *APOE*$^{-/-}$ MICE TRANSPLANTED WITH *IRF8*$^{-/-}$ BM DISPLAY A CML-LIKE PHENOTYPE

As Kallies *et al.* reported that *Irf8*$^{-/-}$ monocytes exhibit an only marginal expression of CD115, possibly related to its enhanced proteolytic degradation[177], a new gating strategy had to be established to distinguish between PMN and monocytes in these mice. This strategy identified monocytes by staining for CD11b and Gr1$^{high/low}$ but the absence of PMN-specific Ly6G, while PMN expressed CD11b, Gr1, and Ly6G (Figure 3-1).

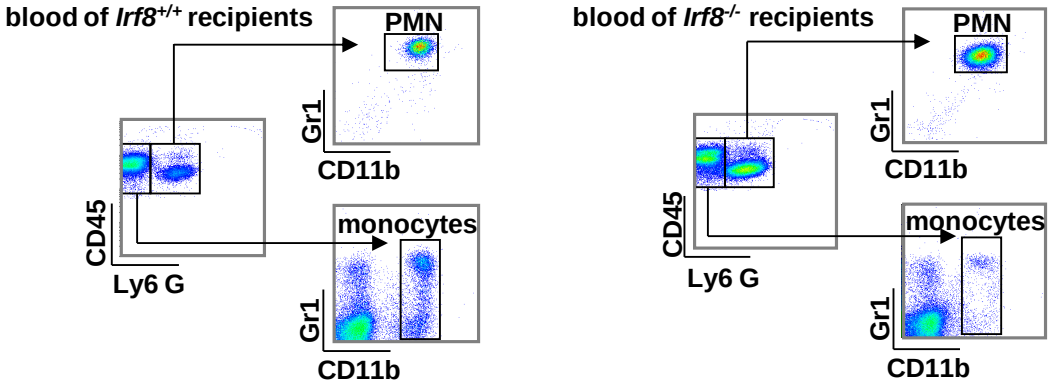

Figure 3-1. Gating strategy for monocytes in *Irf8*$^{-/-}$ mice.
Gating strategy for PMN (Ly6G^{+} CD11b^{+} Gr1^{+}) and monocytes (Ly6G^{-} CD11b^{+} Gr1$^{high/low}$); representative dot plots are shown.

Next it was investigated whether or not the phenotype of *Irf8*$^{-/-}$ mice[164] is retained in *Apoe*$^{-/-}$ mice transplanted with *Irf8*$^{-/-}$ bone marrow. For this purpose relative leukocyte distribution was examined by flow cytometry identifying neutrophils and monocytes as described, DCs by staining for MHCII and CD11c, while T cells and B cells were defined by CD3 and CD19 expression, respectively. CD45 was used as a pan marker for all leukocytes. Absolute numbers of leukocytes in blood of *Irf8*$^{+/+}$►*Apoe*$^{-/-}$ and *Irf8*$^{-/-}$►*Apoe*$^{-/-}$were analyzed according to the method section 2.5.6. Similar to the distribution of peripheral blood cells in donor *Irf8*$^{-/-}$ mice, lethally irradiated *Apoe*$^{-/-}$ mice reconstituted with *Irf8*$^{-/-}$ BM (*Irf8*$^{-/-}$►*Apoe*$^{-/-}$) displayed a trend for expansion in the number of leukocytes and a significant increase in the frequency of PMN in peripheral blood, while relative numbers of circulating monocytes, DCs and T cells but not B cells were reduced when compared to *Irf8*$^{+/+}$►*Apoe*$^{-/-}$ mice (Figure 3-2).

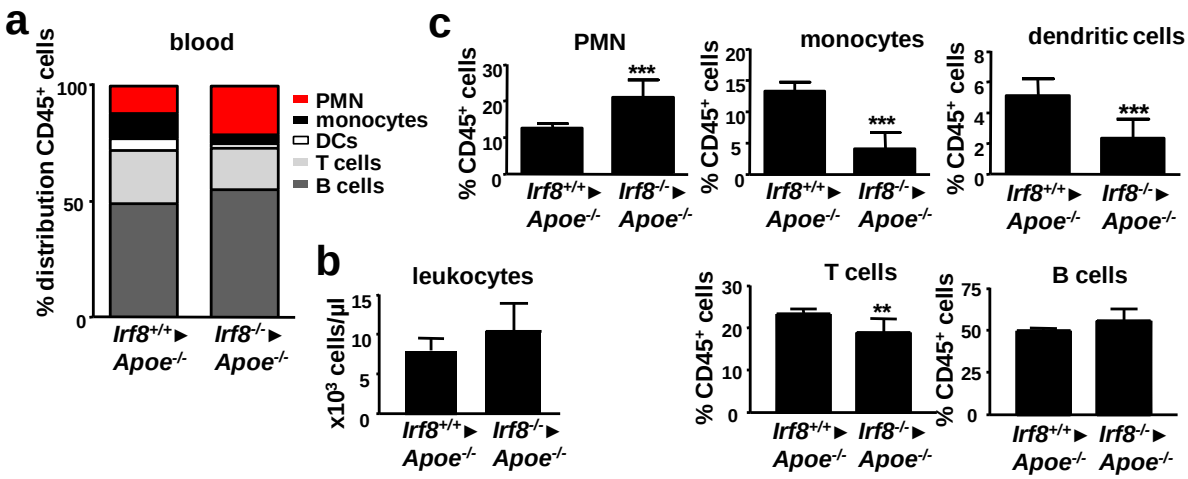

Figure3-2. Leukocyte distribution in blood of *IRF8*$^{-/-}$►*Apoe*$^{-/-}$ mice.
(a) FACS analysis of the CD45^{+} subset distribution in blood of *Irf8*$^{-/-}$►*Apoe*$^{-/-}$ (n=7) and *Irf8*$^{+/+}$►*Apoe*$^{-/-}$ mice (n=10) after 12 weeks of high fat diet; **(b)** total leukocyte counts in BM-recipients. **(c)** relative frequencies of PMN, monocytes, T cells, B cells and dendritic cells in *Irf8*$^{-/-}$►*Apoe*$^{-/-}$mice. Data are expressed as mean±SD, $^{**}p<0.005$; $^{***}p<0.001$.

A comparable distribution of leukocyte subsets was also observed in the BM of transplanted mice, with an even more pronounced expansion of PMN in *Irf8*$^{-/-}$►*Apoe*$^{-/-}$ mice compared to *Irf8*$^{+/+}$►*Apoe*$^{-/-}$ mice, as shown by flow cytometry analysis and HE-stained bone marrow sections (Figure 3-3).

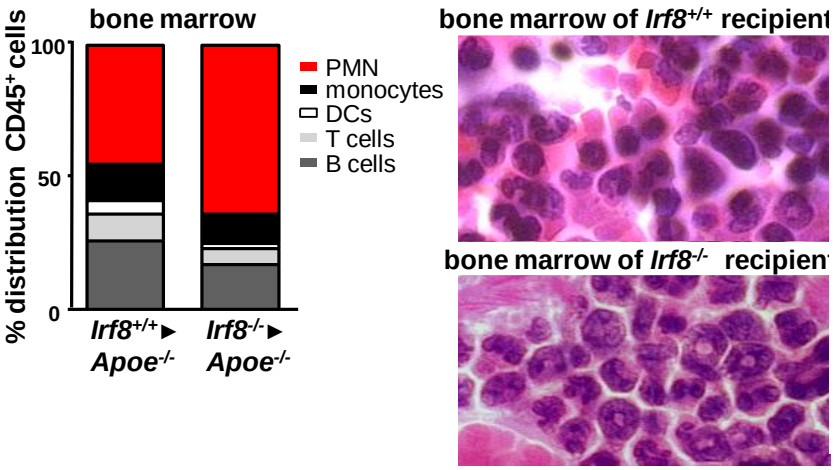

Figure 3-3. Leukocyte distribution in bone marrow of *Irf8*$^{-/-}$►*Apoe*$^{-/-}$ mice.
Representative HE-stained sections of *Irf8*$^{+/+}$and *Irf8*$^{-/-}$ bone marrow recipients and FACS analysis of the CD45^{+} subset distribution in bone marrow of *Irf8*$^{+/+}$►*Apoe*$^{-/-}$ (n=10) and *Irf8*$^{-/-}$►*Apoe*$^{-/-}$ mice (n=7) after 12 weeks of high fat diet.

These data indicate that the CML-like phenotype observed in *Irf8*$^{-/-}$ mice is sustained in transplanted *Irf8*$^{-/-}$►*Apoe*$^{-/-}$ mice, allowing the investigation of its consequences in atherosclerosis. Of note, no changes in the nuclear morphology of PMN were observed in blood smears of *Irf8*$^{-/-}$►*Apoe*$^{-/-}$and *Irf8*$^{+/+}$►*Apoe*$^{-/-}$ mice (Figure 3-4). This is in line with a chronic disease course with no signs of an accumulation of progenitor or immature myeloid cells in blood, which would be a characteristic of the late progressive blast phase.[164,178]

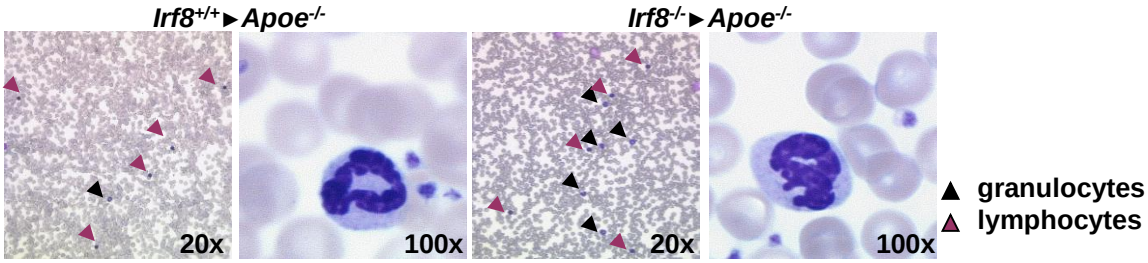

Figure 3-4. Representative Blood Smears.
Representative blood smears of *Irf8*$^{+/+}$►*Apoe*$^{-/-}$ and *Irf8*$^{-/-}$►*Apoe*$^{-/-}$ mice. PMN and lymphocytes are indicated by black or red arrow heads, respectively.

3.2.2 INCREASED ATHEROSCLEROTIC LESION FORMATION IN *IRF8*$^{-/-}$►*APOE*$^{-/-}$MICE

Following the confirmation of a neutrophilic phenotype in *Irf8*$^{-/-}$►*Apoe*$^{-/-}$mice, serum lipid levels and the degree of atherosclerotic lesion formation in *Irf8*$^{-/-}$►*Apoe*$^{-/-}$mice and controls were analyzed after 12 weeks of HFD. Total serum cholesterol and low density lipoprotein (LDL) levels were increased in *Irf8*$^{-/-}$►*Apoe*$^{-/-}$ in comparison to *Irf8*$^{+/+}$►*Apoe*$^{-/-}$ mice (Table 1). Furthermore the quantification of lipid depositions in *en face* preparations of aortas and aortic roots with oil-red-O revealed a significant exacerbation in lesion formation in *Irf8*$^{-/-}$►*Apoe*$^{-/-}$ compared to *Irf8*$^{+/+}$►*Apoe*$^{-/-}$ mice (Figure 3-5).

Table 3-1. Serum lipid levels

	total cholesterol [mg/dL]	LDL [mg/dL]	HDL [mg/dL]	triglycerides [mg/dL]
***Irf8*$^{+/+}$ ►*Apoe*$^{-/-}$**	196.3 ± 84.5	123.5 ± 57.6	104.2 ± 45.0	84.5 ± 32.3
***Irf8*$^{-/-}$►*Apoe*$^{-/-}$**	298.2 ± 80.8*	198.5 ± 53.7*	111.2 ± 43.2	73.5 ± 12.6
***Irf8*$^{+/+}$►*Ldlr*$^{-/-}$**	250.8 ± 44.1	121.9 ± 19.2	91.3 ± 6.8	138.7 ± 62.9
***Irf8*$^{-/-}$►*Ldlr*$^{-/-}$**	249.2 ± 25.9	121.8 ± 12.3	82.4 ± 33.5	107.3 ± 26.0
***Irf8*$^{-/-}$►*Ldlr*$^{-/-}$anti-PMN**	324.6 ± 34.3	127.2 ± 102.5	100.5 ± 9.0	95.0 ± 28.9

LDL, low-densitiy lipoprotein
HDL, high-density lipoprotein * p<0.05

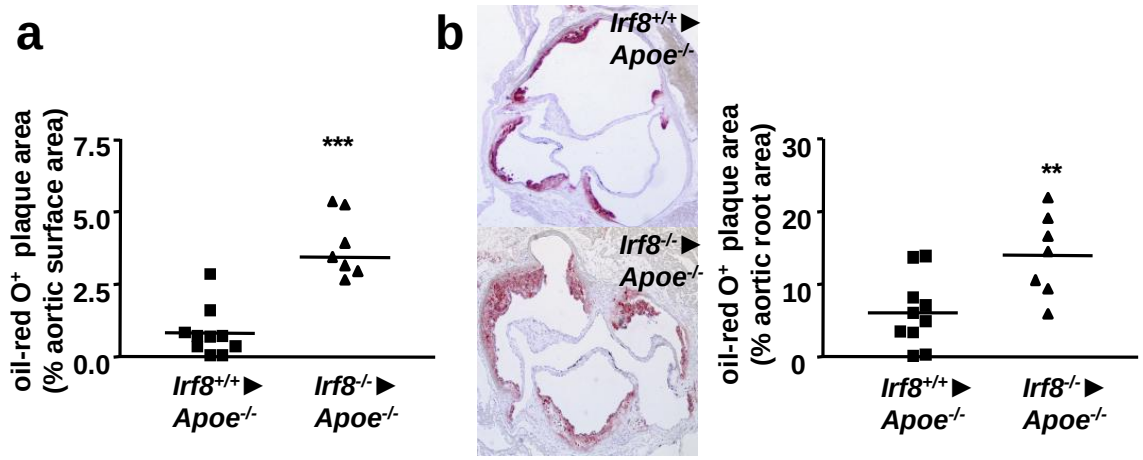

Figure 3-5. Increased atherosclerotic lesion formation in *Irf8*$^{-/-}$►*Apoe*$^{-/-}$ mice. (a, b) Quantification of oil-red-O^{+} lipid depositions in the thoracoabdominal aorta **(a)** and aortic root **(b)** of *Irf8*$^{+/+}$►*Apoe*$^{-/-}$(n= 10) and *Irf8*$^{-/-}$►*Apoe*$^{-/-}$(n=7) mice; representative images are displayed. Data is expressed as mean±SD, **p<0.01, ***p<0.001.

To clearly attribute the changes in lesion size to the lack of IRF8 in our transplantation model we also investigated the effect of 12 weeks HFD in *Irf8*$^{+/+}$ and *Irf8*$^{-/-}$ control mice without an *Apoe*$^{-/-}$ background. These mice showed a similar tendency in plaque development after 12 weeks, even though they had very small lesions only detectable in aortic roots (Figure 3-6). In conclusion, IRF8-deficiency increases plaque formation.

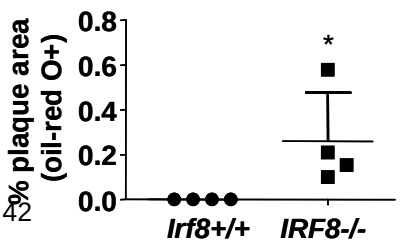

Figure 3-6. Increased plaque formation in *Irf8*$^{-/-}$ control mice. Quantification of oil-red-O^{+} lipid depositions in aortic roots of *Irf8*$^{+/+-}$ (n= 4) and *Irf8*$^{-/-}$ (n=4) mice. Data is expressed as mean±SD, *p<0.05.

Augmented plaque formation may also be accompanied by changes of plaque composition, plaque stability (SMC content), foam cell formation (macrophage content), and leukocyte accumulation. Further analysis of the cellular plaque composition by quantitative immunofluorescence showed that the number of macrophages ($MOMA^+$), SMC ($smoothelin^+$), and T cells ($CD3^+$) was not altered in aortic root plaques, whereas a significant increase in the relative number of PMN ($Ly6G^+$) was observed in lesions of *Irf8*$^{-/-}$►*Apoe*$^{-/-}$ (Figure 3-7).

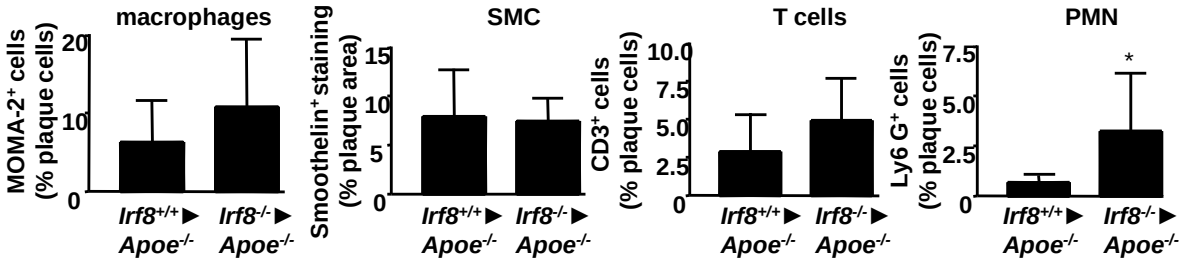

Figure 3-7. Quantitative analysis of plaque composition in *Irf8*$^{+/+}$►*Apoe*$^{-/-}$ and *Irf8*$^{-/-}$►*Apoe*$^{-/-}$.
Quantification of macrophages, SMC-content, T cells and PMN in aortic root plaques. Data is expressed as mean±SD, **p*<0.05.

Increased neutrophil numbers may also be accompanied by enhanced granule protein formation and deposition. Hence, it was investigated if PMN-granule proteins were detectable. Both, the expression of MPO, known to be involved inROS formation (1.2.1.1), and the number of $MMP\text{-}9^+$ cells (MMP-9 facilitates PMN transmigration, 1.2.1.1) were found to be increased (Figure 3-8). Instead, the content of collagen-rich, extracellular matrix, evidenced by Sirius-red staining, was reduced in lesions of *Irf8*$^{-/-}$►*Apoe*$^{-/-}$ mice, implying a more inflammatory and unstable plaque phenotype (Figure 3-9). These results indicate that increased PMN accumulation accompanied by augmented levels of PMN-derived granule proteins drive plaque growth and weaken the fibrous cap.

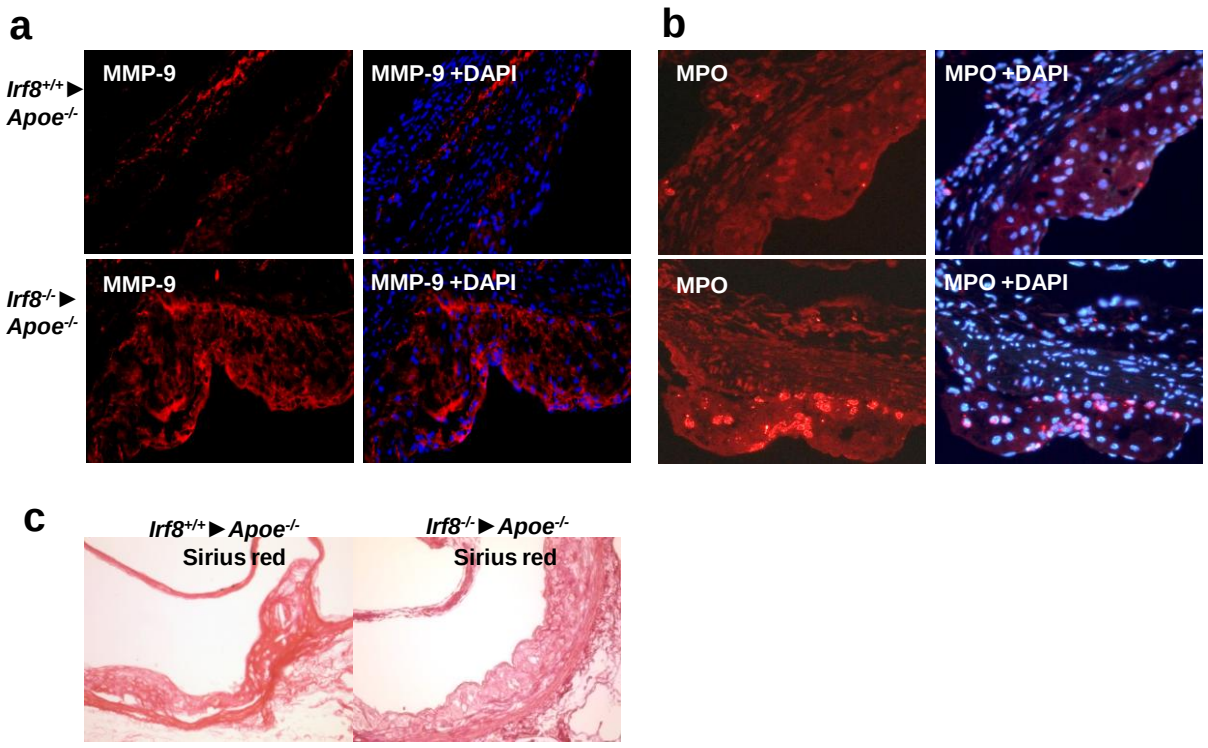

Figure 3-8. MMP-9 and MPO-expressing cells and collagen content in atherosclerotic lesions. **(a, b)** Aortic root plaques of *Irf8*$^{-/-}$►*Apoe*$^{-/-}$ and *Irf8*$^{+/+}$►*Apoe*$^{-/-}$ mice were analyzed after 12 weeks of high fat diet. Representative images of staining for MMP-9^{+} **(a)** and MPO^{+} cells **(b)**; cell nuclei are stained by DAPI. **(c)** Representative images of collagen content Sirius red staining.

In addition, ongoing inflammation in atherosclerotic plaques is accompanied by the accumulation of dead cell debris, referred to as the necrotic core. Growing necrotic cores are one major reason for increased lesion sizes. Therefore we measured the necrotic core area and the amount of DNA fragmentation within the plaque by TUNEL staining. Notably, the size of necrotic cores in lesions of *Irf8*$^{-/-}$►*Apoe*$^{-/-}$ mice as well as their number of lesional TUNEL^{+} apoptotic cells was markedly increased in comparison to *Irf8*$^{+/+}$►*Apoe*$^{-/-}$ mice (Figure 3-9; a). To further unravel the cell type undergoing apoptosis or necrosis, double-immunofluorescence staining was performed. While the macrophage fraction within TUNEL^{+} cells did not differ, a clear increase in relative numbers of TUNEL^{+} Ly6G^{+} PMN could be detected in *Irf8*$^{-/-}$►*Apoe*$^{-/-}$ compared to *Irf8*$^{+/+}$►*Apoe*$^{-/-}$ lesions (Figure 3-9; b,c). These results demonstrate that exacerbated atherosclerotic lesion formation in *Irf8*$^{-/-}$►*Apoe*$^{-/-}$ mice is associated with an enhanced accumulation and subsequent apoptosis of PMN within growing plaques.

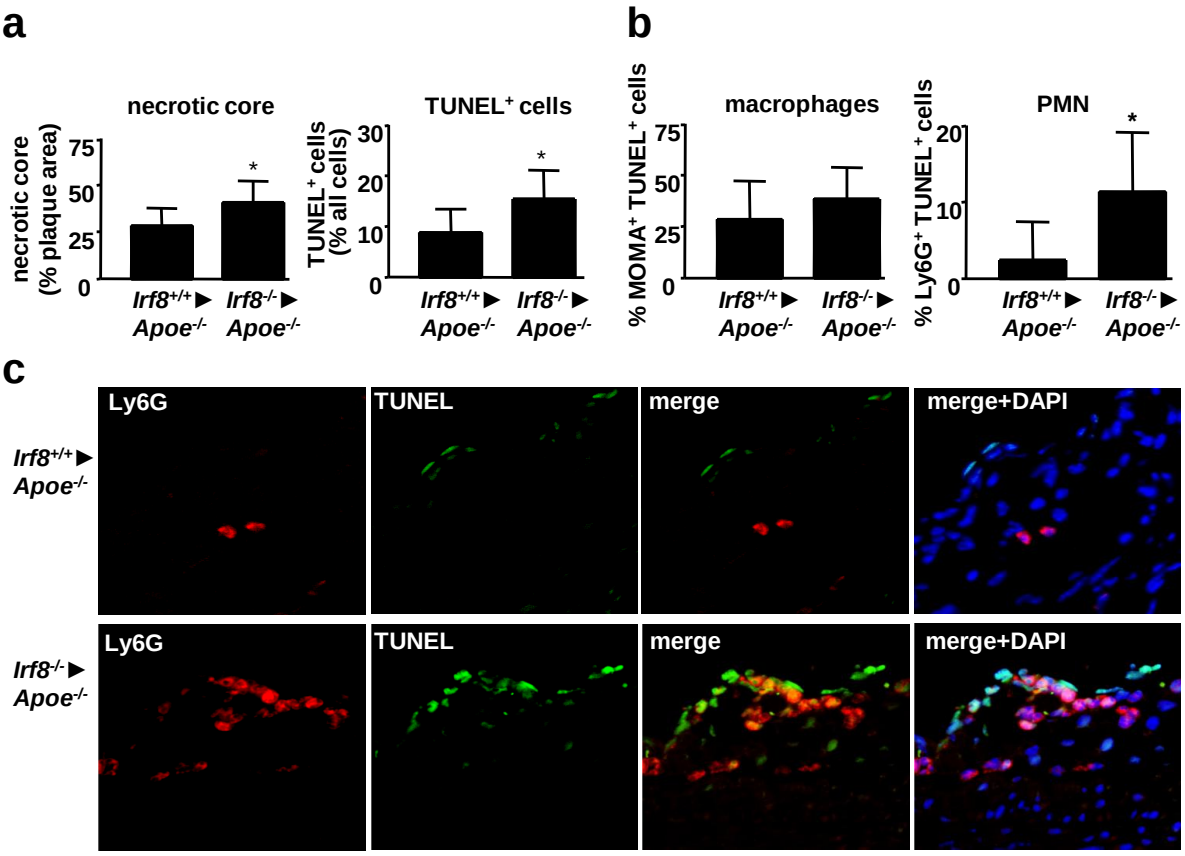

Figure 3-9. Necrotic cores and TUNEL$^+$ cell numbers are increased in *Irf8*$^{-/-}$►*Apoe*$^{-/-}$ lesions. (a) Quantification of acellular necrotic cores and TUNEL$^+$ apoptotic cells within aortic root lesion of *Irf8*$^{+/+}$►*Apoe*$^{-/-}$ and *Irf8*$^{-/-}$►*Apoe*$^{-/-}$ mice, and **(b)** quantification of double-positive TUNEL$^+$ macrophages and TUNEL$^+$ PMN relative to total TUNEL$^+$ cells (n=7-10).**(c)** Representative images of Ly6Gand TUNEL double-immunofluorescence staining. Cell nuclei were stained by DAPI. Data is expressed as mean±SD, *p<0.05.

3.2.3 MACROPHAGE FUNCTIONS BUT NOT ACCUMULATION OR APOPTOSIS ARE IMPAIRED IN *IRF8*$^{-/-}$ MICE

Macrophage phenotype and functions were shown to be regulated by IRF8.[173] Thus, the question arose whether macrophage functions and/or their accumulation under acute and prolonged inflammatory conditions, reflecting inflammation in atherosclerosis, would be altered. To address this question, we first investigated acute inflammatory recruitment into a subcutaneous air pouch. Results therefrom revealed an increase in the total number of leukocytes accumulating in air pouches of *Irf8*$^{-/-}$ mice in response to PAF after 4 hours and a significant decrease in relative frequencies of monocytes compared to *Irf8*$^{+/+}$ mice (Figure 3-10; a,b). Instead, the absolute number of monocytes extravasated into the air pouch did not differ in *Irf8*$^{+/+}$ or *Irf8*$^{-/-}$ mice contrasting decreased absolute and relative monocyte counts in peripheral blood (Figure 3-10; b).

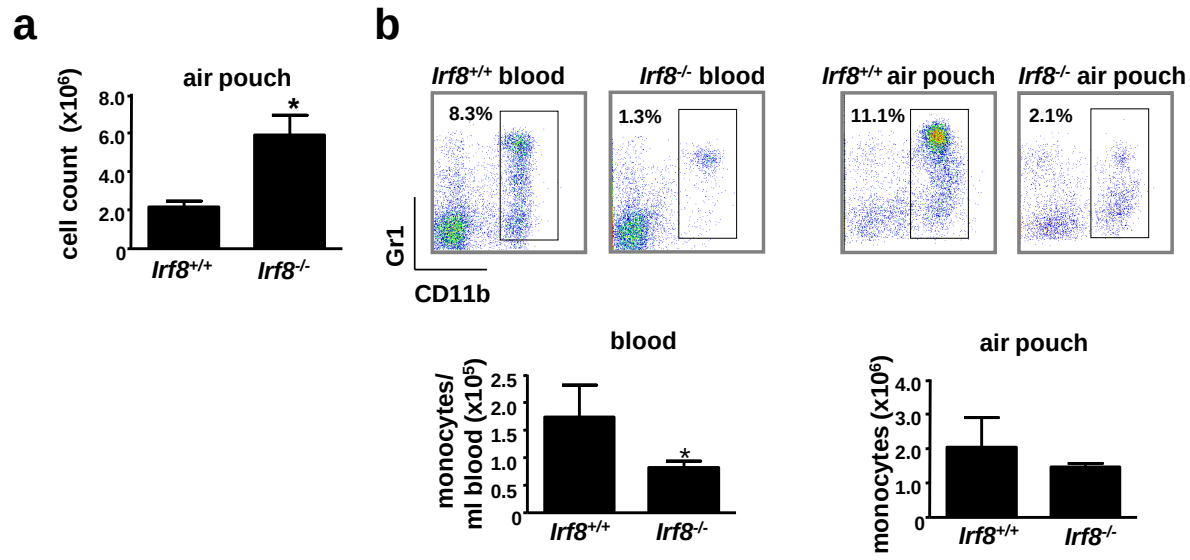

Figure 3-10. Macrophage recruitment in acute inflammation is not affected in *Irf8*$^{-/-}$ mice. **(a)** Total count of cells retrieved from air pouches after stimulation with PAF for 4 h. **(b)** Representative FACS dot plots of monocytes (gated events, inserted numbers indicate percentages relative to CD45^{+} cells) in blood and air pouch lavages of *Irf8*$^{+/+}$ and *Irf8*$^{-/-}$ mice (n=5 each) 4 h after stimulation with PAF. Absolute monocyte counts in blood and air pouch lavages are depicted in bar graphs. Data is expressed as mean±SD, **p*<0.05.

Prolonged inflammation was studied in the peritonitis model by flow cytometry analysis of peritoneal macrophage numbers before thioglycollate injection (untreated) and 4 days after thioglycollate injection. These data did not reveal any difference between *Irf8*$^{-/-}$ peritoneal macrophages and the control group (Figure 3-11).

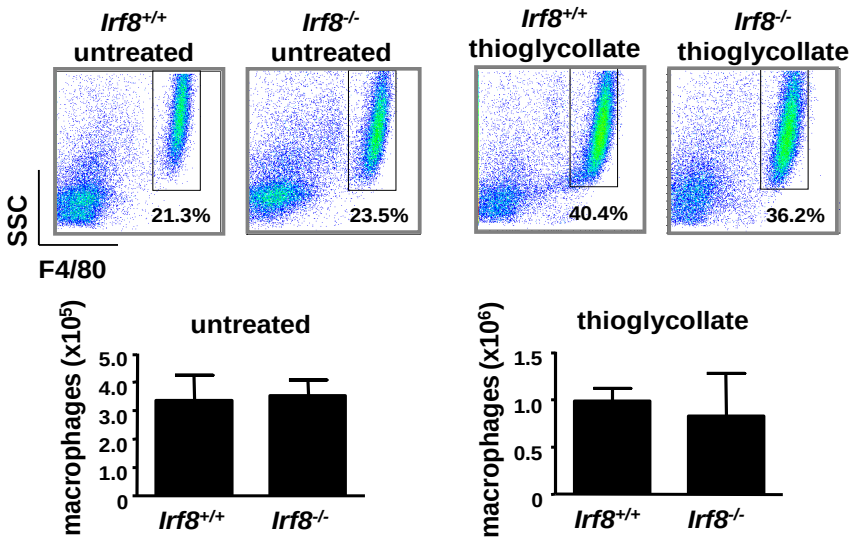

Figure 3-11. Recruitment of *Irf8*$^{-/-}$ macrophages is not altered under prolonged inflammatory conditions. Representative FACS dot plots of monocytes (gated events, inserted numbers represent percentages relative to CD45^{+} cells) in unstimulated and thioglycollate-injected *Irf8*$^{+/+}$ and *Irf8*$^{-/-}$ mice (n=5 each). Absolute macrophage counts are depicted in bar graphs. Data is expressed as mean±SD, **p*<0.05.

Moreover no differences were detectable for the apoptosis rate of *Irf8*$^{-/-}$ peritoneal macrophages compared to *Irf8*$^{+/+}$ macrophages (Data not shown). In summary, these results suggest that inflammatory monocyte recruitment under acute or chronic conditions is not impaired and apoptosis and proliferation rates are not altered in IRF8-deficient mice.

Further, we examined an IRF8-related impact on macrophage phenotype analyzing the surface expression of major histocompatibility complex class II (MHCII), co-stimulatory molecule CD40 and scavenger receptors in peritoneal macrophages from *Irf8*$^{+/+}$ or *Irf8*$^{-/-}$ mice by FACS analysis. The expression of MHCII and CD40 (Figure 3-12) but also surface class B scavenger receptor CD36 were significantly decreased in peritoneal macrophages of *Irf8*$^{-/-}$ macrophages compared to *Irf8*$^{+/+}$ controls, while the expression of class A scavenger receptors CD68 and CD204 were not affected (Figure 3-13).

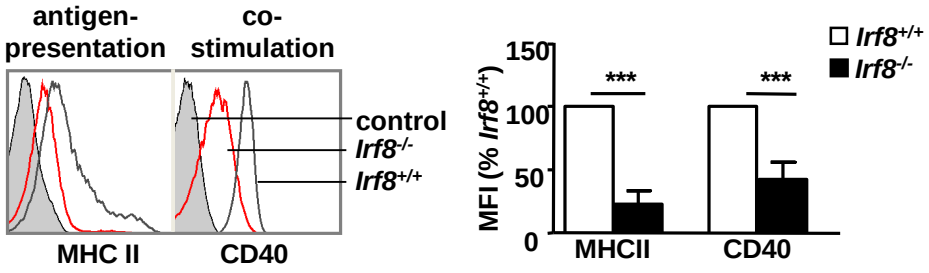

Figure 3-12. Decreased expression of MHCII and CD40 on *Irf8*$^{-/-}$ macrophages. FACS analysis and representative histograms of MHCII and co-stimulatory CD40 expression by peritoneal macrophages isolated from *Irf8*$^{+/+}$ (black line) or *Irf8*$^{-/-}$ mice (red line) (n=5 each). Filled histograms (grey) represent FMO controls. Quantification of staining is shown as MFI relative to expression by *Irf8*$^{+/+}$ macrophages. Data are expressed as mean±SD, ***p<0.001.

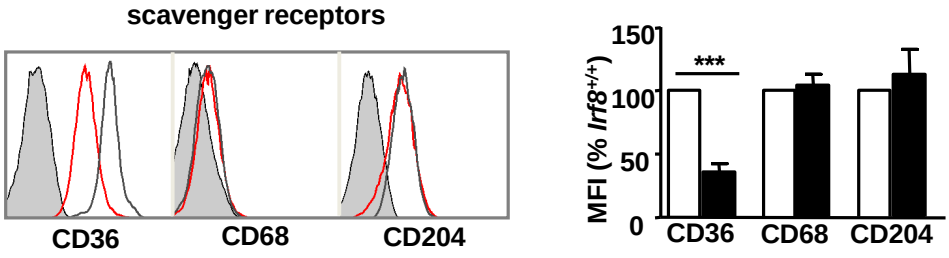

Figure 3-13. Decreased expression of CD36, but not CD68 and CD204 in *Irf8*$^{-/-}$ macrophages. FACS analysis and representative histograms of CD36, CD68 and CD204 expression by peritoneal macrophages isolated from *Irf8*$^{+/+}$ (black line) or *Irf8*$^{-/-}$ mice (red line) (n=5 each). Filled histograms (grey) represent FMO controls. Quantification of staining is given as MFI relative to expression by *Irf8*$^{+/+}$ macrophages. Data are expressed as mean±SD, ***p<0.001.

CD36 is one the most important receptors for the uptake of oxLDL and the clearance of apoptotic cells.[179,180] Therefore one may ask whether phagocytosis of oxLDL or apoptotic debris by *Irf8*$^{-/-}$ macrophages would be affected by a reduced expression of CD36. To address this question labeled oxLDL or apoptotic PMN were incubated with peritoneal macrophages isolated from *Irf8*$^{+/+}$ or *Irf8*$^{-/-}$ mice for 1 h. Flow cytometry analysis of these cells revealed a significantly decreased phagocytosis of both - oxLDL and apoptotic neutrophils when comparing *Irf8*$^{-/-}$ to *Irf8*$^{+/+}$ macrophages (Figure 3-14).

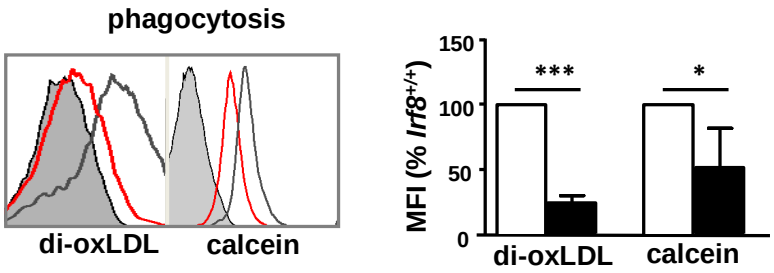

Figure 3-14. Decreased phagocytic capacity of *Irf8*$^{-/-}$ macrophages. FACS analysis and representative histograms of peritoneal macrophages isolated from *Irf8*$^{+/+}$ (black line) or *Irf8*$^{-/-}$ mice (red line) incubated with di-oxLDL and calcein-labelled apoptotic PMN for 1 h in comparison to untreated control macrophages (grey, filled histogram). Uptake efficiency is quantified by analyzing mean fluorescence intensity (MFI) and expressed relative to *Irf8*$^{+/+}$ mice (n=5 each). Data are expressed as mean±SD,*p<0.05; ***p<0.001.

In addition, phagocytosis of apoptotic cells is known to exert immunosuppressive effects by inducing the production of anti-inflammatory cytokines including IL-10 in phagocytes.[181] Thus, *Irf8*$^{-/-}$ and *Irf8*$^{+/+}$ peritoneal macrophages were incubated in the presence of apoptotic PMN for 12 h. Subsequent analysis of the cell culture supernatant by ELISA showed a strong secretion of IL-10 by *Irf8*$^{+/+}$ macrophages in response to the uptake of apoptotic PMN, but IL-10 release was substantially impaired in *Irf8*$^{-/-}$ macrophages (Figure 3-15).

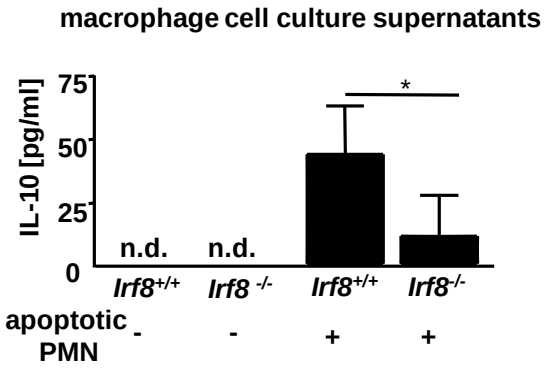

Figure 3-15. Impaired IL-10 secretion by *Irf8*$^{-/-}$ macrophages. Peritoneal macrophages from *Irf8*$^{+/+}$ or *Irf8*$^{-/-}$ mice were incubated with apoptotic PMN for 12 h and IL-10 concentrations assessed in the cell-free supernatant by ELISA (n=5 each); n.d., non detectable. Data are expressed as mean±SD,*p<0.05.

These differences may also relate to reduced IL-10 serum levelsin *Irf8*$^{-/-}$►*Apoe*$^{-/-}$ compared to *Irf8*$^{+/+}$►*Apoe*$^{-/-}$ mice (Figure 3-16; a). Moreover, lower concentrations of IFNγ and IL-6 were observed in air pouches of *Irf8*$^{-/-}$ in comparison to *Irf8*$^{+/+}$mice (Figure 3-16; b), suggesting a global insufficiency in cytokine production in *Irf8*$^{-/-}$ macrophages.

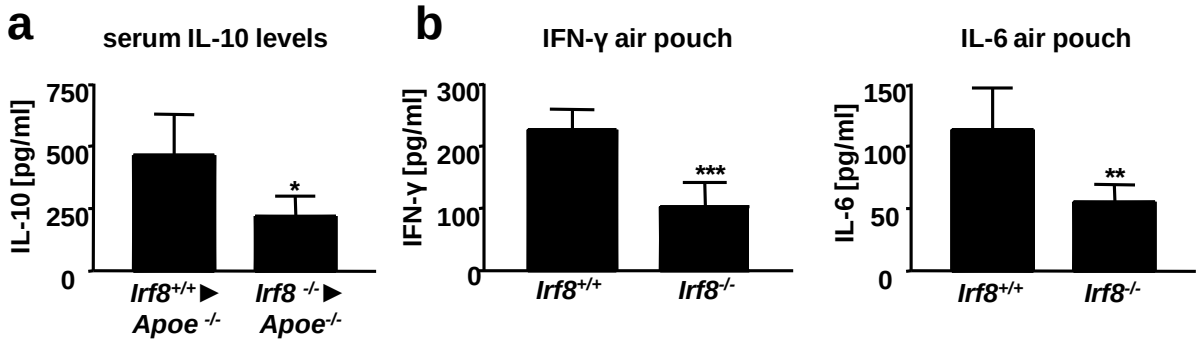

Figure 3-16. Cytokine production is impaired in *Irf8*$^{-/-}$ mice. (a) Serum IL-10 concentrations in *Irf8*$^{-/-}$►*Apoe*$^{-/-}$ and *Irf8*$^{+/+}$►*Apoe*$^{-/-}$ mice (n=7-10) after 12 weeks of HFD determined by ELISA. **(b)** IFNγ and IL-6 concentration in air pouch lavages of *Irf8*$^{+/+}$ or *Irf8*$^{-/-}$ mice 4 h after the injection of PAF (n=5 each). Data are expressed as mean±SD, **p*<0.05, ***p*<0.01. ****p*<0.001.

In summary, although apoptosis and proliferation rates are not altered in *Irf8*$^{-/-}$ macrophages, their functionality is impaired, as demonstrated by decreased expression of CD36 in line with reduced uptake of oxLDL and apoptotic PMN accompanied withlimited production of IL-10, IFNγ and IL-6.

3.2.4 THE INFLAMMATORY ACCUMULATION OF *IRF8*$^{-/-}$ PMN IS DUE TO ENHANCED EXTRAVASATION

Taking into account, that macrophages are functionally impaired *in Irf8*$^{-/-}$ mice, but lesion size is increased in *Irf8*$^{-/-}$►*Apoe*$^{-/-}$ transplanted animals, a more detailed analysis of how PMN may drive plaque progression is necessary.

The enhanced frequency of PMN in *Irf8*$^{-/-}$►*Apoe*$^{-/-}$ aortic root plaques led us to further address the recruitment of PMN. Similarly, the number of emigrated PMN in the air pouch lavage in response to PAF was significantly increased in *Irf8*$^{-/-}$ mice after 4 h (Figure 3-17). However, the ratio of PMN numbers in blood relative to air pouches was identical in either strain (0.37±0.04in *Irf8*$^{+/+}$*vs*. 0.40±0.09 in *Irf8*$^{-/-}$ mice), suggesting that PMN are recruited with similar efficiencies and that their enhanced accumulation at sites of inflammation in mice with *Irf8*$^{-/-}$ BM reflects an influx proportional to their numbers in blood.

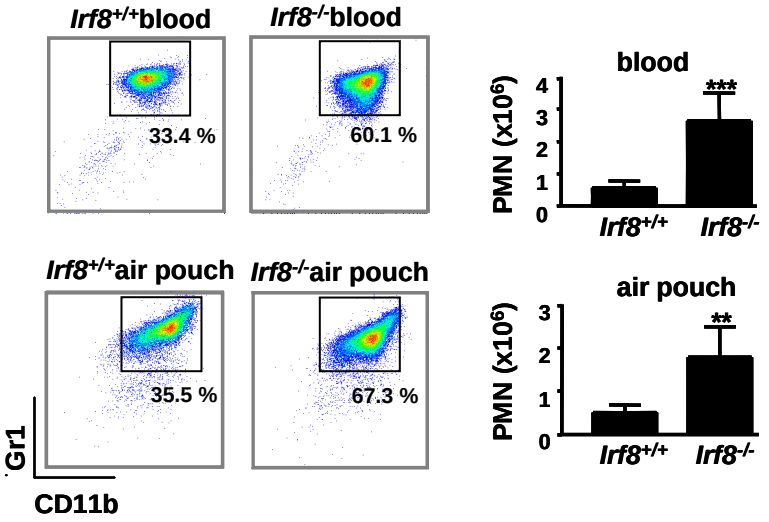

Figure 3-17. Accumulation of PMN in *Irf8*$^{-/-}$ mice is due to their enhanced extravasation. Representative FACS dot plots of PMN (gates events, inserted numbers indicate percentages relative to CD45^{+} cells) in blood and air pouch lavages 4 h after PAF stimulation in *Irf8*$^{+/+}$ and *Irf8*$^{-/-}$ mice (n= 5 each). Absolute PMN counts in blood and air pouch lavages are depicted in bar graphs representing mean±SD, ** p<0.01, *** p<0.001.

An increased frequency of apoptotic PMN in *Irf8*$^{-/-}$►*Apoe*$^{-/-}$ lesions (Figure 3-9) may indicate an enhanced susceptibility of *Irf8*$^{-/-}$PMN to undergo cell death. While fewer apoptotic blood and air pouch-derived *Irf8*$^{-/-}$ PMN could be detected early after the induction of serum starvation, no differences were detectable after 36 h with about 50% Annexin V^{+} PMN, and at later time points, as revealed by FACS analysis and when compared to *Irf8*$^{+/+}$ PMN (Figure 3-18; a). Of note, bone marrow-derived *Irf8*$^{-/-}$ PMN were less susceptible to apoptosis compared to *Irf8*$^{+/+}$controls (not shown), confirming previous findings.[175] Enhanced proliferation of extravasated cells may yet be another mechanism contributing to PMN accumulation. Cell cycle analysis of PMN from blood and air pouches of *Irf8*$^{+/+}$ and *Irf8*$^{-/-}$ mice, however, could not reveal any differences in the number of proliferating cells in the S and M phase, excluding this possibility (Figure 3-18; b). This indicates that apoptosis and proliferation of PMN in blood and at sites of inflammation are not substantially affected by the lack of IRF8. Thus, increased numbers of PMN and TUNEL^{+} PMN in atherosclerotic lesions are likely due to an overflow with extravasated PMN.

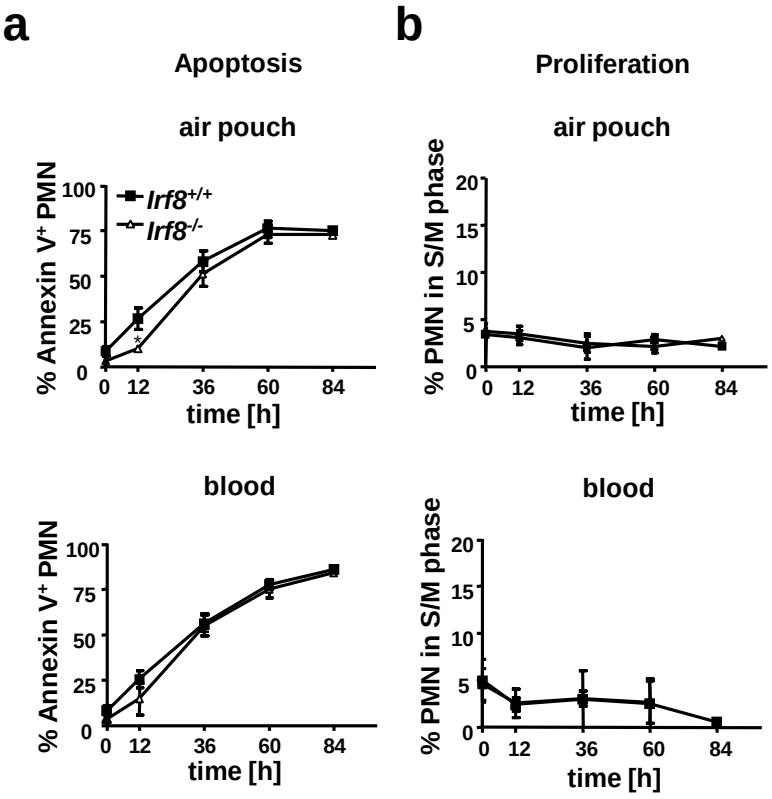

Figure 3-18. Apoptosis and proliferation rates do not differ between *Irf8*$^{-/-}$ and *Irf8*$^{+/+}$ neutrophils.
FACS analysis of the frequencies of Annexin V^{+} apoptotic **(a)** and propidium iodide (PI)$^{+}$ **(b)** proliferation cells in the S and M phase as determined by cell cycle analysis after intracellular staining in PMN sorted from blood and air pouch lavages of *Irf8*$^{+/+}$ and *Irf8*$^{-/-}$ mice (n=5 each) and after serum-starvation for indicated time periods. Data are expressed as mean±SD, **p*<0.05.

In conclusion, increased numbers of PMN within lesions are likely due to enhanced extravasation, but neutrophil numbers are not influenced by their apoptosis or proliferation rate.

3.2.5 ROS FORMATION AND GRANULE DISCHARGE ARE NOT IMPAIRED IN *IRF8*$^{-/-}$ PMN

ROS play a central role in the development of atherosclerosis and initiate and sustain key mechanisms of atheroprogression.[182] As PMN are a major source of ROS, we assessed the ROS-forming aptitude of peripheral PMN FACS-sorted from blood and BM. Both the treatment with TNF or PMA triggered an equal release of ROS over baseline in *Irf8*$^{+/+}$ compared to *Irf8*$^{-/-}$ PMN (Figure 3-19).

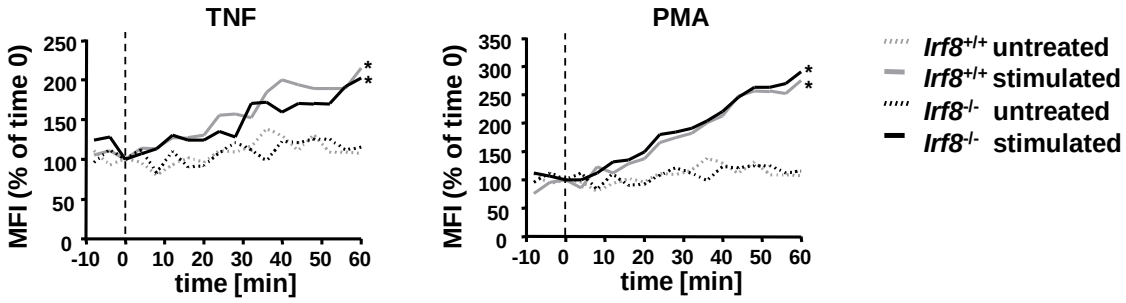

Figure 3-19. ROS formation is not impaired in *Irf8*$^{-/-}$ mice. ROS release from PMN sorted from peripheral blood of *Irf8*$^{+/+}$ and *Irf8*$^{-/-}$ mice (n=5 each) in response to TNF or PMA in comparison to untreated cells. Lines represent ROS formation over time (measured by MFI), **p*<0.05.

PMN contain preformed granules, which are rapidly released upon extravasation. This process can be assessed by the upregulation of membrane-bound receptors translocated from the granule membrane or by measurement of granule proteins in the cell-free supernatant.[29,146] Compared to circulating blood PMN, the surface expression of CD11b and CD14 derived from secretory vesicles and tertiary granules[29] were markedly upregulated on both *Irf8*$^{+/+}$ and *Irf8*$^{-/-}$ PMN after extravasation to the air pouch (Figure 3-20; a).

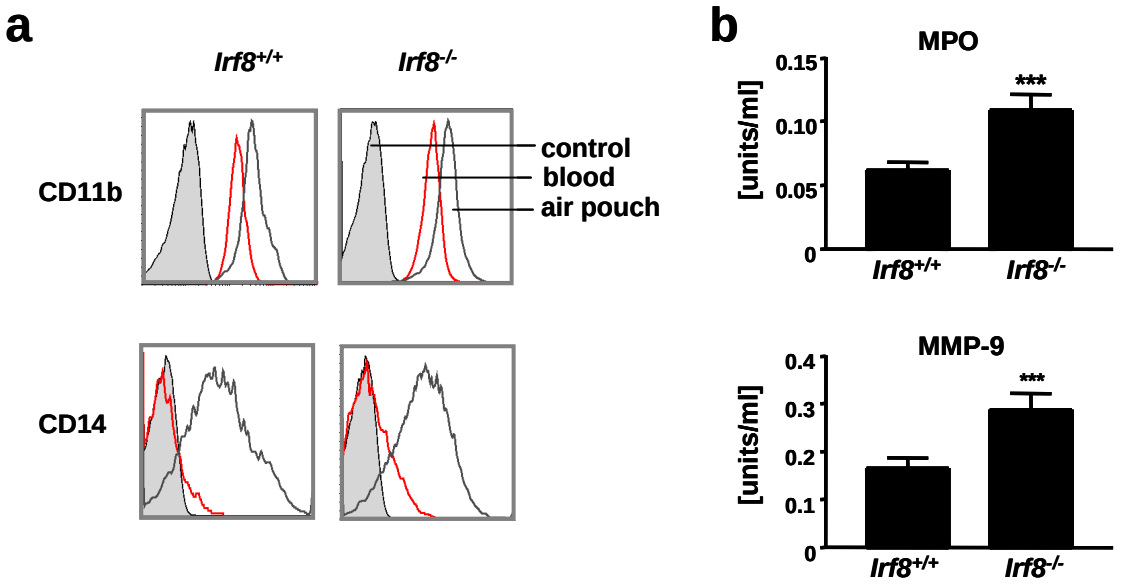

Figure 3-20. Granule protein discharge is not affected by lack of IRF8. (a) FACS analysis of the surface expression of CD11b and CD14 in PMN in blood (red line) and air pouches (black line) of *Irf8*$^{+/+}$ and *Irf8*$^{-/-}$ mice. Filled histograms (grey) represent FMO controls. One representative histogram of five independent experiments is shown. **(b)** Activity of MPO and MMP-9 in air pouch lavages collected from *Irf8*$^{+/+}$ and *Irf8*$^{-/-}$ mice (n=5 for each group) after 4 hours of PAF stimulation and PMN extravasation. Data are expressed as mean±SD, ****p*<0.001.

Concentrations of MMP-9 and MPO, which are stored in primary and secondary PMN granules[183], were found to be significantly increased in the air pouch lavage from *Irf8*$^{-/-}$ compared to *Irf8*$^{+/+}$ mice (Figure 3-20, b). However, a correlation of enzyme activity with PMN numbers in the air pouch revealed no significant differences in the amount of enzyme released per cell when comparing both strains (not shown). This indicates that *Irf8*$^{-/-}$ PMN are functionally intact and that enhanced numbers of extravasated PMN likely contribute to an overall increased ROS- and granule-releasing capacity which may contribute to inflammation and enhanced atherosclerosis observed in *Irf8*$^{-/-}$►*Apoe*$^{-/-}$mice.

3.2.6 PMN-DEPLETION IN *IRF8*$^{-/-}$►*LDLR*$^{-/-}$MICE PREVENTS AGGRAVATED ATHEROSCLEROTIC LESION FORMATION

To scrutinizethe contribution of PMN to aggravated lesion formation in mice reconstituted with *Irf8*$^{-/-}$ bone marrow, a PMN-depleting antibody was employed. Preliminary evaluation of the antibody depletion efficiency revealed an almost complete clearing of neutrophils from blood 4 h after injection of 100 µg antibody *i.p*. in *Irf8*$^{+/+}$and *Irf8*$^{-/-}$ mice (Figure 3-21).

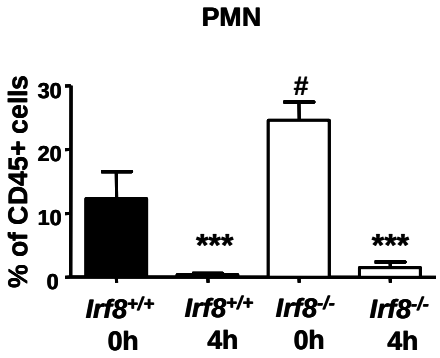

Figure 3-21. Antibody depletion efficiency. FACS analysis of the relative frequencies of PMN before (0h) and after (4h) treatment with PMN depletion antibody. Data are expressed as mean±SD, ***p<0.001 comparing 4h to 0h, # p<0.05 comparing 0h to 0h.

Recapitulating results obtained in transplanted *Apoe*$^{-/-}$ mice, *Irf8*$^{-/-}$►LDL-receptor deficient (*Ldlr*$^{-/-}$) mice displayed an expansion of leukocytes and a significant increase of neutrophils in blood and bone marrow (Figure 3-22).

Furthermore early atherosclerotic lesionsin aortas and aortic rootsof *Irf8*$^{-/-}$►*Ldlr*$^{-/-}$ mice after 5 weeks of HFD also revealed enhanced plaque formation compared to *Irf8*$^{+/+}$►*Ldlr*$^{-/-}$ mice (Figure 3-23; a,b). Importantly, depletion of PMN with 100 µg depletion antibody every other day over this time period prevented the exacerbation in lesion formation in *Irf8*$^{-/-}$►*Ldlr*$^{-/-}$ mice (Figure 3-23; a,b).

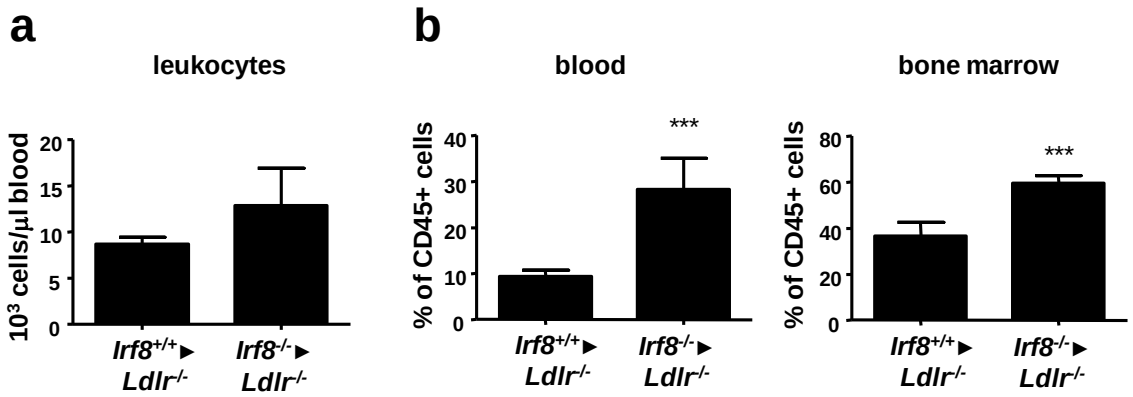

Figure 3-22. Absolute leukocyte numbers and relative PMN frequencies in *Ldlr*$^{-/-}$ BM recipients. **(a)** Total leukocyte counts in BM-recipients and **(b)** relative frequencies of PMN in blood and bone marrow of *Irf8*$^{-/-}$►*Ldlr*$^{-/-}$ and controls (n=5-7). Data are expressed as mean±SD, ****p*<0.001.

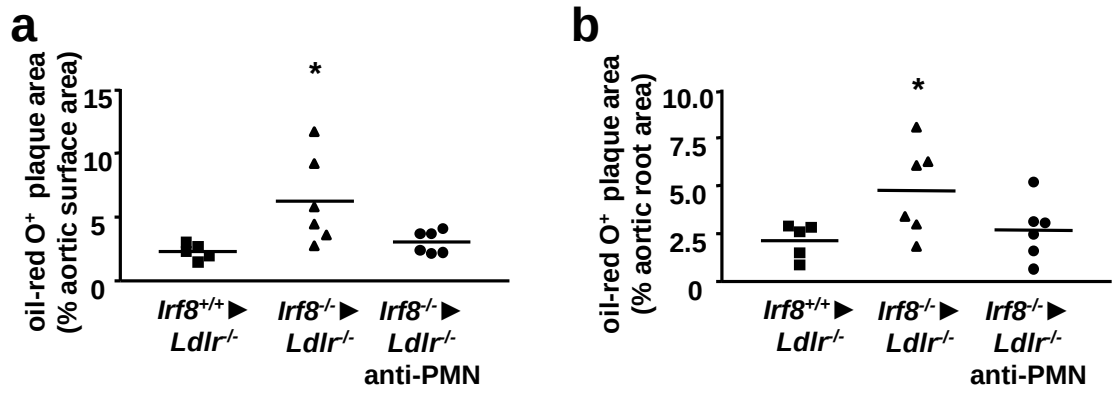

Figure 3-23. PMN depletion in *Irf8*$^{-/-}$►*Ldlr*$^{-/-}$ mice prevents exacerbated atherosclerotic lesion formation. Quantification of oil-red-O^{+} lipid depositions in the thoracoabdominal aorta **(a)** and aortic roots **(b)** of *Irf8*$^{+/+}$►*Ldlr*$^{-/-}$ and *Irf8*$^{-/-}$►*Ldlr*$^{-/-}$ mice and in*Irf8*$^{-/-}$►*Ldlr*$^{-/-}$ mice treated with anti-PMN Ab after 5 weeks of high fat diet (n=5-6 each). Data are expressed as mean±SD, **p*<0.05 compared to *Irf8*$^{+/+}$►*Ldlr*$^{-/-}$ mice.

Further analysis of the plaque composition in these bone marrow recipients revealed, that macrophage numbers in atherosclerotic lesions were not affected in either group. Instead,the enhanced accumulating of Ly6G^{+}PMN and TUNEL^{+} cells in *Irf8*$^{-/-}$►*Ldlr*$^{-/-}$ mice was preventedby the treatment with the PMN-depleting antibody (Figure 3-24). No changes in serum lipid levels were observed between the different treatments (Table 3-1), while IL-10 serum levels were again significantly diminished in *Irf8*$^{-/-}$►*Ldlr*$^{-/-}$ animals compared to *Irf8*$^{+/+}$►*Ldlr*$^{-/-}$ mice. *Irf8*$^{-/-}$►*Ldlr*$^{-/-}$ mice treated with a PMN depletion antibody showed an upward trend in IL-10 serum levels (Figure 3-25).

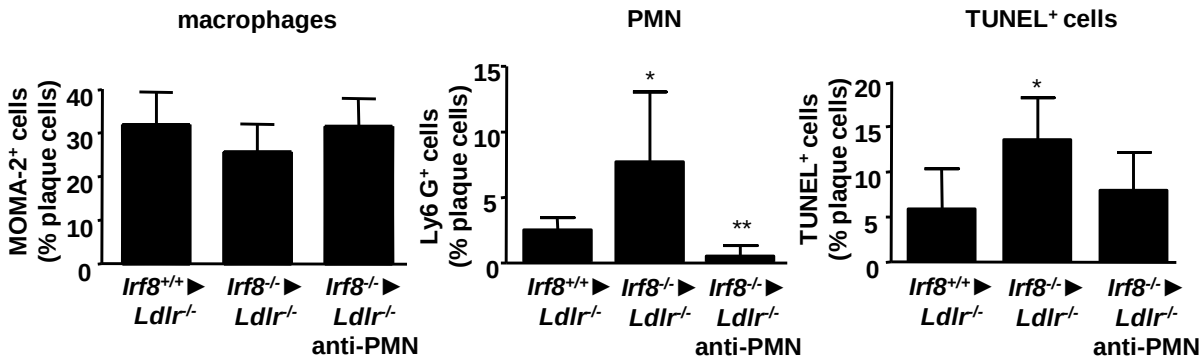

Figure 3-24. PMN depletion decreasesPMN and TUNEL$^+$ cells in*Irf8*$^{-/-}$►*Ldlr*$^{-/-}$ lesions. Quantification of macrophages, PMN and TUNEL$^+$ apoptotic cells in aortic root plaques. Data are expressed as mean±SD, **p*<0.05 compared to *Irf8*$^{+/+}$►*Ldlr*$^{-/-}$ mice, and ***p*<0.01 compared to both *Irf8*$^{+/+}$► *Ldlr*$^{-/-}$ and *Irf8*$^{-/-}$► *Ldlr*$^{-/-}$ mice.

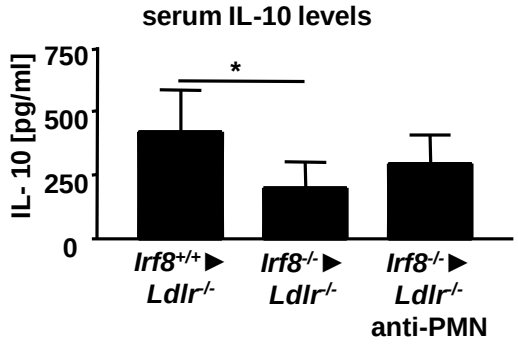

Figure 3-25. Cytokine production is impaired in *Irf8*$^{-/-}$ *Ldlr*$^{-/-}$mice. Serum IL-10 concentrations in *Irf8*$^{+/+}$► *Ldlr*$^{-/-}$ and*Irf8*$^{-/-}$► *Ldlr*$^{-/-}$mice (n=5-6) after 12 weeks of HFD determined by ELISA. Data are expressed as mean±SD, **p*<0.05.

Taken together, these data establish that the expansion of PMN in blood and at sites of inflammation causally determines the enhanced development of atherosclerosis in mice with *Irf8*$^{-/-}$ bone marrow.

3.3 ROLE OF PLASMACYTOID DENDRITIC CELLS IN THE DEVELOPMENT OF ATHEROSCLEROSIS

PDCs are a subtype of DCs, which are highly specialized for recognition of viral pathogens followed by the release of great amounts of type I interferons to eliminate the intruder and induce a general immune response. However, although TLR7 and TL9 are expressed intracellularly to prevent recognition of self antigens (nucleic acids), several autoimmune diseases are known in which pDCs and their release of type I interferons trigger disease progression (ref. 1.2.2.2).[97] So far, the role of pDCs in atherosclerosis has only been marginally addressed. Although Niessner *et al*.[154,155] showed that pDCs can be found in the shoulder region of human plaques, it is not clear if pDCs have a significant impact on the development and progression of atherosclerosis and how they are activated in this context. Therefore, a murine mouse model of atherosclerosis (*Apoe*$^{-/-}$) was used to study the role of pDCs in atherosclerosis employing various complementary approaches.

3.3.1 PDCS ARE PRESENT IN ATHEROSCLEROTIC LESIONS OF *APOE*$^{-/-}$ MICE

Murine pDCs are described as B220^{+}, CD11c^{low}, CD11b^{-}, PDCA1^{+} and SiglecH (440c^{+}) of which the last two markers are supposed to be specific for this DC-subpopulation.[86,87] PDCs are very low in numbers and discrimination of pDCs varies between published studies, in this thesis they are identified by PDCA1^{+} and SiglecH (440c^{+}) as depicted in Figure 3-26 for blood, bone marrow, lymph node and spleen in flow cytometry analysis.

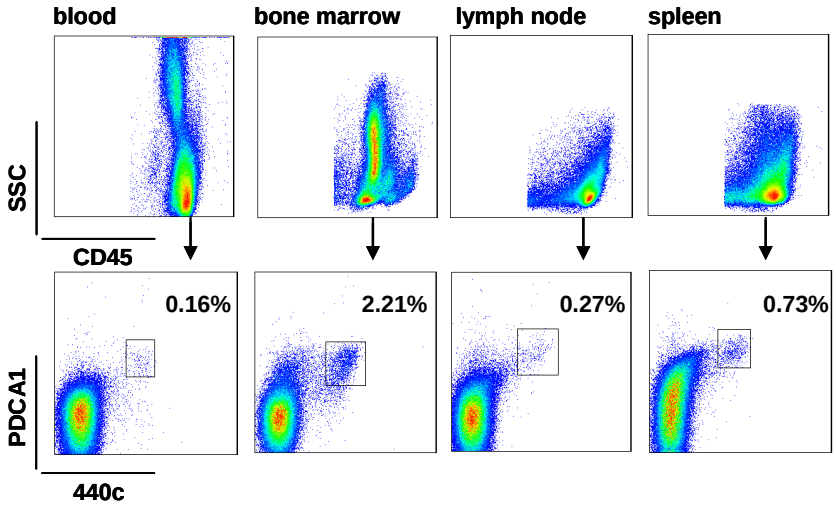

Figure 3-26. Gating strategy and frequencies of pDCs in various organs. PDCs are identified by CD45^{+} PDCA1^{+} 440c^{+}; representative dot plots are shown (gated events, inserted numbers indicate percentages relative to CD45^{+} cells).

In addition, numbers indicated in the representative dot plots depict pDC frequencies in *Apoe*$^{-/-}$ mice relative to all leukocytes in blood, bone marrow, lymph node and spleen, demonstrating that bone marrow cells are the richest source of pDCs (Figure 3-26).

To address the question if pDCs are present in murine atherosclerotic lesions immunofluorescent stainings of aortic roots and spleen (positive control) of 12 week old *Apoe*$^{-/-}$ mice fed a HFD over 4 weeks were performed. Representative images show pDCs identified by SiglecH (440c^{+}) staining in spleen and aortic root (Figure 3-27).

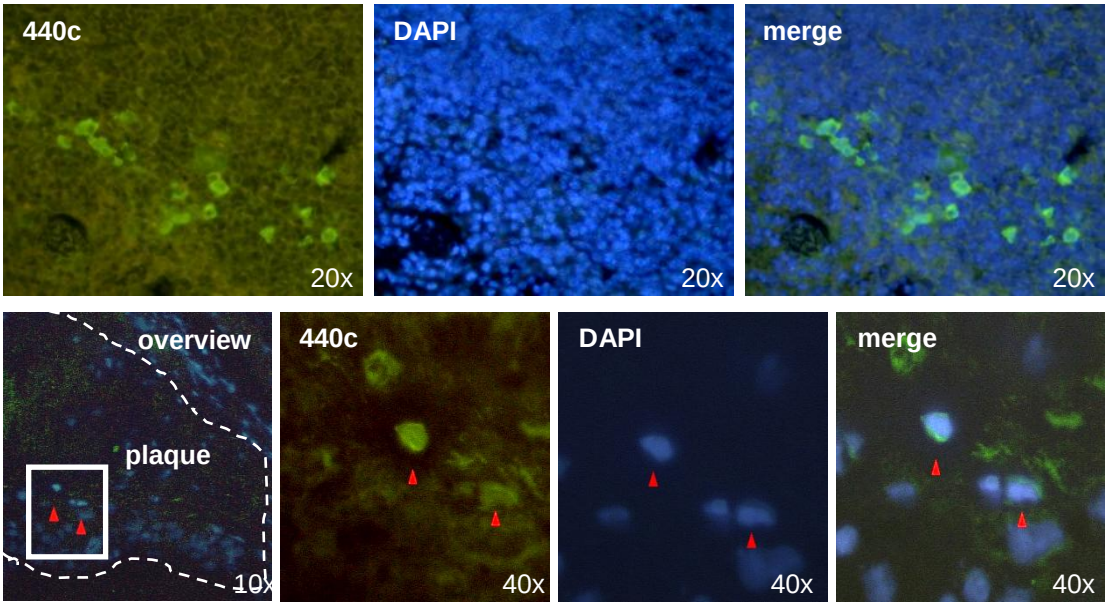

Figure 3-27. Identification of pDCs in aortic roots of *Apoe*$^{-/-}$ mice. Representative immunofluorescent images of 440c^{+} pDCs in spleen (upper panel) and aortic root (lower panel) in an *Apoe*$^{-/-}$ mouse are depicted. Cell nuclei were stained by DAPI.

To confirm the identification of pDCs in atherosclerotic lesions of *Apoe*$^{-/-}$ mice on HFD and in *Apoe*$^{-/-}$ mice fed a normal chow, enzymatically digested aortas of *Apoe*$^{+/+}$ and *Apoe*$^{-/-}$ mice were stained for 440c^{+} and PDCA1 and analysed by flow cytometry. As depicted in Figure 3-28 (a) only few pDCs could be detected in the aorta of *Apoe*$^{+/+}$ mice, but their frequencies markedly increased in *Apoe*$^{-/-}$ mice fed a high fat diet for 3 month. Furthermore, IFNα serum levels in *Apoe*$^{-/-}$ mice on high fat diet were significantly elevated, together with increased mRNA transcripts of *SiglecH* and *Ifn*α in aortic tissue compared to *Apoe*$^{-/-}$ on normal chow (Figure 3-28; b,c). These data substantiate the presence of pDCs in murine atherosclerotic lesions.

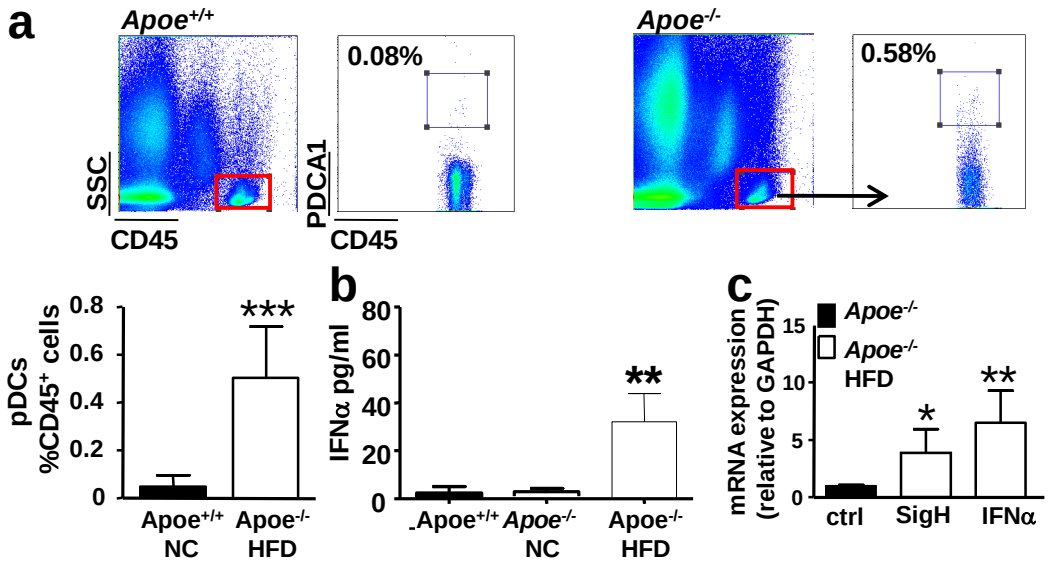

Figure 3-28. Gating strategy and pDC frequencies in mouse aortas. (a) Representative Dot Plots of aorta lysates are shown, pDCs are identified by low SSC, $CD45^+$ and $PDCA1^+$. **(b)** Quantification of pDC numbers by flow cytometry analysis of aortas from *Apoe*$^{+/+}$, *Apoe*$^{-/-}$ 6 month old and *Apoe*$^{-/-}$ fed a HFD for 3 month (n= 5 per group). Data are expressed as mean±SD, ***p<0.001.

3.3.2 MANIPULATION OF PDC COUNTS AND ACTIVITY CORRELATES WITH ATHEROSCLEROTIC LESION FORMATION

3.3.2.1 ANALYSIS AFTER 4 WEEKS HIGH FAT DIET

To investigate a general role of pDCs in atherosclerosis, *Apoe*$^{-/-}$ mice fed a HFD for 4 weeks received *i.v.* injections of a pDC depletion antibody (PDCA1, ref. to 2.9.1.1) at the beginning of HFD feeding and again after 7 days. Atherosclerotic lesion formation in the aortic root and aorta was substantially reduced in *Apoe*$^{-/-}$ mice treated with the PDCA1 antibody compared to IgG injected controls (Figure 3-29; a, b). Furthermore pDC depletion was associated with a decrease in the relative content of lesional macrophages (Figure 3-29; c).

As pointed out before, pDCs are known to specifically secrete large amounts of type I interferons upon stimulation with CpG motives via binding murine TLR9.[169] To monitor a CpG responst *in vivo* we injected 25 µg of CpG complexed to DOTAP *i.v.* in *Apoe*$^{+/+}$ mice and examined the IFNα and Chemerin serum levels as well as pDC numbers in blood, bone marrow, spleen and lymph node after 4h and 12 h. These data confirmed a significant secretion of IFNα after 4h, which was still detectable after 12h (Figure 3-30; a) and a significant increase of chemerin serum levels 12 h after CpG injections (Figure 3-30; b). PDC numbers in blood, bone marrow, lymph node and spleen were significantly increased after 4 h, but were lowered to control level again 12 h after treatment, indicating that pDCs numbers are

tightly regulated as soon as the pathogen level ("CpGs") decreases again. Furthermore CpG stimulation eventually induces pDC maturation resulting in pDC emigration to sites of inflammation. Of note, IFNα levels decreased again after 48 h (data not shown), an observation also reported by Swiecki *et al.*[184] in murine cytomegalovirus infected mice. From these results we concluded that 3 doses of CpG motives per week would be sufficient to stimulate pDCs for longer time periods *in vivo*.

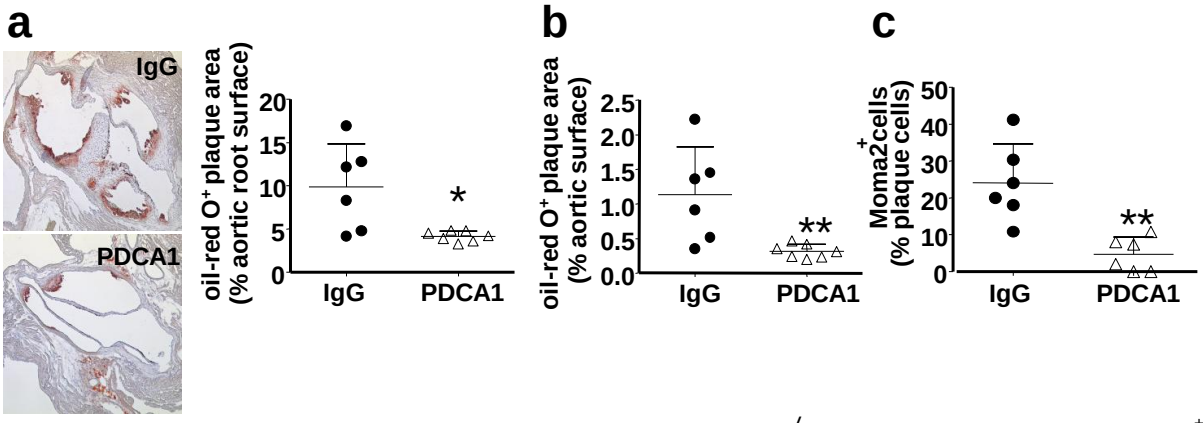

Figure 3-29. PDC depletion decreased plaque formation in *Apoe*$^{-/-}$ mice. Quantification of oil-red-O^{+} lipid depositions in **(a)** aortic roots and **(b)** thoracoabdominal aortas of *Apoe*$^{-/-}$ mice treated with PDCA1 Ab or Isotype control Ab. **(c)** Quantification of macrophage contents in aortic roots. Mice were fed a HFD over 4 weeks (Isotyp n=6; PDCA1 n=6-7).Representative images of aortic roots are displayed. Data are expressed as mean±SD; **p*<0.05;** *p*<0.01.

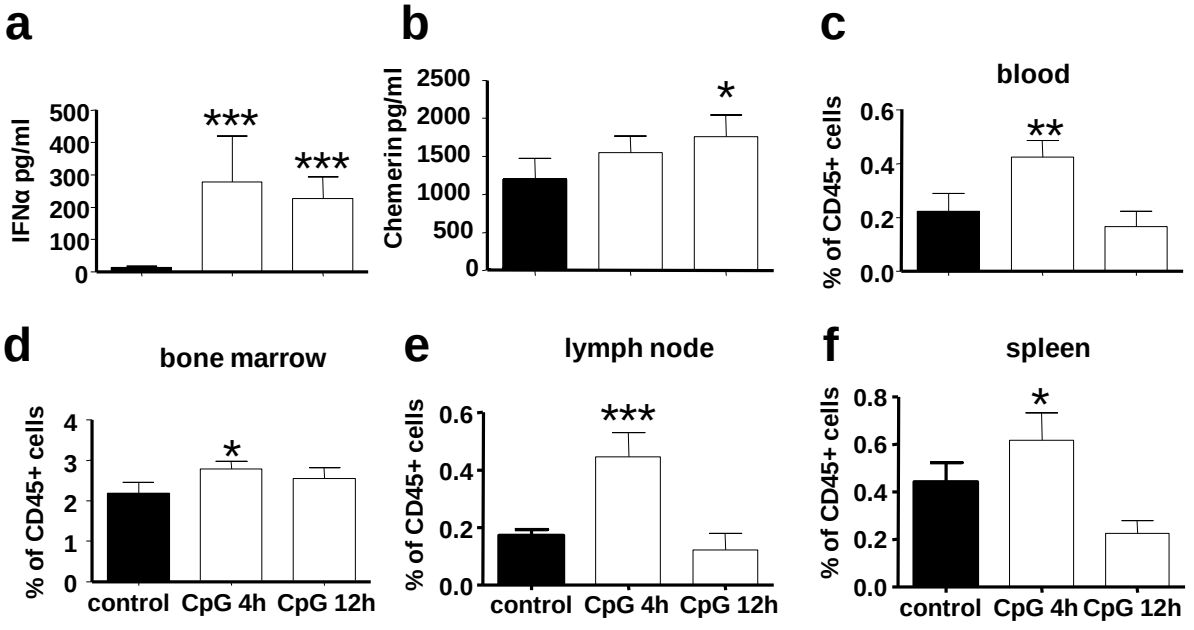

Figure 3-30. Monitoring of an immune response after CpG treatment over time. (a, b) IFNα and chemerin concentrations (pg/ml) in sera of *Apoe*$^{+/+}$control mice (untreated) or 4 h and 12 h after CpG treatment. **(c-f)** Quantification of pDC numbers by flow cytometry analysis of blood, bone marrow, lymph node and spleen in *Apoe*$^{+/+}$ control mice (untreated) or 4 h and 12 h after CpG treatment (n=5 per group). Data are expressed as mean±SD; **p*<0.05;** *p*<0.01, ****p*<0.005.

Given the presence of pDCs within atherosclerotic lesions, we further wanted to unravel whether a specific stimulation of pDCs would affect plaque formation. Quantification of lipid depositions in the aorta and aortic roots revealed a significant exacerbation in lesion formation in CpG-injected *Apoe*$^{-/-}$ mice compared to control treated mice (Figure 3-31; a,b), which was associated with a significant increase in the content of macrophages in the aortic root (Figure 3-31; c). Notably, the CpG-induced increase in plaque formation together with the augmented numbers of macrophages were abrogated in *Apoe*$^{-/-}$ mice depleted of pDCs by PDCA1 antibody injections (Figure 3-31; a-c). These data indicate that stimulated pDCs accounted for the effects of the CpG treatment exclusively. To confirm the assumption that IFNα secretion by activated pDCs promotes atherosclerosis, 6 week old *Apoe*$^{-/-}$mice were fed a HFD over 4 weeks accompanied by a repetitive *i.p.* injection of IFNα. Plaque analysis of these animals revealed an increase in lesion formation and macrophage content in *Apoe*$^{-/-}$ mice treated with IFNα (Figure 3-31; c,d), suggesting that IFNα may be the main trigger of pDC-induced plaque formation.

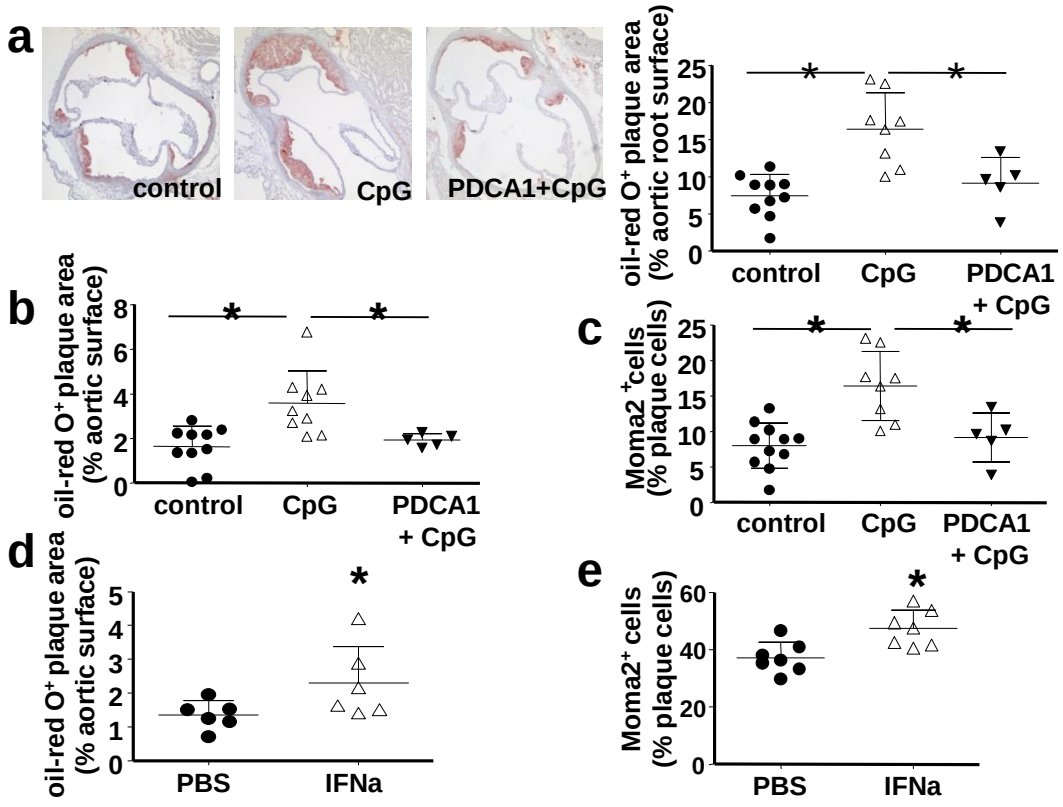

Figure 3-31. Increased plaque formation in *Apoe*$^{-/-}$ mice treated with CpGs or IFNα. Quantification of oil-red-O^{+} lipid depositions in **(a)** aortic roots and **(b)** thoracoabdominal aortas of *Apoe*$^{-/-}$ mice treated with DOTAP (control), CpG and CpG+PDCA1. **(c, e)** Analysis of macrophage contents in aortic roots. **(d)** Quantification of oil-red-O^{+} lipid depositions in thoracoabdominal aortas of *Apoe*$^{-/-}$ mice treated with PBS or IFNα. All mice were fed a HFD over 4 weeks (control n=9-11, CpG n=7-9, PDCA1+CpG n=5, PBS n= 6-7 and IFNα n=6-7). Representative images of aortic roots are given. Data is expressed as mean±SD, **p*<0.05.

3.3.2.2 ANALYSIS AFTER 8 WEEKS HIGH FAT DIET

To analyse the stage specific contribution of pDCs in atherosclerotic lesion formation, we depleted pDCs in *Apoe*$^{-/-}$ mice four weeks after initiation of HFD. In these experiments, pDC depletion did not affect the lesion size in aortic roots and aortas after an additional 4 weeks of HFD compared to control-treated mice (Figure 3-32 a, b). Further analysis of the plaque composition in these mice revealed, that macrophage numbers in atherosclerotic lesions did not differ in both groups (Figure 3-32; c). Surprisingly and in contrast to all other experiments relative and absolute T cell numbers in blood were significantly augmented in these mice (Figure 3-32; d), accompanied by a dramatic increase of IL-4 serum levels (Figure 3-32; e). These data may indicate that pDC depletion under inflammatory conditions causes side effects most likely masking results observed during early lesion development.

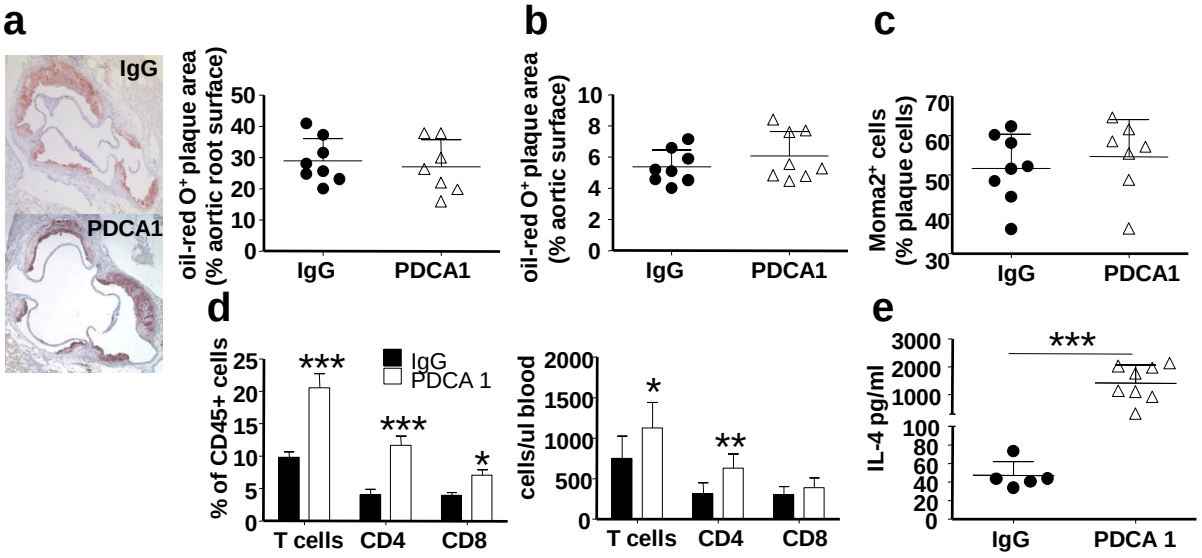

Figure 3-32. No change in plaque development in pDC-depleted mice with prolonged high fat diet. Quantification of oil-red-O^{+} lipid depositions in **(a)** aortic roots and **(b)** thoracoabdominal aortas of *Apoe*$^{-/-}$ mice treated with Isotype IgG or PDCA1 antibody.**(c)** Analysis of macrophage contents in aortic roots.**(d)** Quantification of T cell numbers by flow cytometry analysis for relative and absolute frequencies. **(e)** IL-4 serum titers in IgG and PDCA1 treated mice. All mice were fed a high fat diet over 8 weeks. Representative images of aortic roots are given. Data are expressed as mean±SD,**p*<0.05, ***p*<0.01, ***p*<0.001.

In contrast, prolonged injection of CpGs over 8 weeks, or treatment of mice already bearing early lesions (4 weeks of HFD prior to stimulation) with CpGs for another 4 weeks led to enhanced atherosclerotic plaque size in aortic roots and aortas of *Apoe*$^{-/-}$ mice. The content of lesional macrophages did not further increase (Figure 3-33; a-c). In conclusion these data demonstrate an important role of activated pDCs in the progression of lesion formation, while depletion of pDCs only affects early atherosclersosis.

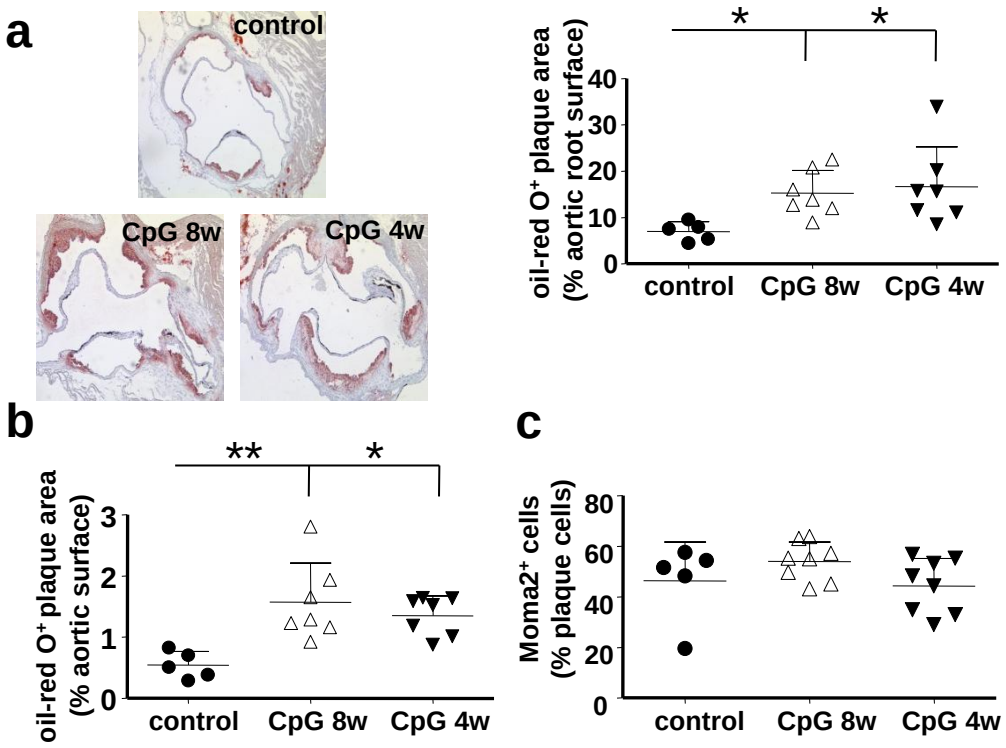

Figure 3-33. Enhanced plaque formation in CpG treated mice with prolonged high fat diet. Quantification of oil-red-O^+ lipid depositions in **(a)** aortic roots and **(b)** thoracoabdominal aortas of *Apoe*$^{-/-}$ mice treated with DOTAP (control) and CpGs for a period of 8 or 4 weeks. **(c)** The relative content of MOMA-2^+ macrophages per total plaque cells was analyzed by quantitative immunofluorescence. All mice were fed a HFD over 8 weeks. Representative images of aortic roots are given. Data are expressed as mean±SD, **p*<0.05, ***p*<0.01.

3.3.3 ALTERATIONS OF PDC FUNCTIONS IN THE PRESENCE OF OXLDL TREATMENT

Modified lipoproteins, *e.g.* oxLDL, accumulate in the arterial wall during atherosclerosis. Thus, following the confirmation of pDCs influencing atherosclerotic lesion development, it was addressed whether or not oxLDL could be taken up by *ex vivo* isolated pDCs and would alter their maturation and function. In addition pDCs were treated with GpG motives as a positive control (ref. to 2.5). In line with conventional DCs[185], pDCs were capable of taking up Di-labeled oxLDL (Figure 3-34; a). However, upregulation of costimulatory molecules was only observed in CpG treated pDCs, but not in the presence of oxLDL (Figure 3-34; b). On the other hand scavenger receptor CD36, implicated in the phagocytosis of oxLDL[179,186], is constitutively expressed by pDCs and even further upregulated by stimulation with oxLDL or CpG motives. The protein expression of the scavenger receptors CD68 and SR-A was not altered in the prescence of oxLDL or CpGs (Figure 3-34; c).

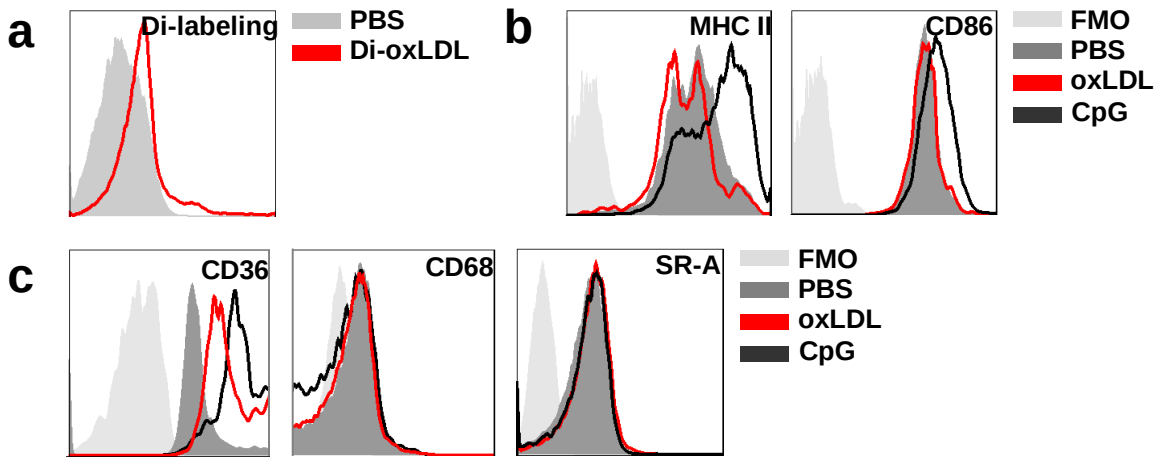

Figure 3-34. Di-oxLDL uptake and MHCII, CD86 and scavenger receptor expression of oxLDL treated pDCs. (a) The uptake of Di-labeled oxLDL after exposure to oxLDL or PBS over 12 h was assessed in sorted pDCs by FACS analysis. **(b, c)** Expression of MHCII and CD86 and the scavenger receptors CD36, CD68 and SR-A in sorted pDCs. Cells were stimulated with/without oxLDL and CpG overnight and analysed by FACS. Representative histograms with FMO controls of 3 independent experiments are shown.

Although pDCs are not as efficient in antigen presentation as cDCs (ref. to 1.2.2), they are fully capable of inducing an antigen specific T cell response.[187] Therefore it was investigated if prestimulation of *ex vivo* isolated pDCs with oxLDL would alter their T cell proliferation capacity *in* vivo. As shown in Figure 3-35 (a,b) oxLDL pretreatment of pDCs for 12 h prior to OVA-2 feeding and subsequent foot pad injection of the cultured pDCs potentiated the antigen-specific T cell response *in vivo* to a similar extend as pretreatment with CpG motives for 12 h did. However, no additive effects were observed in co-cultures simultaneously treated with CpG and oxLDL (Figure 3-35; a, b). To further elucidate whether the enhanced T cell proliferation in the presence of oxLDL could be due to an altered cytokine profile, supernatants of treated pDCs were examined for various proinflammtory mediators by bead array analysis. IFNα was measured by ELISA. While IFNα was not detectable in supernatants of untreated T cells, and an only marginal expression was observed in unpulsed pDCs or in OVA-2 pulsed pDCs interacting with OT-II T cells, an increase in the secretion of IFNα was detectable in pDC-T cell co-cultures upon stimulation with CpGs. OxLDL *per se* did not result in an increase in the secretion of IFNα by pDCs (Figure 3-35; c) or induce IFNα mRNA expression (data not shown). The concentrations of all other cytokines measured (*e.g.* IL-6, TNFα) did not significantly vary among the different treatments (data not shown). Thus, oxLDL does not induce the release of proinflammatory cytokines; therefore engagement of antigen-specific T cell interactions in the prescence of oxLDL must be explained differently.

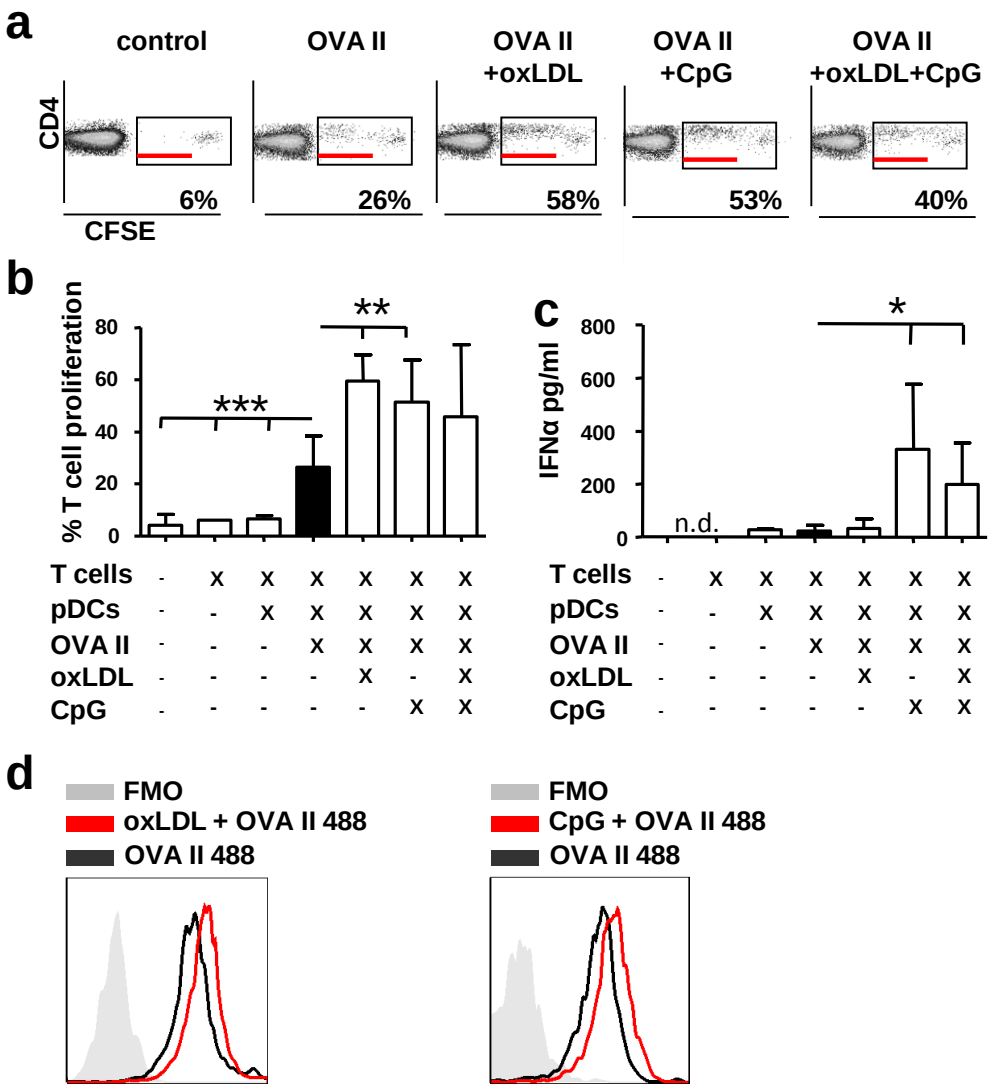

Figure 3-35. oxLDL can be taken up by pDCs and enhances pDC-driven T cell responses. (a) Sorted pDCs (unpulsed control), OVA-2-pulsed pDCs pretreated with or without oxLDL or CpG over 12 h were transferred into wt mice transfused with $CFSE^{+}$OT-II T cells. After 3 days, T-cell proliferation was quantified by CSFE dilution and FACS analysis; representative dot plots and percentage of $CFSE^{+}CD4^{+}$ T cells (red markers) within gates are shown. **(b)** Quantificatin of T cell proliferation shown in **a** (n=4 independent experiments)**.** Data is expressed as mean±SD, $^{**}p<0.01$, $^{***}p<0.001$. **(c)** IFNα secretion in supernatants of the T cell proliferation assay after 12 h *in vitro* culture (n=4 independent experiments). Data is expressed as mean±SD, $^{*}p<0.05$. (**d**) The uptake of 488-labeled OVA-2 peptid pretreated with PBS, oxLDL (left panel) or CpG (right panel) over 12 h was assessed in sorted pDCs by FACS analysis; representative histograms with FMO controls of 3 independent experiments are shown.

Hence, it may be possible that oxLDL promotes T cell proliferation by enhancing the phagocytic uptake of antigens, *e.g.* by inducing the expression of scavenger receptors as already shown for CD36 (Figure 3-34;c). Following this assumption, fluorescently labeled OVA-2 was added to *ex vivo* isolated pDCs either pretreated with oxLDL or CpGs for 12 h or left unstimulated. Notably, as depicted in Figure 3-35 (d), the uptake of OVA-2 by *ex vivo*

isolated pDCs was enhanced after pretreatment with oxLDL comparable to the augmented antigen uptake after CpG stimulation. In summary, enhanced phagocytotic capacity upon exposure to oxLDL may strengthen pDC-driven immune responses in atherosclerosis.

3.3.4 ACTIVATION OF PDCS BY AUTOIMMUNE MECHANISMS

Notably, pDCs are well known for their involvement in the pathogenesis of several autoimmune diseases (ref. to 1.2.2.2), leading to the description of two main mechanisms, which cause breakdown of immune tolerance resulting in pDC activation: Self-nucleic acids, which form complexes with the antimicrobial peptide LL37/Cramp, and DNA-specific IgG autoantibodies produced by autoreactive B cells, which bind self-DNA–Cramp complexes.

As depicted in Figure 3-36 (a) treatment of *ex vivo* sorted pDCs with dying neutrophils, CpG or Cramp complexed with DNA, but not Cramp or DNA alone, induced IFNα production by pDCs. In line with findings by Ganguly *et al.*[171], MHCII (Figure 3-36, b) and CD86 (Data not shown) expression were only altered after CpG treatment, but not after stimulation with Cramp-DNA complexes or dead PMN. The expression of *Cramp* mRNA expression was increased in aortic tissue of diet-fed *Apoe*$^{-/-}$ mice compared with *Apoe*$^{-/-}$ controls on normal chow (Figure 3-36, c). In addition, immunofluorescent stainings with an anti-Cramp antibody displayed Cramp in close vicinity of segment-nucleated neutrophils (white arrow heads) within atherosclerotic lesions (Figure 3-36, d). These findings correlate with a study by Drechsler *et al.*[145], who showed neutrophil accumulation during early lesion development. Furthermore, bone marrow transplantation of *Cramp*$^{-/-}$ BM in *Ldlr*$^{-/-}$ recipient mice and subsequent quantification of lipid depositions in *en face* preparations of aortas and aortic roots after 4 weeks of HFD revealed a significant decrease in lesion formation in *Cramp*$^{-/-}$►*Ldlr*$^{-/-}$ aortas compared to aortas of *Cramp*$^{+/+}$►*Ldlr*$^{-/-}$ mice (Figure 3-36,e). In contrast, *Apoe*$^{-/-}$ mice, receiving repetitive *i. p.* injections of Cramp during a HFD over 4 weeks, displayed a significant increase of plaque formation in aortic roots (Figure 3-36, f). In summary, lesional pDCs may encounter Cramp-complexed self-DNA, the former released by activated neutrophils, while dying neutrophils may be the main source of self-DNA. As a consequence breakdown of immune tolerance to self-DNA resulting in pDC activation leads to lesion progression.

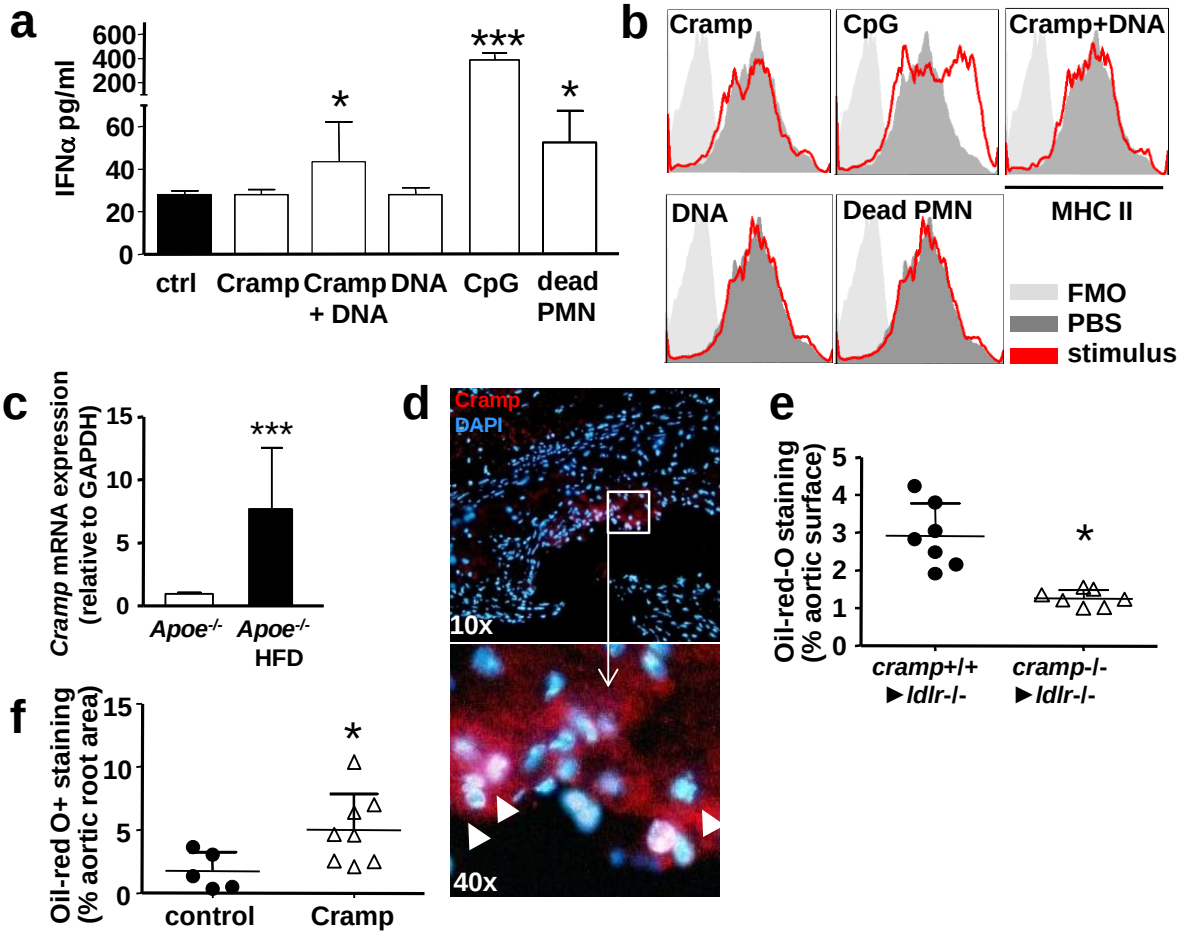

Figure 3-36. Cramp-DNA complexes promote lesion formation. **(a)** Concentration of IFNα in poststimulatory supernatants of FACS-sorted pDCs following stimulation for 12 h as indicated. Data are expressed as mean±SD; displayed are a combination of 3-5 experiment, each experiment was performed in duplicates. **(b)** Expression of MHCII in FACS-sorted pDCs stimulated for 12 h with indicated stimuli and assessed by FACS analysis; representative histograms with FMO controls of 3 independent experiments are shown. **(c)** *Cramp* mRNA expression in aortas of *Apoe*$^{-/-}$ mice (n=9) receiving HFD relative to expression in healthy 6 week old *Apoe*$^{-/-}$ mice (n=5). **(d)** Cramp staining (red) detected by immunofluorescence in the aortic root of *Apoe*$^{-/-}$ mice fed HFD for 12 weeks; cell nuclei are counter-stained with DAPI (blue); arrow heads indicate segment-nucleated neutrophils. **(e, f)** Lipid depositions were quantified in the aorta of *Ldlr*$^{-/-}$ mice reconstituted with *Cramp*$^{+/+}$ or *Cramp*$^{-/-}$ bone marrow or in roots of Cramp-treated *Apoe*$^{-/-}$ mice after staining with oil-red O. All mice were fed HFD for 4 weeks. (*Cramp*$^{+/+}$►*Ldlr*$^{-/-}$, *Cramp*$^{-/-}$►*Ldlr*$^{-/-}$ n=7; control n=5, Cramp n=8). Displayed are means (horizontal lines) and SD,*p<0.05.***P<0.001.

Following the confirmation of pDC activation by Cramp-self-DNA complexes, we further investigated whether DNA-specific IgG autoantibody titers would be altered in *Apoe*$^{-/-}$ on HFD. Notably, serum anti-dsDNA antibody titers were increased in hyperlipidemic *Apoe*$^{-/-}$ mice receiving a HFD for 3 months compared with healthy controls (Figure 3-37; a). Subsequently, *Apoe*$^{-/-}$ mice receiving a PDCA1-depleting antibody showed reduced anti-dsDNA antibody titers compared to isotype treated control mice after 4 weeks of HFD. In contrast, anti-dsDNA titers were elevated in CpG- and IFNα treated *Apoe*$^{-/-}$ mice, but not in CpG-injected mice depleted of pDCs (Figure 3-37; b, c). Furthermore, enhanced anti-dsDNA antibody titers could also be observed in *Apoe*$^{-/-}$ with prolonged injections of CpGs during 8 weeks of high fat diet (Figure 3-37; d). In turn, diminished anti-dsDNA antibody titers were detectable in *Ldlr*$^{-/-}$ mice reconstituted with *Cramp*$^{-/-}$ versus *Cramp*$^{+/+}$ bone marrow; which is in line with the reduced lesion size in these mice (Figure 3-37; e). Interestingly, abundant IgG-deposits could be detected in atherosclerotic plaques of diet-fed *Apoe*$^{-/-}$ mice, predominantly in regions of DNA fragmentation at the border of necrotic plaque areas (Figure 3-37; f). In order to investigate, if these anti-dsDNA antibodies would activate pDCs, *ex vivo* sorted pDCs were stimulated with serum of *Apoe*$^{-/-}$ mice containing high or low levels of anti-dsDNA antibody titers. Remarkably, serum with high titers, but not serum containing low titers of anti-dsDNA antibodies significantly increased IFNα production in pDCs *in vitro* (Figure 3-37; g). Comparable to stimulation experiments with Cramp-DNA complexes, the expression of MHC-II, as a maturation marker of pDCs, was unaltered in the presence of serum, but upregulated after addition of CpGs (Figure 3-37; h). Thus, auto-antibody-self-DNA complexes within lesions, may also contribute to pDC activation and lesion progression in atherosclerosis.

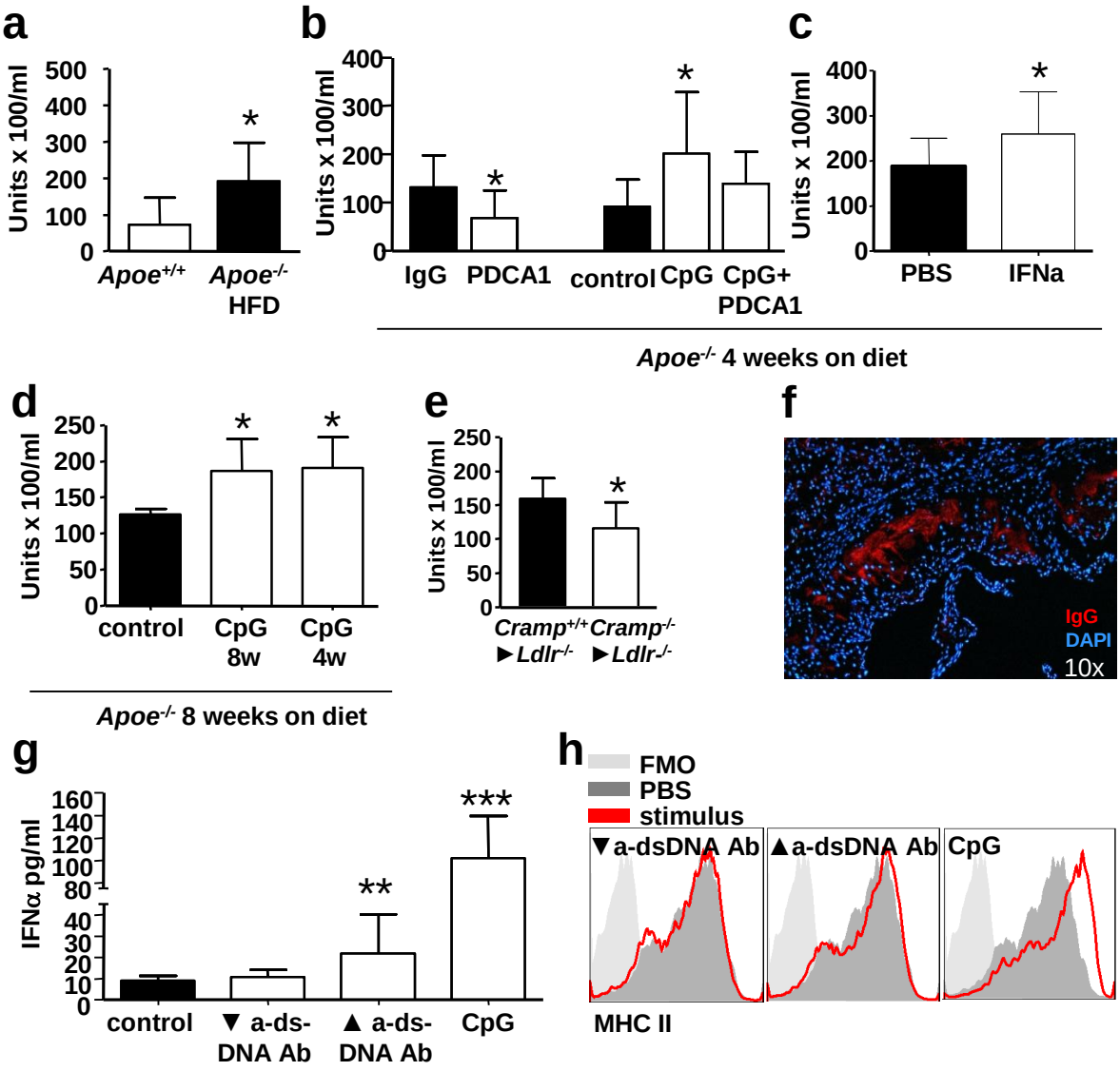

Figure 3-37. Anti-ds-DNA antibody generation correlates with atherosclerotic lesion formation and auto-antigenic protein-DNA complexes stimulate pDCs. (a) Anti-dsDNA antibody titers were quantified in serum of *Apoe*$^{-/-}$ mice fed HFD for 12 weeks (n=18) and in healthy 6 week old *Apoe*$^{+/+}$ mice (n=8 mice). **(b, c)** Further analysis of anti-dsDNA antibody serum titers were accomplished in *Apoe*$^{-/-}$ mice treated with IgG, PDCA1, DOTAP (control), CpG or CpG+PDCA1 or PBS and IFNα for 4 weeks including HFD for this time period (n=5-10 mice). **(d)** Quantification of anti-dsDNA antibody serum titers in *Apoe*$^{-/-}$ mice injected with DOTAP (control) and CpG for 4 or 8 weeks receiving a HFD for 8 weeks. **(e)** Anti-dsDNA antibody serum titers in sera of *Ldlr*$^{-/-}$ mice reconstituted with *Cramp*$^{+/+}$ or *Cramp*$^{-/-}$ bone marrow after 4 weeks of HFD. **(f)** IgG staining (red) detected by immunofluorescence in the aortic root in *Apoe*$^{-/-}$ mice fed HFD for 12 weeks; cell nuclei are counter-stained by DAPI (blue). **(g)** IFNα protein secretion by sorted pDCs stimulated for 12 h with PBS (control), CpGs or serum containing low (▼) or high (▲) anti-dsDNA titers. n=5 independent experiments. Data is expressed as mean±SD, ***P*<0.01, ****P*<0.01. **(h)** MHCII expression in sorted pDCs stimulated for 12 h with CpGs or serum with low (▼) or high (▲) anti-dsDNA antibody titers, assessed by FACS analysis; representative histograms with FMO, one representative image of 5 independent experiments is depicted.

4. DISCUSSION

4.1 IRF8-DEFICIENCY EXACERBATES ATHEROSCLEROSIS

We here show that the development of a CML-like syndrome in *Apoe*$^{-/-}$ or *Ldlr*$^{-/-}$ mice transplanted with bone marrow from *Irf8*$^{-/-}$ mice was associated with a striking increase in atherosclerotic lesion formation compared to mice reconstituted with wt bone marrow. The marked expansion of functionally intact PMN in peripheral blood was accompanied by their enhanced accumulation at sites of inflammation and plaque growth in *Irf8*$^{-/-}$ bone marrow recipients, implicating an enhanced release of ROS and granule components. Despite a reduction in monocyte numbers, the accumulation of macrophages during inflammation was unaffected by IRF8-deficiency, but was associated with an altered phenotype and impaired phagocytic clearance of apoptotic PMN. By demonstrating that the depletion of circulating PMN prevented the exacerbation of atherosclerotic lesion formation in *Irf8*$^{-/-}$ bone marrow recipient *Ldlr*$^{-/-}$ mice we pinpointed PMN to critically contribute to this phenotype.

4.1.1 *IRF8*$^{-/-}$ MACROPHAGES DISPLAY IMPAIRED FUNCTIONALITY

The infiltration of the vessel wall with immune cells is a crucial force driving the development of atherosclerosis.[137,188] Macrophages, which are present throughout all stages of atherosclerosis, hold a key position in the initiation but also progression of this disease. Through the expression of the scavenger receptors CD68, CD204, and CD36, macrophages participate in the phagocytic uptake of lipids contributing to their retention in the vessel wall, as well as in the clearance of apoptotic cells.[137,148,179,180] While moderate expression levels of CD68 and CD204 were unaltered, the strong surface expression of CD36 observed in *Irf8*$^{+/+}$ was markedly reduced in *Irf8*$^{-/-}$ macrophages. Known to account for up to 70% of the accumulation of oxLDL in macrophage foam cells[179], these differences might at least in part explain the impaired uptake of oxLDL by *Irf8*$^{-/-}$ macrophages and possibly relate to higher serum cholesterol and LDL levels in *Irf8*$^{-/-}$►*Apoe*$^{-/-}$ mice after 12 weeks of HFD, which in addition may contribute to enhanced atherosclerosis at later stages. But also lower numbers of ApoE-secreting, bone marrow-derived macrophages after transplantation of *Irf8*$^{-/-}$*Apoe*$^{+/+}$ bone marrow in *Irf8*$^{-/-}$►*Apoe*$^{-/-}$ mice compared to increased *Apoe*$^{+/+}$ monocyte counts in reconstituted *Irf8*$^{+/+}$►*Apoe*$^{-/-}$ mice could contribute to increased serum cholesterol and LDL levels. These differences, however, are unlikely to primarily underlay enhanced lesion formation in *Irf8*$^{-/-}$recipientmice, as a very similar plaque phenotype but no changes in lipid levels were observed in *Irf8*$^{-/-}$►*Ldlr*$^{-/-}$ mice after 5 weeks of diet.

Interestingly, while the deletion of CD36 was previously shown to protect from atherosclerosis[189], an impaired clearance of apoptotic material has been associated with disease acceleration and a reduction in IL-10 production[181]. In line, diminished IL-10 secretion from *Irf8*$^{-/-}$ macrophages was observed in response to phagocytosis of apoptotic PMN but also in sera of *Irf8*$^{-/-}$►*Apoe*$^{-/-}$ mice. However, protein concentrations of the clearly pro-atherogenic cytokines[127] IFNγ and IL-6 were reduced in air pouches of *Irf8*$^{-/-}$ compared to *Irf8*$^{+/+}$mice. Moreover, the surface expression of MHCII and CD40 were substantially diminished in *Irf8*$^{-/-}$ macrophages, pointing at a global insufficiency in cytokine secretion, antigen-presenting and immune priming capacities of this cell type, functions usually associated with atheroprogression[127]. However, anti-inflammatory properties of *Irf8*$^{-/-}$ macrophages are clearly outweighed by pro-inflammatory mechanisms active in mice carrying *Irf8*$^{-/-}$ bone marrow. In light of an essential function of IRF8 in regulating macrophage maturation[173], these differences might also be indicative of a less mature macrophage phenotype.

4.1.2 MONOCYTE EXTRAVASATION IS NOT AFFECTED BY IRF8 DEFICIENCY

In line with their differentiation from extravasated monocytes[190], the depletion of monocytes/macrophages in mice expressing the diphtheria toxin receptor under the control of CD11b or the reduction in blood monocyte levels due to the lack of important mobilization or survival cues was shown to reduce early plaque burden[191-194]. Despite a marked reduction in circulating monocyte numbers in mice reconstituted with *Irf8*$^{-/-}$ bone marrow, unaltered macrophage content and an increase in plaque formation was observed in *Irf8*$^{-/-}$►*Apoe*$^{-/-}$ or *Irf8*$^{-/-}$►*Ldlr*$^{-/-}$ mice. Similarly, the acute and chronic recruitment of monocytes to the air pouch and peritoneum was not impaired in *Irf8*$^{-/-}$ mice. This likely precludes severe functional deficits in the migratory capacity of *Irf8*$^{-/-}$ monocytes *per se*. An enhanced survival of *Irf8*$^{-/-}$ macrophages masking defects in extravasation is unlikely to occur under inflammatory conditions, as previous findings showed a reduction in the susceptibility to apoptosis in *Irf8*$^{-/-}$ myeloid cells under homeostatic conditions but not upon inflammatory stimulation with TNF.[175] In line, we did not detect any differences in the frequency of apoptotic macrophages in atherosclerotic lesions of *Irf8*$^{-/-}$►*Apoe*$^{-/-}$ compared to *Irf8*$^{-/-}$►*Apoe*$^{-/-}$ mice. It remains to be clarified, whether the augmented PMN extravasation and the PMN-induced inflammation in *Irf8*$^{-/-}$►*Apoe*$^{-/-}$ mice provide recruitment cues that enhance subsequent monocyte influx[39], thus compensating reduced monocyte numbers in the circulation. For instance, emigrated PMN release preformed granule components, which can trigger the subsequent recruitment and attraction of inflammatory monocytes by involvement of formyl-peptide receptors.[39]

4.1.3 PMN ACCUMULATION ACCOMPANIED BY GRANULE PROTEIN DISCHARGE DRIVES ATHEROSCLEROSIS IN *IRF8*$^{-/-}$►*APOE*$^{-/-}$MICE

Moreover, granule proteins have been shown to promote pro-inflammatory responses in monocytes and macrophages and induce a classical macrophage polarization.[146] The activation and discharge of granule proteins were not impaired in *Irf8*$^{-/-}$ PMN, as determined by the rapid upregulation of CD11b and CD14 on extravasated PMN due to their incorporation from membranes of secretory vesicles and tertiary granules during discharge, or by the release of MPO and MMP-9 from primary and secondary granules.

Granule proteins also exert pro-inflammatory functions in other cell types. For instance, MPO can limit the bioavailability of nitric oxide and can therefore contribute to the onset of endothelial dysfunction.[195] It was also reported that MPO-generated hyperchlorous acid may contribute to intracoronary endothelial cell desquamation and the engenderment of a prothrombotic phenotype.[196] Due to its proteolytic function, MMP-9 on the other hand was shown to contribute to the degradation and weakening of the fibrous cap ultimately promoting a vulnerable plaque phenotype and plaque rupture.[197] Accordingly, mice devoid of MMP-9 are protected from atherosclerosis.[198]

In addition, also ROS formation was unaltered in *Irf8*$^{-/-}$ PMN, constituting another weapon being at the PMN's immediate demand and proposed to be a key mediator in atherosclerosis.[182] PMN produce large amounts of ROS via MPO, lipoxygenases, and NADPH oxidase, most of which are secreted extracellularly and there contribute to lipid oxidation and retention as well as apoptosis of endothelial cells. Furthermore, ROS enhance the expression of endothelial adhesion molecules contributing to leukocyte recruitment.[182]

PMN are short-lived phagocytes undergoing rapid apoptosis following emigration. The rate of apoptosis of blood or emigrated PMN was not different in *Irf8*$^{-/-}$ compared to control mice. However, likely due to their enhanced accumulation, apoptotic PMN were detected in increased numbers in atherosclerotic plaques. The impaired clearance of apoptotic cells and an overload of reduced phagocytic capacities of macrophages with numerous dying PMN in *Irf8*$^{-/-}$►*Apoe*$^{-/-}$ mice might in consequence lead to secondary necrosis contributing to necrotic core formation, perpetuation of inflammation and plaque instability.[147]

Accumulating evidence suggests that PMN critically contribute to atherosclerosis.[140,141,148,199] *Apoe*$^{-/-}$ or *Ldlr*$^{-/-}$ mice transplanted with *Irf8*$^{-/-}$ bone marrow displayed a marked expansion of neutrophils in peripheral blood and a prominent increase in frequencies of PMN within atherosclerotic lesions. The accumulation of PMN was also found to be increased in air pouches of *Irf8*$^{-/-}$ mice, and to be proportional to the increase in circulating PMN counts. As no

differences in PMN numbers were observed in the air pouch or the peritoneum in *Irf8*$^{+/+}$ compared to *Irf8*$^{-/-}$ mice under physiological conditions or without inflammation, these findings suggest that circulating PMN counts determine the rate of extravasation in the context of inflammation and atherosclerosis. Similarly, it has recently been shown that mice with neutrophilia due to blockade of CXCR4 exhibit an increased accumulation of PMN in atherosclerotic lesions concomitant with increased atherosclerotic burden.[141] In humans it has furthermore been suggested that the degree of atherosclerosis and the frequency of coronary artery symptoms positively correlate with peripheral PMN counts.[142,144,200] The rapid PMN mobilization and leukocytosis in response to inflammation might thus constitute a universal mechanism impressing an enhanced PMN influx at sites of inflammation. In the context of myeloproliferative diseases, however, this might implicate an acceleration of atheroprogression.

4.1.4 MYELOPROLIFERATIVE DISORDERS DRIVE ATHEROGENESIS

Similar to our findings, mice deficient in IRF8 or expressing a mutated *Irf8* gene were shown to display a shift in the myeloid cell homeostasis and a CML-like syndrome, characterized by a marked neutrophilia and defective macrophage maturation.[164,173,201] Notably, reduced IRF8 expression has also been associated with thepathogenesis ofhuman CML[202,203], resulting from the neoplastic generation of the BCR-ABL fusion gene. Here, IRF8 functions as a tumor suppressor by antagonizing the tyrosine kinase activity of BCR-ABL.[178] According to our findings, one would suspect a higher prevalence of atherosclerosis-related diseases in patients with myeloproliferative diseases. Literature reports on the correlation between CML and atherosclerosis or its consequences, however, are scarce. One study including only a small number of patients found a correlation of coronary artery disease with co-existing myeloproliferative syndromes, which was not significant after adjustment for various risk factors.[204]

Notably, effective therapeutic regimens are available for treatment of CML that raise IRF8 expression, *e.g.* therapy with the Imatinib mesylate inhibits the tyrosine kinase of the BCR-ABL fusion gene and subsequently restores IRF8 expression, inducing a complete cytogenic response in 80% of CML patients in the chronic phase.[178] Preliminary experiments revealed that treatment with Imatinib decreased the numbers of PMN in peripheral blood of wt mice (Data not shown). Interestingly, treatment with Imatinib was furthermore already shown to reduce diabetes-associated atherosclerosis in mice.[205]

A current publication by Birnberg *et al.*[206] indicated that a defect in the DC compartment in *Irf8*$^{-}$

$^{/-}$ mice may in addition contribute to the development of a CML-like disease. Although the underlying feedback loop remains to be elucidated, it was proposed that peripheral DC counts connect to myelogenesis through soluble growth factors, such as Fms-like tyrosine kinase 3 receptor (Flt3) ligand. In line with reduced frequencies of circulating dendritic cells, increased Flt3 ligand levels could be observed in serum in *Irf8*$^{-/-}$►*Apoe*$^{-/-}$ mice (Data not shown).

4.1.5 PERSPECTIVES

Taken together, these data clearly demonstratethat the expansion of functionally intact PMN in ill alliance with impaired macrophage functions critically contribute to atherosclerosis and imply that myeloproliferative syndromes or related conditions may give rise to enhanced atherosclerosis. Drechsler *et al.*[145] already showed that hypercholesterolemia-induced neutrophilia promotes early atherogenesis attributed to stimulation of granulopoiesis, enhanced bone marrow mobilization as well as reduced peripheral clearance. In line with our findings, Drechsler *et al.* did also report a correlation of increased peripheral neutrophil counts with the extent of early atherosclerosis formation. Notably, while hypercholesterolemia-inducedneutrophilia may normalize by time, IRF8-deficiency results in a chronic neutrophilia, which may not only initiate vascular damage and atherogenesis. Yet, continuous influx of PMN might exacerbate inflammation in the local plaque environment aggravating disease progression.On the other hand, another very recent study suggests thathypercholesterolemia may cause leukocytosis in general, because of increased proliferation of myeloid progenitors in the bone marrow. The authors conclude that modulation of the cholesterol efflux pathway might be a promising tool for therapeutic treatment of myeloproliferative neoplasms.[207] Subsequently, medical drugs developed for one or the other may be beneficial for the treatment of both diseases. Thus, further studies are necessary to scrutinize a possible enhanced susceptibility to atherosclerosis in patients with myeloproliferative disorders.

4.2 AUTOANTIGENIC PROTEIN-DNA COMPLEXES STIMULATE PLASMACYTOID DENDRITIC CELLS TO PROMOTE ATHEROSCLEROSIS

Beyond the detection of murine pDCs in atherosclerotic lesions, this study further demonstrated that specific pDC activation significantly aggravates atherosclerotic lesion formation, while depletion of pDCs decreases early plaque development. Furthermore, pre-treatment of pDCs with oxLDL increases their antigen uptake capacity, leading to enhanced antigen specific T cell proliferation *in vivo*. Notably, not only oxLDL stimulation of pDCs, but also mechanisms accounting for breakdown of immune tolerance resulting in pDC activationin autoimmune diseases, could be identified for atherosclerosis. Cramp-self-DNA complexes stimulated IFNα secretion by pDCs *in vitro*, while *Cramp*$^{-/-}$►*Ldlr*$^{-/-}$ mice displayed reduced plaque formation. In contrast, *Apoe*$^{-/-}$ mice stimulated with Cramp exhibited enlarged atherosclerotic lesion development. In addition, exacerbated plaque formation was always accompanied by increased anti-ds-DNA antibody serum titers and stimulation of pDCs with high anti-ds-DNA sera *in vitro* induced IFNα secretion. Thus, chronic stimulation of pDCs by modified lipoproteins and autoimmune mechanisms may critically drive inflammation in atherosclerosis.

4.2.1 ACTIVATED PDCS INITIATE ATHEROSCLEROTIC LESION FORMATION

Atherosclerosis, being a chronic inflammatory disease of the vessel wall, critically involves immune cells in its pathomechanism.[127] However, definite conclusions on DC implications in atherosclerosis, also attributed to their multifaceted functions, are still to be drawn.[153] Recently, Niessner *et al.*[154] identified pDCs in the shoulder region of human atherosclerotic lesions and correlated IFNα secretion with plaque instability by inducing apoptosis of vascular smooth muscle cells. In addition, he and his colleagues described IFNα as an inflammatory amplifier inducing upregulation of TLR4 on cDCs, resulting in a synergistic effect of different danger signals within the two DC subsets.[155] Nevertheless, *in vivo* studies of pDC activation and depletion in appropriate atherosclerotic mouse models remain elusive, which underlines the importance of this work. We did show that pDC activation *in vivo* increases plaque formation in initial and advanced atherosclerotic lesions. Furthermore, IFNα injections enhanced lesion progression, confirming the identification of IFNα as a critical disease trigger.An observation also reported by Levy *et al.*[208], who examined plaque development in *Ldlr*$^{-/-}$ mice after repetitive IFNα injections. Moreover, increased plaque formation was accompanied by enhanced macrophage influx, supporting a study by Goosen *et al*.[209], which

showed that type I interferon signaling promotes atherosclerosis by stimulating macrophage recruitment to lesions. In line with these findings, not only activation of pDCs, but already hyperlipidemia led to a detectable, hence increased, IFNα titer compared to baseline level in mice sera after high fat diet treatment. This was accompanied bythe accumulation of pDCs in aortas of these animals. In contrast and supportive to the latter, patients with CAD display a decreased number of circulating pDCs, emphasizing a possible role of pDCs in plaque progression.[210] Taken together, these findings corroborate that type I interferons progress atherosclerosis throughout lesion development.

IFNα secretion by pDCs may be stimulated by various ligands, including autoantigens (also ref. 4.2.3), and plays a critical role in response to viral[61] and bacterial[211] infections. CpG stimulation of pDCs “mimics” such infection, although stimulation with a “real pathogen” would result in a much higher type I interferon response.[212,213] This raises the question whether or not pathogen related infections drive atherosclerosis. An issue that is still a matter of debate.[214,215] However, the sensitivity of pDCs to multiple pathogens correlates well with the concept of an infectious burden, highlighting the importance of numerous or chronic infections driving atherosclerosis, rather than pointing at one infection or pathogen.[216] On the other hand one infectious event may be enough to break down immune tolerance.[217,218] Thus, investigation of pathogen associated pDC activation with regard to atherosclerosis may be another important piece in the puzzle.

Yet, reduced plaque formation after pDC depletion could only be observed in early atherosclerotic lesions, while cell depletion in mice with ongoing atherosclerosis did not reduce the plaque burden. These results came along with increased T cell numbers and dramatically enhanced IL-4 serum titers, suggesting that pDC depletion under inflammatory conditions may cause a complex imbalance of the immune response. Although, IL-4 is known to stimulate a Th2 response and induces alternative macrophage activation[127,219], its role in atherosclerosis seems to be variable, depending on the disease stage.[220] Of note, alternative macrophage activation may not always be beneficial, but can result in macrophage accumulation in inflamed tissue.[208] Furthermore it is well known, that type I interferons are critical regulators of DC and T cell homeostasis.[221] Baseline type I interferon expression[222] is assumed to play a considerable role in the regulation of Treg homeostasis[223], potentially by influencing their thymic selection process. The latter may explain, why the relative number of $CD4^+$ $CD25^+$ T cells was significantly decreased (Data not shown), while numbers of $CD4^+$ T cells in total were increased in pDC depleted mice. Moreover and in line with the findings above, *Apoe*$^{-/-}$ mice transplanted with *Ikaros*$^{L/L}$ bone marrow (a mouse model which lacks pDCs[224]) displayed no changes in plaque formation, but dysregulated T cell homeostasis after

high fat diet treatment (Data not shown). Thus, reduced type I interferon levels (beneath baseline) possibly cause disturbed T cell homeostasis, manifesting in increased T cell numbers accompanied by augmented T cell derived IL-4 serum titers and decreased Treg frequencies. In conclusion, this may explain why pDC depletion under inflammatory conditions does not reduce plaque formation.

Recruitment of DCs into atherosclerotic lesions seems to be mediated by CCL2, CCL5 and fractalkine (CX_3CL1), abundantly expressed in inflamed atheromas.[153] Nevertheless, one may only speculate, whether these mechanisms do also account for pDC recruitment in particular. It has been shown that pDCs not only migrate in response to CCL5, but also to CCL3, CCL25, CXCL9, CXCL10 and, CXCL12 depending on the pathological conditions involved.[73] Though, recruitment assays in the context of an inflammatory air pouch model within this thesis did not clearly show an involvement of CCL5 in the recruitment of pDCs to sites of inflammation (Data not shown), which may also be explained by the recruitment model chosen. However, administration of IFNα into the air pouch cavity did lead to an increased number of pDCs after 4h (Data not shown). The latter may perhaps point at an autocrine feedback loop between pDC derived type I interferons and subsequent cell recruitment. Notably, chemerin injections into pouches resulted in significantly increased pDC accumulation (Data not shown), most likely reflecting increased pDC numbers and enhanced chemerin titers in CpG stimulated mice. Thus, neutrophil derived chemerin could not only be a potent chemotactic factor directing pDC migration in psoriasis[74,225], but also drive pDC recruitment to aortic lesions.

4.2.2 OXLDL CRITICALLY INFLUENCES PDC FUNCTIONS

Modified lipoproteins, in particular oxLDL, are main triggers of atherosclerosis. OxLDL induces foam cell formation, alteration of nitric oxide signaling, initiation of endothelial activation, and expression of adhesion molecules that accelerate leukocyte homing to the site of atherosclerosis.[226] Additionally, accumulating evidence shows that oxLDL affects DC migration, maturation and the expression of scavenger receptors.[186,227,228] Furthermore, induction of hypercholesterolemia in mice triggers rapid ingestion of lipids by resident intimal DCs. In turn, these cells initiate early foam cell formation in atherosclerotic lesions.[229] However, similar to the lack of general data on how pDCs in detail may influence atherosclerosis, studies investigating the influence of oxLDL on pDCs are absent. In our hands pDCs were able to take up oxLDL and oxLDL-treated pDCs upregulated the expression of scavenger receptor CD36, which is one of the most important receptors for oxLDL uptake[179]. In contrast to cDCs[186,228,230], pDCs did not increase the expression of MHCII and

CD86 in the presence of oxLDL, but oxLDL treatment enhanced their capacity to induce antigen specific T cell proliferation. An observation also reported for cDCs, which also maintain their ability to prime $CD4^+$ T cells after oxLDL uptake.[230,231] According to our data, augmented induction of T cell proliferation by oxLDL stimulatated pDCs may be explained by their increased antigen uptake. Though, uptake of exogenous antigen by pDCs is impaired compared to cDCs because of their diminished ability for phagocytosis or macropinocytosis.[58] However, pDCs possibly internalize exogenous antigens by receptor mediated endocytosis via specific receptors of the c-type lectin[232] or siglec[233] family, of which some are highly or exclusively expressed on pDCs[234-236]. Subsequently, their expression may also be affected by oxLDL treatment.[186] Taken together, oxLDL may force pDC-driven immune responses in the context of atherosclerosis.

4.2.3 AUTOIMMUNE MECHANISMS DRIVE PDC ACTIVATION IN ATHEROSCLEROSIS

Besides the recognition of atherosclerosis as a chronic inflammatory disease, a growing group of scientists hold the opinion that it may also be an autoimmune disorder. According to the "Koch's postulates" it fulfills the criteria for an inflammation of autoimmune origin: (i) presence of autoantibodies or evidence of cellular reactivity to self; (ii) documentation of lymphocyte infiltrate in the pathologic lesion; (iii) demonstration that autoantibodies or activated T cells can cause tissue pathology.[218] However, the reduction of atherosclerosis as being "simply" an autoimmune disease would not take into account other triggers such as metabolic and hemodynamic factors.[237] But not only the disease classification may be complex also the (auto)antigens considered to be responsible for the autoimmune activation are multifaceted. Best characterized autoantigens for atherosclerosis are oxLDL and heat shock proteins (HSPs), particularly HSP60.[218,238] Both can form immune complexes with their cognate antibodies and modulate inflammation in atherosclerosis.[239]

Another group of postulated immune stimulators in autoimmune diseases are nuclear antigens derived from apoptotic or necrotic cells, which are known to play an important role in the stimulation of pDCs in the pathomechanisms of psoriasis and SLE.[97] In addition, both diseases are associated with increased prevalence of atherosclerosis.[112,114] Notably, we were able to show that similar mechanisms may also trigger plaque development in atherosclerosis. We could confirm that, Cramp-DNA complexes, in line with previous findings in the pathogenesis of psoriasis[42,171,240], stimulate IFNα secretion by pDCs *in vitro*. As a novelty, the same results were obtained by pDC activation with dead PMN, emphasizing an ill-alliance of apoptotic neutrophils and pDCs within atherosclerotic lesions. Further evidence approving Cramp as a disease amplifier in atherosclerosis were revealed after analyzing plaque

formation in *Apoe*$^{-/-}$ mice treated with Cramp. These mice displayed an increase in plaque formation, while *Cramp*$^{-/-}$►*Ldlr*$^{-/-}$ mice exhibited a decrease in lesion size. Moreover, supporting a study by Edfeldt *et al.*[241], who encountered LL-37 in human atherosclerotic lesions, we could visualize lesional Cramp in murine plaques and corroborated enhanced Cramp mRNA transcripts in atherosclerotic murine aortas. Hence, complex formation of self-DNA and antimicrobial peptides resulting in pDC activation may be a shared pathomechanism[112] between psoriasis and atherosclerosis. Thus, increased prevalence of atherosclerosis in patients with psoriasis[242] may be explained by chronically activated pDCs.

SLEis identified by complex formation between self-DNA and anti-DNA antibodies. These DNA containing immune complexes (IC) accumulate within various tissues leading to unspecific immune activation eventually resulting in breakdown of immune tolerance. One hallmark of SLE diagnostic is the detection of anti-nuclear antibodies (ANAs), including anti-dsDNA antibodies.[243] Interestingly, Aprahamian *et al.*[244] already proposed defects in apoptotic cell clearance as pathogenic trigger in atherogenesis and SLE development in a combined mouse model of lupus and atherosclerosis. In contrast to this work he and his colleagues did not report augmented ANA levels in *Apoe*$^{-/-}$ mice on high fat diet. According to our findings, determination of ANAs in high fat diet fed *Apoe*$^{-/-}$ mice revealed increased ANA titers in sera of these mice (Data not shown). Further investigations of anti-dsDNA antibody levels in all sera of the mice included in this thesis even displayed significantly elevated anti-dsDNA titers in correlation with enhanced plaque formation. Thus, IC may also form in the context of atherosclerosis and DNA containing immune complexes have also been implicated in the activation of pDCs with subsequent IFNα release.[245,246] Remarkably, we were also able to demonstrate that sera of *Apoe*$^{-/-}$ mice with a high anti-dsDNA titer did induce IFNα secretion by pDCs *in vitro*. A similar observation was made for isolated DNA containing IC from SLE patients.[246] Noteworthy, comparable results were reported by Pertovaara *et al.*[247], who showed that elevated anti-nuclear antibody titers were associated with decreased carotid elasticity in young Finns, which might confirm their participation in the development of early atherosclerosis. Ultimately, we demonstrated the presence of IgGs within atherosclerotic lesions, which concentrated in the plaque center highlighting their availability in inflammatory, growing lesions. Hence, increased pDC numbers and elevated IFNα levels in SLE patients may be one explanation for their increased risk to develop atherosclerosis.[248]

In conclusion, Cramp-induced recognition of self-DNA triggering activation of pDCs and secretion of IFNα may be critical in promoting auto-antibody production, which in turn may enhance pDC activation.[108,246]

4.2.4 PERSPECTIVES

Summarizing the novelty of the data presented and discussed above, we showed that specific pDC depletion or stimulation severly affects atherogenesis. Furthermore, mechanisms relevant to pDC activation in autoimmune diseases may be pertinent in chronic arterial inflammation, namely atherosclerosis. Especially further insight in the ill-alliance of neutrophils and their secretory products during pDC activation may improve our understanding of pathomechanisms underlying atherosclerosisin particular (Figure 4-1) and of autoimmune diseases in general.

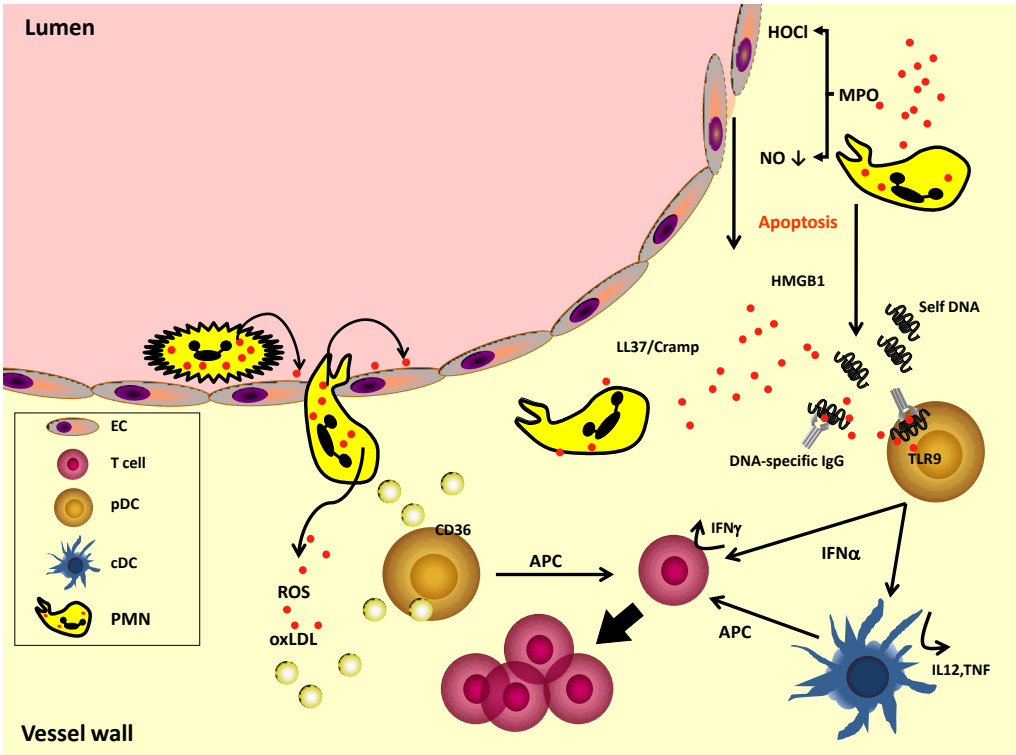

Figure 4-1: Summary of potential mechanisms of pDC activation by neutrophil secretory products in atherosclerosis. PMN-derived ROS facilitate LDL modification leading to oxLDL accumulation. Lesional oxLDL may be encoutered by pDCs resulting in enhanced CD36 surface expression and antigen uptake by pDCs. Subsequently, augmented antigen uptake by pDCs stimulates increased antigen-specific T cell proliferation. In parallel, MPO reduces the bioavailability of NO and leads to production of HOCl. The latter may induce endothelial cell apoptosis and desquamation. LL37/Cramp secreted by infiltrating neutrophilsbinds self-DNA fragments released from dying cells to form aggregates of self-DNA–LL37/Cramp. Dying cells also set free high-mobility group box 1 protein (HMGB1), which binds self-DNA–LL37/Cramp complexes and promotes their association with TLR9. In addition, DNA-specific IgG autoantibodies produced by autoreactive B cells bind to self-DNA–LL37/Cramp–HMGB1 complexes and potently increase their translocation into TLR9-containing endosomes in pDCs. These complexes activate pDCs and lead to a robust type I interferon production. In turn, IFNα activates cDCs, which produce proinflammatory cytokines and induce antigen-specific T cell proliferation (extracted from[97,148,153]).

Overall, the aberrant conversion of self-nucleicacids into ligands for TLR7/9 in pDCs may represent a common step of several pathogenic cascades not only in psoriasis and SLE, but possibly also for other autoimmune diseases.[249] Consequential therapeutic approaches targeting *e.g.* the specific release of granule proteins (*e.g.* LL37) may be a promising tool for diseases in this context. Hence, one should also not ignore that the mechanisms discussed above may only be true for TLR9, although TLR7 is also involved in nucleic acid recognition. Shlomchik *et al.*[250] already reported opposing roles of TLR7/9 in the pathogenesis of SLE. On the other hand, it should be kept in mind that the complete depletion of pDCs, beyond the increased susceptibilityto viral infections, seems to disturb T cell homeostasis. Thus, therapeutic approaches should aim carefully at very specific drugs, only intervening with distinct functions rather than blocking or depleting whole cell subsets.

5. SUMMARY

This study focuses on the understanding of the pathophysiological role of neutrophils and plasmacytoid dendritic cells in atherosclerosis.

Atherosclerosis is now agreed to be a chronic inflammatory disease of the vessel wall driven by intense immunological activity, of both, innate and adaptive immunity. Whereas monocytes/macrophages are of paramount importance, polymorphonuclear neutrophilic leukocytes (PMN) have recently also been implicated in lesion formation. Given the expansion of these cell types in myeloproliferative disease, we here investigated atherosclerotic lesion formation in Interferon regulatory factor 8-deficient (*Irf8*$^{-/-}$) mice. Thechronic myelogenous leukemia (CML)-like phenotype with expanded PMN but reduced frequencies of monocytes in bone marrow and peripheral blood in atherosclerosis-prone apolipoprotein E-deficient (*Apoe*$^{-/-}$) mice reconstituted with *Irf8*$^{-/-}$ bone marrow was associated with an increased lesional accumulation of PMN, apoptotic cells, a more pro-inflammatory plaque phenotype, and exacerbated atherosclerotic lesion formation in comparison to *Irf8*$^{+/+}$ bone marrow-recipient *Apoe*$^{-/-}$ mice. Although accumulating in equal numbers at sites of inflammation and plaque growth, *Irf8*$^{-/-}$ macrophages were defective in phagocytosis of apoptotic cells and lipids as well as cytokine production, contrasting unaffected reactive oxygen species formation, and discharge of PMN granule components by *Irf8*$^{-/-}$ compared to *IRF8*$^{+/+}$ PMN. Depletion of PMN in atherosclerotic mice reconstituted with *Irf8*$^{-/-}$ bone marrow abrogated increased lesion formation. These data indicate that the expansion of functionally intact PMN in ill alliance with impaired macrophage functions critically contribute to atherosclerosis and imply that long-standing CML-syndroms may associate with enhanced atherosclerosis.

Dendritic cells are very heterogenous group of antigen presenting cells and their role in atherosclerotic lesion formation is not clear. Even less is known about plasmacytoid dendritic cells (pDCs) in this context. Thus, this study wanted to unravel the role of pDC in atherosclerosis. Besides the detection of murine pDCs in atherosclerotic lesions, it could be further demonstrated, that specific pDC activation significantly aggravates atherosclerotic lesion formation, while depletion of pDCs decreases early plaque development. Furthermore, pre-treatment of pDCs with oxLDL increases their antigen uptake capacity, leading to enhanced antigen specific T cell proliferation *in vivo*. Notably, not only oxLDL stimulation of pDCs, but also mechanisms accounting for breakdown of immune tolerance resulting in pDC activation in autoimmune diseases, could be identified for atherosclerosis. Cramp-self-DNA complexes stimulated IFNα secretion by pDCs *in vitro*, while *Cramp*$^{-/-}$►*Ldlr*$^{-/-}$ mice displayed reduced plaque formation. In contrast, *Apoe*$^{-/-}$ mice stimulated with Cramp exhibited enlarged

atherosclerotic lesion development. In addition, exacerbated plaque formation was always accompanied by increased anti-ds-DNA antibody serum titers and stimulation of pDCs with high anti-ds-DNA sera *in vitro* induced IFNα secretion. Thus, chronic stimulation of pDCs by modified lipoproteins and autoimmune mechanisms may critically drive inflammation in atherosclerosis.

6. ZUSAMMENFASSUNG

Die Atherosklerose ist als eine chronische Entzündung der Gefäßwand zu verstehen, in deren Pathomechanismus die inflammatorische Rekrutierung leukozytärer Zellen eine zentrale Bedeutung für die Initiierung und Progression atherosklerotischer Läsionen spielt.

Die Rolle von Phagozyten in der Pathophysiologie der Atherosklerose, vorrangig Monozyten und Makrophagen, unterlag in den letzten Jahrzehnten weitreichenden Untersuchungen. Der kausale Beitrag von Neutrophilen Granulozyten (NG) zur Atherogenese ist dagegen weitestgehend unverstanden. Epidemiologische Studien weisen auf eine positive Korrelation zirkulierender NG-Zahlen und der Inzidenz von koronaren Herzerkrankungen hin. Daher werden hier atherosklerotische Apolipoprotein E-defiziente (*Apoe*$^{-/-}$) Mäuse mit dem Knochenmark Interferon-regulierenden-Faktor-8-defizienter (*Irf8*$^{-/-}$) Tiere transplantiert. Mit erhöhter Zahl peripherer NG, weisen letztere ein Blutbild auf, das dem der chronisch myeloischen Leukämie (CML) ähnelt. Mit Hilfe dieser Transplantation kann man somit die Zahl der NG im atherosklerotischen Kontext deutlich erhöhen, um so ihren Einfluss auf die Atherogenese besser untersuchen und verstehen zu können. In dieser Arbeit konnte gezeigt werden, dass *Apoe*$^{-/-}$ Tiere, die mit *Irf8*$^{-/-}$ Knochenmark transplantiert wurden, eine deutlich vermehrte Plaquebildung zeigen. Durch die Reversion der Läsionsgröße in NG-depletierten Tieren konnte der kausale Beitrag von NG in diesem Modell bewiesen werden. Insbesondere die durch NG freigesetzten Granulaproteine und die Akkumulation apoptotischer NG im nekrotischen Kern des Plaques trugen zur erhöhten Läsionsbildung bei. Aus diesen Ergebnissen lässt sich eindeutig ableiten, dass NG eine entscheidende Rolle bei der Entstehung und Progression von atherosklerotischen Läsionen spielen und eine Erhöhung ihrer Zahl, nicht nur für Patienten mit CML, sondern auch im Rahmen anderer chronischer Inflammationen einen kardiovaskulären Risikofaktor darstellen.

Dendritische Zellen sind spezialisierte Antigen-präsentierende Zellen, die zur Attraktion und Aktivierung von T-Zellen beitragen.Allerdings handelt es sich hier um eine sehr heterogene Zellpopulation mit mehreren Subtypen. Im Fokus dieser Arbeit stehen die plasmazytoiden dendritischen Zellen (pDC). Diese sind durch ihre Fähigkeit gekennzeichnet grosse Mengen proinflammatorischer Typ I Interferone als Antwort auf virale und bakterielle Pathogene auszuschütten. Ihre Bedeutung in der Atherosklerose ist kaum untersucht. Es war daher Ziel dieser Doktorarbeit zum Einen abzuklären, ob pDC in murinen Läsionen von *Apoe*$^{-/-}$ Mäusen nachweisbar sind. Weiterhin sollte untersucht werden, ob eine Depletion oder Stimulation dieser Zellpopulation *in vivo* die Plaquentwicklung beeinflusst. Nach Auswertung der Stimulationsstudien in *Apoe*$^{-/-}$ Tieren zeigte sich eine signifikant erhöhte Plaqueentwicklung

und ließ die Frage offen, welche Mechanismen *in vivo* ursächlich zu einer Stimulation von pDC führen können. Neben den bereits beschriebenen Ursachen, die zur Entstehung von Atherosklerose beitragen, wird im Kontext neuerer Studien auch diskutiert, welchen Einfluss autoimmune Mechanismen auf die Entwicklung von Atherosklerose haben. Die pathologische Relevanz von pDC und die von ihnen ausgeschütteten Typ I Interferone ist bereits für verschiedene autoimmune Erkrankungen wie z.B. Psoriasis und Sytemischen Lupus Erythematodes (SLE) beschrieben. Die dort gezeigten Pathomechanismen sind auch für die Entstehung von Atherosklerose von Bedeutung. Im Rahmen dieser Arbeit konnte gezeigt werden, dass z.B. die Konzentration von anti-Doppelstrang-DNA Antikörpern (a-dsDNA-AK), die an körpereigene DNA binden und somit zur Bildung von Immunkomplexen (IC) beitragen, in *Apoe*$^{-/-}$ Tieren unter fettreicher Diät erhöht ist. Ausserdem weisen *Apoe*$^{-/-}$ Tiere unter fettreicher Diät *per se* einen erhöhten Type I Interferon Spiegel auf. Darüber hinaus konnte *in vitro* nachgewiesen werden, dass IC-reiche Seren pDC aktivieren. Ähnlich verhält es sich mit Komplexen aus körpereigener DNA und dem antimikrobiellen Peptid LL-37/Cramp (human/murin). Hier konnte u.a. gezeigt werden, dass *Cramp*$^{-/-}$ Mäuse weniger Plaque entwickeln. Aus diesen Ergebnissen lässt sich eindeutig ableiten, dass die konstante autoantigene Stimulation von pDC und die damit verbundene Sekretion von Typ I Interferonen zur Entstehung und Progression von atherosklerotischen Läsionen beiträgt.

7. REFERENCES

1. Hansson, G.K., Robertson, A.K. & Soderberg-Naucler, C. Inflammation and atherosclerosis. *Annu Rev Pathol* **1**, 297-329 (**2006**).
2. Janeway, C.A., Jr. & Medzhitov, R. Introduction: the role of innate immunity in the adaptive immune response. *Semin Immunol* **10**, 349-350 (**1998**).
3. Janeway, C.A., Jr. & Medzhitov, R. Innate immune recognition. *Annu Rev Immunol* **20**, 197-216 (**2002**).
4. Hoebe, K., Janssen, E. & Beutler, B. The interface between innate and adaptive immunity. *Nat Immunol* **5**, 971-974 (**2004**).
5. Iwasaki, A. & Medzhitov, R. Regulation of adaptive immunity by the innate immune system. *Science* **327**, 291-295 (**2010**).
6. Katsura, Y. Redefinition of lymphoid progenitors. *Nat Rev Immunol* **2**, 127-132 (**2002**).
7. Abraham, S.N. & St John, A.L. Mast cell-orchestrated immunity to pathogens. *Nat Rev Immunol* **10**, 440-452 (**2010**).
8. Ardavin, C. Origin, precursors and differentiation of mouse dendritic cells. *Nat Rev Immunol* **3**, 582-590 (**2003**).
9. Ehrlich, P. La leukocytose. in *XIII Congres International de Medicine* (Paris, 1900).
10. Borregaard, N., Miller, L.J. & Springer, T.A. Chemoattractant-regulated mobilization of a novel intracellular compartment in human neutrophils. *Science* **237**, 1204-1206 (**1987**).
11. von Vietinghoff, S. & Ley, K. Homeostatic regulation of blood neutrophil counts. *J Immunol* **181**, 5183-5188 (**2008**).
12. Mestas, J. & Hughes, C.C. Of mice and not men: differences between mouse and human immunology. *J Immunol* **172**, 2731-2738 (**2004**).
13. Brinkmann, V., Reichard, U., Goosmann, C., Fauler, B., Uhlemann, Y., Weiss, D.S., Weinrauch, Y. & Zychlinsky, A. Neutrophil extracellular traps kill bacteria. *Science* **303**, 1532-1535 (**2004**).
14. Papayannopoulos, V. & Zychlinsky, A. NETs: a new strategy for using old weapons. *Trends Immunol* **30**, 513-521 (**2009**).
15. Borregaard, N., Sorensen, O.E. & Theilgaard-Monch, K. Neutrophil granules: a library of innate immunity proteins. *Trends Immunol* **28**, 340-345 (**2007**).
16. Scapini, P., Lapinet-Vera, J.A., Gasperini, S., Calzetti, F., Bazzoni, F. & Cassatella, M.A. The neutrophil as a cellular source of chemokines. *Immunol Rev* **177**, 195-203 (**2000**).

17. Ethuin, F., Gerard, B., Benna, J.E., Boutten, A., Gougereot-Pocidalo, M.A., Jacob, L. & Chollet-Martin, S. Human neutrophils produce interferon gamma upon stimulation by interleukin-12. *Lab Invest* **84**, 1363-1371 (**2004**).
18. Tamassia, N., Cassatella, M.A. & Bazzoni, F. Fast and accurate quantitative analysis of cytokine gene expression in human neutrophils by reverse transcription real-time PCR. *Methods Mol Biol* **412**, 455-471 (**2007**).
19. Kantari, C., Pederzoli-Ribeil, M. & Witko-Sarsat, V. The role of neutrophils and monocytes in innate immunity. *Contrib Microbiol* **15**, 118-146 (**2008**).
20. Nathan, C. Neutrophils and immunity: challenges and opportunities. *Nat Rev Immunol* **6**, 173-182 (**2006**).
21. Ma, Q., Jones, D. & Springer, T.A. The chemokine receptor CXCR4 is required for the retention of B lineage and granulocytic precursors within the bone marrow microenvironment. *Immunity* **10**, 463-471 (**1999**).
22. Semerad, C.L., Liu, F., Gregory, A.D., Stumpf, K. & Link, D.C. G-CSF is an essential regulator of neutrophil trafficking from the bone marrow to the blood. *Immunity* **17**, 413-423 (**2002**).
23. Friedman, A.D. Transcriptional control of granulocyte and monocyte development. *Oncogene* **26**, 6816-6828 (**2007**).
24. Lalezari, P., Murphy, G.B. & Allen, F.H., Jr. NB1, a new neutrophil-specific antigen involved in the pathogenesis of neonatal neutropenia. *J Clin Invest* **50**, 1108-1115 (**1971**).
25. Knapp, W. (ed.) *Leucocyte Typing IV. White Cell Differentiation Antigens.*, Pp. 1182 (Oxford University Press, 1990).
26. Fleming, T.J., Fleming, M.L. & Malek, T.R. Selective expression of Ly-6G on myeloid lineage cells in mouse bone marrow. RB6-8C5 mAb to granulocyte-differentiation antigen (Gr-1) detects members of the Ly-6 family. *J Immunol* **151**, 2399-2408 (**1993**).
27. Murayama, T., Yokode, M., Kataoka, H., Imabayashi, T., Yoshida, H., Sano, H., Nishikawa, S. & Kita, T. Intraperitoneal administration of anti-c-fms monoclonal antibody prevents initial events of atherogenesis but does not reduce the size of advanced lesions in apolipoprotein E-deficient mice. *Circulation* **99**, 1740-1746 (**1999**).
28. Witko-Sarsat, V., Rieu, P., Descamps-Latscha, B., Lesavre, P. & Halbwachs-Mecarelli, L. Neutrophils: molecules, functions and pathophysiological aspects. *Lab Invest* **80**, 617-653 (**2000**).
29. Borregaard, N. Development of neutrophil granule diversity. *Ann N Y Acad Sci* **832**, 62-68 (**1997**).
30. Faurschou, M. & Borregaard, N. Neutrophil granules and secretory vesicles in

inflammation. *Microbes Infect* **5**, 1317-1327 (**2003**).

31. Hager, M., Cowland, J.B. & Borregaard, N. Neutrophil granules in health and disease. *J Intern Med* **268**, 25-34 (**2010**).
32. Soehnlein, O., Weber, C. & Lindbom, L. Neutrophil granule proteins tune monocytic cell function. *Trends Immunol* **30**, 538-546 (**2009**).
33. Gudmundsson, G.H., Agerberth, B., Odeberg, J., Bergman, T., Olsson, B. & Salcedo, R. The human gene FALL39 and processing of the cathelin precursor to the antibacterial peptide LL-37 in granulocytes. *Eur J Biochem* **238**, 325-332 (**1996**).
34. Burton, M.F. & Steel, P.G. The chemistry and biology of LL-37. *Nat Prod Rep* **26**, 1572-1584 (**2009**).
35. Gallo, R.L., Kim, K.J., Bernfield, M., Kozak, C.A., Zanetti, M., Merluzzi, L. & Gennaro, R. Identification of CRAMP, a cathelin-related antimicrobial peptide expressed in the embryonic and adult mouse. *J Biol Chem* **272**, 13088-13093 (**1997**).
36. Chromek, M., Slamova, Z., Bergman, P., Kovacs, L., Podracka, L., Ehren, I., Hokfelt, T., Gudmundsson, G.H., Gallo, R.L., Agerberth, B. & Brauner, A. The antimicrobial peptide cathelicidin protects the urinary tract against invasive bacterial infection. *Nat Med* **12**, 636-641 (**2006**).
37. Kai-Larsen, Y. & Agerberth, B. The role of the multifunctional peptide LL-37 in host defense. *Front Biosci* **13**, 3760-3767 (**2008**).
38. De, Y., Chen, Q., Schmidt, A.P., Anderson, G.M., Wang, J.M., Wooters, J., Oppenheim, J.J. & Chertov, O. LL-37, the neutrophil granule- and epithelial cell-derived cathelicidin, utilizes formyl peptide receptor-like 1 (FPRL1) as a receptor to chemoattract human peripheral blood neutrophils, monocytes, and T cells. *J Exp Med* **192**, 1069-1074 (**2000**).
39. Soehnlein, O., Zernecke, A., Eriksson, E.E., Rothfuchs, A.G., Pham, C.T., Herwald, H., Bidzhekov, K., Rottenberg, M.E., Weber, C. & Lindbom, L. Neutrophil secretion products pave the way for inflammatory monocytes. *Blood* **112**, 1461-1471 (**2008**).
40. Davidson, D.J., Currie, A.J., Reid, G.S., Bowdish, D.M., MacDonald, K.L., Ma, R.C., Hancock, R.E. & Speert, D.P. The cationic antimicrobial peptide LL-37 modulates dendritic cell differentiation and dendritic cell-induced T cell polarization. *J Immunol* **172**, 1146-1156 (**2004**).
41. Di Nardo, A., Braff, M.H., Taylor, K.R., Na, C., Granstein, R.D., McInturff, J.E., Krutzik, S., Modlin, R.L. & Gallo, R.L. Cathelicidin antimicrobial peptides block dendritic cell TLR4 activation and allergic contact sensitization. *J Immunol* **178**, 1829-1834 (**2007**).
42. Lande, R., Gregorio, J., Facchinetti, V., Chatterjee, B., Wang, Y.H., Homey, B., Cao, W., Su, B., Nestle, F.O., Zal, T., Mellman, I., Schroder, J.M., Liu, Y.J. & Gilliet, M.

Plasmacytoid dendritic cells sense self-DNA coupled with antimicrobial peptide. *Nature* **449**, 564-569 (**2007**).

43. Scott, M.G., Davidson, D.J., Gold, M.R., Bowdish, D. & Hancock, R.E. The human antimicrobial peptide LL-37 is a multifunctional modulator of innate immune responses. *J Immunol* **169**, 3883-3891 (**2002**).
44. Masure, S., Proost, P., Van Damme, J. & Opdenakker, G. Purification and identification of 91-kDa neutrophil gelatinase. Release by the activating peptide interleukin-8. *Eur J Biochem* **198**, 391-398 (**1991**).
45. Van den Steen, P.E., Proost, P., Wuyts, A., Van Damme, J. & Opdenakker, G. Neutrophil gelatinase B potentiates interleukin-8 tenfold by aminoterminal processing, whereas it degrades CTAP-III, PF-4, and GRO-alpha and leaves RANTES and MCP-2 intact. *Blood* **96**, 2673-2681 (**2000**).
46. Hu, J., Van den Steen, P.E., Sang, Q.X. & Opdenakker, G. Matrix metalloproteinase inhibitors as therapy for inflammatory and vascular diseases. *Nat Rev Drug Discov* **6**, 480-498 (**2007**).
47. Klebanoff, S.J. Myeloperoxidase: friend and foe. *J Leukoc Biol* **77**, 598-625 (**2005**).
48. Triantafilou, M. & Triantafilou, K. Lipopolysaccharide recognition: CD14, TLRs and the LPS-activation cluster. *Trends Immunol* **23**, 301-304 (**2002**).
49. Lynch, R.G. Regulatory roles for FcgammaRIII (CD16) and FcgammaRII (CD32) in the development of T- and B-lineage lymphoid cells. *J Leukoc Biol* **67**, 279-284 (**2000**).
50. D'Autreaux, B. & Toledano, M.B. ROS as signalling molecules: mechanisms that generate specificity in ROS homeostasis. *Nat Rev Mol Cell Biol* **8**, 813-824 (**2007**).
51. Fang, F.C. Antimicrobial reactive oxygen and nitrogen species: concepts and controversies. *Nat Rev Microbiol* **2**, 820-832 (**2004**).
52. Nathan, C. & Shiloh, M.U. Reactive oxygen and nitrogen intermediates in the relationship between mammalian hosts and microbial pathogens. *Proc Natl Acad Sci U S A* **97**, 8841-8848 (**2000**).
53. Geissmann, F., Manz, M.G., Jung, S., Sieweke, M.H., Merad, M. & Ley, K. Development of monocytes, macrophages, and dendritic cells. *Science* **327**, 656-661 (**2010**).
54. Shortman, K. & Naik, S.H. Steady-state and inflammatory dendritic-cell development. *Nat Rev Immunol* **7**, 19-30 (**2007**).
55. Chicha, L., Jarrossay, D. & Manz, M.G. Clonal type I interferon-producing and dendritic cell precursors are contained in both human lymphoid and myeloid progenitor populations. *J Exp Med* **200**, 1519-1524 (**2004**).
56. Lennert, K. & Remmele, W. [Karyometric research on lymph node cells in man. I.

Germinoblasts, lymphoblasts & lymphocytes.]. *Acta Haematol* **19**, 99-113 (**1958**).

57. Facchetti, F. & Vergoni, F. The plasmacytoid monocyte: from morphology to function. *Adv Clin Path* **4**, 187-190 (**2000**).
58. Grouard, G., Rissoan, M.C., Filgueira, L., Durand, I., Banchereau, J. & Liu, Y.J. The enigmatic plasmacytoid T cells develop into dendritic cells with interleukin (IL)-3 and CD40-ligand. *J Exp Med* **185**, 1101-1111 (**1997**).
59. Siegal, F.P., Kadowaki, N., Shodell, M., Fitzgerald-Bocarsly, P.A., Shah, K., Ho, S., Antonenko, S. & Liu, Y.J. The nature of the principal type 1 interferon-producing cells in human blood. *Science* **284**, 1835-1837 (**1999**).
60. Trinchieri, G. & Santoli, D. Anti-viral activity induced by culturing lymphocytes with tumor-derived or virus-transformed cells. Enhancement of human natural killer cell activity by interferon and antagonistic inhibition of susceptibility of target cells to lysis. *J Exp Med* **147**, 1314-1333 (**1978**).
61. Cella, M., Jarrossay, D., Facchetti, F., Alebardi, O., Nakajima, H., Lanzavecchia, A. & Colonna, M. Plasmacytoid monocytes migrate to inflamed lymph nodes and produce large amounts of type I interferon. *Nat Med* **5**, 919-923 (**1999**).
62. Asselin-Paturel, C., Boonstra, A., Dalod, M., Durand, I., Yessaad, N., Dezutter-Dambuyant, C., Vicari, A., O'Garra, A., Biron, C., Briere, F. & Trinchieri, G. Mouse type I IFN-producing cells are immature APCs with plasmacytoid morphology. *Nat Immunol* **2**, 1144-1150 (**2001**).
63. Bjorck, P. Isolation and characterization of plasmacytoid dendritic cells from Flt3 ligand and granulocyte-macrophage colony-stimulating factor-treated mice. *Blood* **98**, 3520-3526 (**2001**).
64. Nakano, H., Yanagita, M. & Gunn, M.D. CD11c(+)B220(+)Gr-1(+) cells in mouse lymph nodes and spleen display characteristics of plasmacytoid dendritic cells. *J Exp Med* **194**, 1171-1178 (**2001**).
65. Schotte, R., Nagasawa, M., Weijer, K., Spits, H. & Blom, B. The ETS transcription factor Spi-B is required for human plasmacytoid dendritic cell development. *J Exp Med* **200**, 1503-1509 (**2004**).
66. Spits, H., Couwenberg, F., Bakker, A.Q., Weijer, K. & Uittenbogaart, C.H. Id2 and Id3 inhibit development of CD34(+) stem cells into predendritic cell (pre-DC)2 but not into pre-DC1. Evidence for a lymphoid origin of pre-DC2. *J Exp Med* **192**, 1775-1784 (**2000**).
67. Corcoran, L., Ferrero, I., Vremec, D., Lucas, K., Waithman, J., O'Keeffe, M., Wu, L., Wilson, A. & Shortman, K. The lymphoid past of mouse plasmacytoid cells and thymic dendritic cells. *J Immunol* **170**, 4926-4932 (**2003**).

68. Cisse, B., Caton, M.L., Lehner, M., Maeda, T., Scheu, S., Locksley, R., Holmberg, D., Zweier, C., den Hollander, N.S., Kant, S.G., Holter, W., Rauch, A., Zhuang, Y. & Reizis, B. Transcription factor E2-2 is an essential and specific regulator of plasmacytoid dendritic cell development. *Cell* **135**, 37-48 (**2008**).
69. Esashi, E. & Liu, Y.J. E-box protein E2-2 is a crucial regulator of plasmacytoid DC development. *Eur J Immunol* **38**, 2386-2388 (**2008**).
70. Esashi, E., Wang, Y.H., Perng, O., Qin, X.F., Liu, Y.J. & Watowich, S.S. The signal transducer STAT5 inhibits plasmacytoid dendritic cell development by suppressing transcription factor IRF8. *Immunity* **28**, 509-520 (**2008**).
71. Esashi, E. & Watowich, S.S. Dendritic cells: transcriptional control of plasmacytoid dendritic cell development by E2-2. *Immunol Cell Biol* **87**, 1-2 (**2009**).
72. O'Keeffe, M., Hochrein, H., Vremec, D., Caminschi, I., Miller, J.L., Anders, E.M., Wu, L., Lahoud, M.H., Henri, S., Scott, B., Hertzog, P., Tatarczuch, L. & Shortman, K. Mouse plasmacytoid cells: long-lived cells, heterogeneous in surface phenotype and function, that differentiate into CD8(+) dendritic cells only after microbial stimulus. *J Exp Med* **196**, 1307-1319 (**2002**).
73. Sozzani, S., Vermi, W., Del Prete, A. & Facchetti, F. Trafficking properties of plasmacytoid dendritic cells in health and disease. *Trends Immunol* **31**, 270-277 (**2010**).
74. Vermi, W., Riboldi, E., Wittamer, V., Gentili, F., Luini, W., Marrelli, S., Vecchi, A., Franssen, J.D., Communi, D., Massardi, L., Sironi, M., Mantovani, A., Parmentier, M., Facchetti, F. & Sozzani, S. Role of ChemR23 in directing the migration of myeloid and plasmacytoid dendritic cells to lymphoid organs and inflamed skin. *J Exp Med* **201**, 509-515 (**2005**).
75. Randolph, G.J., Ochando, J. & Partida-Sanchez, S. Migration of dendritic cell subsets and their precursors. *Annu Rev Immunol* **26**, 293-316 (**2008**).
76. Salio, M., Palmowski, M.J., Atzberger, A., Hermans, I.F. & Cerundolo, V. CpG-matured murine plasmacytoid dendritic cells are capable of in vivo priming of functional CD8 T cell responses to endogenous but not exogenous antigens. *J Exp Med* **199**, 567-579 (**2004**).
77. Young, L.J., Wilson, N.S., Schnorrer, P., Proietto, A., ten Broeke, T., Matsuki, Y., Mount, A.M., Belz, G.T., O'Keeffe, M., Ohmura-Hoshino, M., Ishido, S., Stoorvogel, W., Heath, W.R., Shortman, K. & Villadangos, J.A. Differential MHC class II synthesis and ubiquitination confers distinct antigen-presenting properties on conventional and plasmacytoid dendritic cells. *Nat Immunol* **9**, 1244-1252 (**2008**).
78. LeibundGut-Landmann, S., Waldburger, J.M., Reis e Sousa, C., Acha-Orbea, H. & Reith, W. MHC class II expression is differentially regulated in plasmacytoid and conventional

dendritic cells. *Nat Immunol* **5**, 899-908 (**2004**).

79. Colonna, M., Trinchieri, G. & Liu, Y.J. Plasmacytoid dendritic cells in immunity. *Nat Immunol* **5**, 1219-1226 (**2004**).
80. Asselin-Paturel, C., Brizard, G., Pin, J.J., Briere, F. & Trinchieri, G. Mouse strain differences in plasmacytoid dendritic cell frequency and function revealed by a novel monoclonal antibody. *J Immunol* **171**, 6466-6477 (**2003**).
81. Lande, R. & Gilliet, M. Plasmacytoid dendritic cells: key players in the initiation and regulation of immune responses. *Ann N Y Acad Sci* **1183**, 89-103 (**2010**).
82. Gerlini, G., Mariotti, G., Bianchi, B. & Pimpinelli, N. Massive recruitment of type I interferon producing plasmacytoid dendritic cells in varicella skin lesions. *J Invest Dermatol* **126**, 507-509 (**2006**).
83. Blomberg, S., Eloranta, M.L., Cederblad, B., Nordlin, K., Alm, G.V. & Ronnblom, L. Presence of cutaneous interferon-alpha producing cells in patients with systemic lupus erythematosus. *Lupus* **10**, 484-490 (**2001**).
84. Lande, R., Gafa, V., Serafini, B., Giacomini, E., Visconti, A., Remoli, M.E., Severa, M., Parmentier, M., Ristori, G., Salvetti, M., Aloisi, F. & Coccia, E.M. Plasmacytoid dendritic cells in multiple sclerosis: intracerebral recruitment and impaired maturation in response to interferon-beta. *J Neuropathol Exp Neurol* **67**, 388-401 (**2008**).
85. Dzionek, A., Sohma, Y., Nagafune, J., Cella, M., Colonna, M., Facchetti, F., Gunther, G., Johnston, I., Lanzavecchia, A., Nagasaka, T., Okada, T., Vermi, W., Winkels, G., Yamamoto, T., Zysk, M., Yamaguchi, Y. & Schmitz, J. BDCA-2, a novel plasmacytoid dendritic cell-specific type II C-type lectin, mediates antigen capture and is a potent inhibitor of interferon alpha/beta induction. *J Exp Med* **194**, 1823-1834 (**2001**).
86. Blasius, A.L., Cella, M., Maldonado, J., Takai, T. & Colonna, M. Siglec-H is an IPC-specific receptor that modulates type I IFN secretion through DAP12. *Blood* **107**, 2474-2476 (**2006**).
87. Blasius, A.L., Giurisato, E., Cella, M., Schreiber, R.D., Shaw, A.S. & Colonna, M. Bone marrow stromal cell antigen 2 is a specific marker of type I IFN-producing cells in the naive mouse, but a promiscuous cell surface antigen following IFN stimulation. *J Immunol* **177**, 3260-3265 (**2006**).
88. Fitzgerald-Bocarsly, P., Dai, J. & Singh, S. Plasmacytoid dendritic cells and type I IFN: 50 years of convergent history. *Cytokine Growth Factor Rev* **19**, 3-19 (**2008**).
89. Kadowaki, N., Ho, S., Antonenko, S., Malefyt, R.W., Kastelein, R.A., Bazan, F. & Liu, Y.J. Subsets of human dendritic cell precursors express different toll-like receptors and respond to different microbial antigens. *J Exp Med* **194**, 863-869 (**2001**).

90. Blasius, A.L. & Beutler, B. Intracellular toll-like receptors. *Immunity* **32**, 305-315 (**2010**).
91. Heil, F., Hemmi, H., Hochrein, H., Ampenberger, F., Kirschning, C., Akira, S., Lipford, G., Wagner, H. & Bauer, S. Species-specific recognition of single-stranded RNA via toll-like receptor 7 and 8. *Science* **303**, 1526-1529 (**2004**).
92. Hemmi, H., Kaisho, T., Takeuchi, O., Sato, S., Sanjo, H., Hoshino, K., Horiuchi, T., Tomizawa, H., Takeda, K. & Akira, S. Small anti-viral compounds activate immune cells via the TLR7 MyD88-dependent signaling pathway. *Nat Immunol* **3**, 196-200 (**2002**).
93. Hemmi, H., Takeuchi, O., Kawai, T., Kaisho, T., Sato, S., Sanjo, H., Matsumoto, M., Hoshino, K., Wagner, H., Takeda, K. & Akira, S. A Toll-like receptor recognizes bacterial DNA. *Nature* **408**, 740-745 (**2000**).
94. Honda, K., Yanai, H., Negishi, H., Asagiri, M., Sato, M., Mizutani, T., Shimada, N., Ohba, Y., Takaoka, A., Yoshida, N. & Taniguchi, T. IRF-7 is the master regulator of type-I interferon-dependent immune responses. *Nature* **434**, 772-777 (**2005**).
95. Kawai, T., Sato, S., Ishii, K.J., Coban, C., Hemmi, H., Yamamoto, M., Terai, K., Matsuda, M., Inoue, J., Uematsu, S., Takeuchi, O. & Akira, S. Interferon-alpha induction through Toll-like receptors involves a direct interaction of IRF7 with MyD88 and TRAF6. *Nat Immunol* **5**, 1061-1068 (**2004**).
96. Honda, K., Ohba, Y., Yanai, H., Negishi, H., Mizutani, T., Takaoka, A., Taya, C. & Taniguchi, T. Spatiotemporal regulation of MyD88-IRF-7 signalling for robust type-I interferon induction. *Nature* **434**, 1035-1040 (**2005**).
97. Gilliet, M., Cao, W. & Liu, Y.J. Plasmacytoid dendritic cells: sensing nucleic acids in viral infection and autoimmune diseases. *Nat Rev Immunol* **8**, 594-606 (**2008**).
98. Pestka, S., Langer, J.A., Zoon, K.C. & Samuel, C.E. Interferons and their actions. *Annu Rev Biochem* **56**, 727-777 (**1987**).
99. Ito, T., Kanzler, H., Duramad, O., Cao, W. & Liu, Y.J. Specialization, kinetics, and repertoire of type 1 interferon responses by human plasmacytoid predendritic cells. *Blood* **107**, 2423-2431 (**2006**).
100. Ito, T., Amakawa, R., Inaba, M., Ikehara, S., Inaba, K. & Fukuhara, S. Differential regulation of human blood dendritic cell subsets by IFNs. *J Immunol* **166**, 2961-2969 (**2001**).
101. Kadowaki, N., Antonenko, S., Lau, J.Y. & Liu, Y.J. Natural interferon alpha/beta-producing cells link innate and adaptive immunity. *J Exp Med* **192**, 219-226 (**2000**).
102. Le Bon, A., Schiavoni, G., D'Agostino, G., Gresser, I., Belardelli, F. & Tough, D.F. Type i interferons potently enhance humoral immunity and can promote isotype switching by stimulating dendritic cells in vivo. *Immunity* **14**, 461-470 (**2001**).

103. Barton, G.M., Kagan, J.C. & Medzhitov, R. Intracellular localization of Toll-like receptor 9 prevents recognition of self DNA but facilitates access to viral DNA. *Nat Immunol* **7**, 49-56 (**2006**).
104. Barrat, F.J., Meeker, T., Gregorio, J., Chan, J.H., Uematsu, S., Akira, S., Chang, B., Duramad, O. & Coffman, R.L. Nucleic acids of mammalian origin can act as endogenous ligands for Toll-like receptors and may promote systemic lupus erythematosus. *J Exp Med* **202**, 1131-1139 (**2005**).
105. Ronnblom, L., Eloranta, M.L. & Alm, G.V. Role of natural interferon-alpha producing cells (plasmacytoid dendritic cells) in autoimmunity. *Autoimmunity* **36**, 463-472 (**2003**).
106. Blanco, P., Palucka, A.K., Gill, M., Pascual, V. & Banchereau, J. Induction of dendritic cell differentiation by IFN-alpha in systemic lupus erythematosus. *Science* **294**, 1540-1543 (**2001**).
107. Jego, G., Palucka, A.K., Blanck, J.P., Chalouni, C., Pascual, V. & Banchereau, J. Plasmacytoid dendritic cells induce plasma cell differentiation through type I interferon and interleukin 6. *Immunity* **19**, 225-234 (**2003**).
108. Means, T.K., Latz, E., Hayashi, F., Murali, M.R., Golenbock, D.T. & Luster, A.D. Human lupus autoantibody-DNA complexes activate DCs through cooperation of CD32 and TLR9. *J Clin Invest* **115**, 407-417 (**2005**).
109. Guiducci, C., Gong, M., Xu, Z., Gill, M., Chaussabel, D., Meeker, T., Chan, J.H., Wright, T., Punaro, M., Bolland, S., Soumelis, V., Banchereau, J., Coffman, R.L., Pascual, V. & Barrat, F.J. TLR recognition of self nucleic acids hampers glucocorticoid activity in lupus. *Nature* **465**, 937-941 (**2010**).
110. Sandgren, S., Wittrup, A., Cheng, F., Jonsson, M., Eklund, E., Busch, S. & Belting, M. The human antimicrobial peptide LL-37 transfers extracellular DNA plasmid to the nuclear compartment of mammalian cells via lipid rafts and proteoglycan-dependent endocytosis. *J Biol Chem* **279**, 17951-17956 (**2004**).
111. Tian, J., Avalos, A.M., Mao, S.Y., Chen, B., Senthil, K., Wu, H., Parroche, P., Drabic, S., Golenbock, D., Sirois, C., Hua, J., An, L.L., Audoly, L., La Rosa, G., Bierhaus, A., Naworth, P., Marshak-Rothstein, A., Crow, M.K., Fitzgerald, K.A., Latz, E., Kiener, P.A. & Coyle, A.J. Toll-like receptor 9-dependent activation by DNA-containing immune complexes is mediated by HMGB1 and RAGE. *Nat Immunol* **8**, 487-496 (**2007**).
112. Ghazizadeh, R., Shimizu, H., Tosa, M. & Ghazizadeh, M. Pathogenic mechanisms shared between psoriasis and cardiovascular disease. *Int J Med Sci* **7**, 284-289 (**2010**).

113. Lopez-Pedrera, C., Aguirre, M.A., Barbarroja, N. & Cuadrado, M.J. Accelerated Atherosclerosis in Systemic Lupus Erythematosus: Role of Proinflammatory Cytokines and Therapeutic Approaches. *J Biomed Biotechnol* **2010**(**2010**).
114. Sherer, Y., Zinger, H. & Shoenfeld, Y. Atherosclerosis in systemic lupus erythematosus. *Autoimmunity* **43**, 98-102 (**2010**).
115. Gordon, S. & Taylor, P.R. Monocyte and macrophage heterogeneity. *Nat Rev Immunol* **5**, 953-964 (**2005**).
116. Strauss-Ayali, D., Conrad, S.M. & Mosser, D.M. Monocyte subpopulations and their differentiation patterns during infection. *J Leukoc Biol* **82**, 244-252 (**2007**).
117. Geissmann, F., Jung, S. & Littman, D.R. Blood monocytes consist of two principal subsets with distinct migratory properties. *Immunity* **19**, 71-82 (**2003**).
118. Metchnikoff, E. Zur Lehre über die intracelluläre Verdauung niederer Tiere. *Zoologischer Anzeiger* **5**, 310-316 (**1882**).
119. Gordon, S. Pattern recognition receptors: doubling up for the innate immune response. *Cell* **111**, 927-930 (**2002**).
120. Mantovani, A., Sica, A. & Locati, M. Macrophage polarization comes of age. *Immunity* **23**, 344-346 (**2005**).
121. Mosser, D.M. & Edwards, J.P. Exploring the full spectrum of macrophage activation. *Nat Rev Immunol* **8**, 958-969 (**2008**).
122. Martinez, F.O., Helming, L. & Gordon, S. Alternative activation of macrophages: an immunologic functional perspective. *Annu Rev Immunol* **27**, 451-483 (**2009**).
123. Fitch, F.W., McKisic, M.D., Lancki, D.W. & Gajewski, T.F. Differential regulation of murine T lymphocyte subsets. *Annu Rev Immunol* **11**, 29-48 (**1993**).
124. Zhu, J. & Paul, W.E. CD4 T cells: fates, functions, and faults. *Blood* **112**, 1557-1569 (**2008**).
125. Kaiko, G.E., Horvat, J.C., Beagley, K.W. & Hansbro, P.M. Immunological decision-making: how does the immune system decide to mount a helper T-cell response? *Immunology* **123**, 326-338 (**2008**).
126. Smith-Garvin, J.E., Koretzky, G.A. & Jordan, M.S. T cell activation. *Annu Rev Immunol* **27**, 591-619 (**2009**).
127. Galkina, E. & Ley, K. Immune and inflammatory mechanisms of atherosclerosis (*). *Annu Rev Immunol* **27**, 165-197 (**2009**).
128. Mayerl, C., Lukasser, M., Sedivy, R., Niederegger, H., Seiler, R. & Wick, G. Atherosclerosis research from past to present--on the track of two pathologists with opposing views, Carl von Rokitansky and Rudolf Virchow. *Virchows Arch* **449**, 96-103

(**2006**).

129. Anitschkow, N.C., S. . Ueber experimentelle Cholesterinsteatose und ihre Bedeutung für die Entstehung einiger pathologischer Prozesse. *Zentralbl Allg Pathol* **24**, 1-9 (**1913**).
130. Windaus, A. Ueber den Gehalt normaler und atheromatoeser Aorten an Cholesterol and Cholesterinester. *Zeitschrift Physiol Chem* **67**, 174-176 (**1910**).
131. Ross, R. & Glomset, J.A. Atherosclerosis and the arterial smooth muscle cell: Proliferation of smooth muscle is a key event in the genesis of the lesions of atherosclerosis. *Science* **180**, 1332-1339 (**1973**).
132. Ross, R. & Glomset, J.A. The pathogenesis of atherosclerosis (second of two parts). *N Engl J Med* **295**, 420-425 (**1976**).
133. Ross, R. & Glomset, J.A. The pathogenesis of atherosclerosis (first of two parts). *N Engl J Med* **295**, 369-377 (**1976**).
134. Steinberg, D. Arterial metabolism of lipoproteins in relation to atherogenesis. *Ann N Y Acad Sci* **598**, 125-135 (**1990**).
135. Ross, R. The pathogenesis of atherosclerosis: a perspective for the 1990s. *Nature* **362**, 801-809 (**1993**).
136. Skalen, K., Gustafsson, M., Rydberg, E.K., Hulten, L.M., Wiklund, O., Innerarity, T.L. & Boren, J. Subendothelial retention of atherogenic lipoproteins in early atherosclerosis. *Nature* **417**, 750-754 (**2002**).
137. Weber, C., Zernecke, A. & Libby, P. The multifaceted contributions of leukocyte subsets to atherosclerosis: lessons from mouse models. *Nat Rev Immunol* **8**, 802-815 (**2008**).
138. Hansson, G.K. & Libby, P. The immune response in atherosclerosis: a double-edged sword. *Nat Rev Immunol* **6**, 508-519 (**2006**).
139. Libby, P. Inflammation in atherosclerosis. *Nature* **420**, 868-874 (**2002**).
140. van Leeuwen, M., Gijbels, M.J., Duijvestijn, A., Smook, M., van de Gaar, M.J., Heeringa, P., de Winther, M.P. & Tervaert, J.W. Accumulation of myeloperoxidase-positive neutrophils in atherosclerotic lesions in LDLR-/- mice. *Arterioscler Thromb Vasc Biol* **28**, 84-89 (**2008**).
141. Zernecke, A., Bot, I., Djalali-Talab, Y., Shagdarsuren, E., Bidzhekov, K., Meiler, S., Krohn, R., Schober, A., Sperandio, M., Soehnlein, O., Bornemann, J., Tacke, F., Biessen, E.A. & Weber, C. Protective role of CXC receptor 4/CXC ligand 12 unveils the importance of neutrophils in atherosclerosis. *Circ Res* **102**, 209-217 (**2008**).
142. Naruko, T., Ueda, M., Haze, K., van der Wal, A.C., van der Loos, C.M., Itoh, A., Komatsu, R., Ikura, Y., Ogami, M., Shimada, Y., Ehara, S., Yoshiyama, M., Takeuchi, K.,

Yoshikawa, J. & Becker, A.E. Neutrophil infiltration of culprit lesions in acute coronary syndromes. *Circulation* **106**, 2894-2900 (**2002**).

143. Kawaguchi, H., Mori, T., Kawano, T., Kono, S., Sasaki, J. & Arakawa, K. Band neutrophil count and the presence and severity of coronary atherosclerosis. *Am Heart J* **132**, 9-12 (**1996**).
144. Sweetnam, P.M., Thomas, H.F., Yarnell, J.W., Baker, I.A. & Elwood, P.C. Total and differential leukocyte counts as predictors of ischemic heart disease: the Caerphilly and Speedwell studies. *Am J Epidemiol* **145**, 416-421 (**1997**).
145. Drechsler, M., Megens, R.T., van Zandvoort, M., Weber, C. & Soehnlein, O. Hyperlipidemia-triggered neutrophilia promotes early atherosclerosis. *Circulation* **122**, 1837-1845 (**2010**).
146. Soehnlein, O., Kai-Larsen, Y., Frithiof, R., Sorensen, O.E., Kenne, E., Scharffetter-Kochanek, K., Eriksson, E.E., Herwald, H., Agerberth, B. & Lindbom, L. Neutrophil primary granule proteins HBP and HNP1-3 boost bacterial phagocytosis by human and murine macrophages. *J Clin Invest* **118**, 3491-3502 (**2008**).
147. Tabas, I. Consequences and therapeutic implications of macrophage apoptosis in atherosclerosis: the importance of lesion stage and phagocytic efficiency. *Arterioscler Thromb Vasc Biol* **25**, 2255-2264 (**2005**).
148. Soehnlein, O. & Weber, C. Myeloid cells in atherosclerosis: initiators and decision shapers. *Semin Immunopathol* **31**, 35-47 (**2009**).
149. Yilmaz, A., Lochno, M., Traeg, F., Cicha, I., Reiss, C., Stumpf, C., Raaz, D., Anger, T., Amann, K., Probst, T., Ludwig, J., Daniel, W.G. & Garlichs, C.D. Emergence of dendritic cells in rupture-prone regions of vulnerable carotid plaques. *Atherosclerosis* **176**, 101-110 (**2004**).
150. Jongstra-Bilen, J., Haidari, M., Zhu, S.N., Chen, M., Guha, D. & Cybulsky, M.I. Low-grade chronic inflammation in regions of the normal mouse arterial intima predisposed to atherosclerosis. *J Exp Med* **203**, 2073-2083 (**2006**).
151. Bobryshev, Y.V. & Lord, R.S. Ultrastructural recognition of cells with dendritic cell morphology in human aortic intima. Contacting interactions of Vascular Dendritic Cells in athero-resistant and athero-prone areas of the normal aorta. *Arch Histol Cytol* **58**, 307-322 (**1995**).
152. Bobryshev, Y.V. & Lord, R.S. S-100 positive cells in human arterial intima and in atherosclerotic lesions. *Cardiovasc Res* **29**, 689-696 (**1995**).
153. Niessner, A. & Weyand, C.M. Dendritic cells in atherosclerotic disease. *Clin Immunol* **134**, 25-32 (**2010**).

154. Niessner, A., Sato, K., Chaikof, E.L., Colmegna, I., Goronzy, J.J. & Weyand, C.M. Pathogen-sensing plasmacytoid dendritic cells stimulate cytotoxic T-cell function in the atherosclerotic plaque through interferon-alpha. *Circulation* **114**, 2482-2489 (**2006**).
155. Niessner, A., Shin, M.S., Pryshchep, O., Goronzy, J.J., Chaikof, E.L. & Weyand, C.M. Synergistic proinflammatory effects of the antiviral cytokine interferon-alpha and Toll-like receptor 4 ligands in the atherosclerotic plaque. *Circulation* **116**, 2043-2052 (**2007**).
156. Goossens, P., Gijbels, M.J., Zernecke, A., Eijgelaar, W., Vergouwe, M.N., van der Made, I., Vanderlocht, J., Beckers, L., Buurman, W.A., Daemen, M.J., Kalinke, U., Weber, C., Lutgens, E. & de Winther, M.P. Myeloid type I interferon signaling promotes atherosclerosis by stimulating macrophage recruitment to lesions. *Cell Metab* **12**, 142-153 (**2010**).
157. Hadeiba, H., Sato, T., Habtezion, A., Oderup, C., Pan, J. & Butcher, E.C. CCR9 expression defines tolerogenic plasmacytoid dendritic cells able to suppress acute graft-versus-host disease. *Nat Immunol* **9**, 1253-1260 (**2008**).
158. Ochando, J.C., Homma, C., Yang, Y., Hidalgo, A., Garin, A., Tacke, F., Angeli, V., Li, Y., Boros, P., Ding, Y., Jessberger, R., Trinchieri, G., Lira, S.A., Randolph, G.J. & Bromberg, J.S. Alloantigen-presenting plasmacytoid dendritic cells mediate tolerance to vascularized grafts. *Nat Immunol* **7**, 652-662 (**2006**).
159. Sambrook, J. & Russell, D.W. (eds.). *Molecular cloning : a laboratory manual.*, (Cold Spring Harbor Laboratory Press., Cold Spring Harbor, 2001).
160. Piedrahita, J.A., Zhang, S.H., Hagaman, J.R., Oliver, P.M. & Maeda, N. Generation of mice carrying a mutant apolipoprotein E gene inactivated by gene targeting in embryonic stem cells. *Proc Natl Acad Sci U S A* **89**, 4471-4475 (**1992**).
161. Plump, A.S., Smith, J.D., Hayek, T., Aalto-Setala, K., Walsh, A., Verstuyft, J.G., Rubin, E.M. & Breslow, J.L. Severe hypercholesterolemia and atherosclerosis in apolipoprotein E-deficient mice created by homologous recombination in ES cells. *Cell* **71**, 343-353 (**1992**).
162. Ishibashi, S., Brown, M.S., Goldstein, J.L., Gerard, R.D., Hammer, R.E. & Herz, J. Hypercholesterolemia in low density lipoprotein receptor knockout mice and its reversal by adenovirus-mediated gene delivery. *J Clin Invest* **92**, 883-893 (**1993**).
163. Barnden, M.J., Allison, J., Heath, W.R. & Carbone, F.R. Defective TCR expression in transgenic mice constructed using cDNA-based alpha- and beta-chain genes under the control of heterologous regulatory elements. *Immunol Cell Biol* **76**, 34-40 (**1998**).
164. Holtschke, T., Lohler, J., Kanno, Y., Fehr, T., Giese, N., Rosenbauer, F., Lou, J., Knobeloch, K.P., Gabriele, L., Waring, J.F., Bachmann, M.F., Zinkernagel, R.M., Morse,

H.C., 3rd, Ozato, K. & Horak, I. Immunodeficiency and chronic myelogenous leukemia-like syndrome in mice with a targeted mutation of the ICSBP gene. *Cell* **87**, 307-317 (**1996**).

165. Nizet, V., Ohtake, T., Lauth, X., Trowbridge, J., Rudisill, J., Dorschner, R.A., Pestonjamasp, V., Piraino, J., Huttner, K. & Gallo, R.L. Innate antimicrobial peptide protects the skin from invasive bacterial infection. *Nature* **414**, 454-457 (**2001**).
166. Krieg, A.M., Yi, A.K., Matson, S., Waldschmidt, T.J., Bishop, G.A., Teasdale, R., Koretzky, G.A. & Klinman, D.M. CpG motifs in bacterial DNA trigger direct B-cell activation. *Nature* **374**, 546-549 (**1995**).
167. Bauer, S., Kirschning, C.J., Hacker, H., Redecke, V., Hausmann, S., Akira, S., Wagner, H. & Lipford, G.B. Human TLR9 confers responsiveness to bacterial DNA via species-specific CpG motif recognition. *Proc Natl Acad Sci U S A* **98**, 9237-9242 (**2001**).
168. Krug, A., Rothenfusser, S., Hornung, V., Jahrsdorfer, B., Blackwell, S., Ballas, Z.K., Endres, S., Krieg, A.M. & Hartmann, G. Identification of CpG oligonucleotide sequences with high induction of IFN-alpha/beta in plasmacytoid dendritic cells. *Eur J Immunol* **31**, 2154-2163 (**2001**).
169. Ballas, Z.K., Krieg, A.M., Warren, T., Rasmussen, W., Davis, H.L., Waldschmidt, M. & Weiner, G.J. Divergent therapeutic and immunologic effects of oligodeoxynucleotides with distinct CpG motifs. *J Immunol* **167**, 4878-4886 (**2001**).
170. Suzuki, K., Ota, H., Sasagawa, S., Sakatani, T. & Fujikura, T. Assay method for myeloperoxidase in human polymorphonuclear leukocytes. *Anal Biochem* **132**, 345-352 (**1983**).
171. Ganguly, D., Chamilos, G., Lande, R., Gregorio, J., Meller, S., Facchinetti, V., Homey, B., Barrat, F.J., Zal, T. & Gilliet, M. Self-RNA-antimicrobial peptide complexes activate human dendritic cells through TLR7 and TLR8. *J Exp Med* **206**, 1983-1994 (**2009**).
172. Davies, J.Q. & Gordon, S. Isolation and culture of murine macrophages. *Methods Mol Biol* **290**, 91-103 (**2005**).
173. Tamura, T., Nagamura-Inoue, T., Shmeltzer, Z., Kuwata, T. & Ozato, K. ICSBP directs bipotential myeloid progenitor cells to differentiate into mature macrophages. *Immunity* **13**, 155-165 (**2000**).
174. Scheller, M., Foerster, J., Heyworth, C.M., Waring, J.F., Lohler, J., Gilmore, G.L., Shadduck, R.K., Dexter, T.M. & Horak, I. Altered development and cytokine responses of myeloid progenitors in the absence of transcription factor, interferon consensus sequence binding protein. *Blood* **94**, 3764-3771 (**1999**).
175. Gabriele, L., Phung, J., Fukumoto, J., Segal, D., Wang, I.M., Giannakakou, P., Giese,

N.A., Ozato, K. & Morse, H.C., 3rd. Regulation of apoptosis in myeloid cells by interferon consensus sequence-binding protein. *J Exp Med* **190**, 411-421 (**1999**).

176. Wu, C.Y., Maeda, H., Contursi, C., Ozato, K. & Seder, R.A. Differential requirement of IFN consensus sequence binding protein for the production of IL-12 and induction of Th1-type cells in response to IFN-gamma. *J Immunol* **162**, 807-812 (**1999**).
177. Kallies, A., Rosenbauer, F., Scheller, M., Knobeloch, K.P. & Horak, I. Accumulation of c-Cbl and rapid termination of colony-stimulating factor 1 receptor signaling in interferon consensus sequence binding protein-deficient bone marrow-derived macrophages. *Blood* **99**, 3213-3219 (**2002**).
178. Ren, R. Mechanisms of BCR-ABL in the pathogenesis of chronic myelogenous leukaemia. *Nat Rev Cancer* **5**, 172-183 (**2005**).
179. Kunjathoor, V.V., Febbraio, M., Podrez, E.A., Moore, K.J., Andersson, L., Koehn, S., Rhee, J.S., Silverstein, R., Hoff, H.F. & Freeman, M.W. Scavenger receptors class A-I/II and CD36 are the principal receptors responsible for the uptake of modified low density lipoprotein leading to lipid loading in macrophages. *J Biol Chem* **277**, 49982-49988 (**2002**).
180. Greenberg, M.E., Sun, M., Zhang, R., Febbraio, M., Silverstein, R. & Hazen, S.L. Oxidized phosphatidylserine-CD36 interactions play an essential role in macrophage-dependent phagocytosis of apoptotic cells. *J Exp Med* **203**, 2613-2625 (**2006**).
181. Savill, J., Dransfield, I., Gregory, C. & Haslett, C. A blast from the past: clearance of apoptotic cells regulates immune responses. *Nat Rev Immunol* **2**, 965-975 (**2002**).
182. Griendling, K.K. & FitzGerald, G.A. Oxidative stress and cardiovascular injury: Part II: animal and human studies. *Circulation* **108**, 2034-2040 (**2003**).
183. Borregaard, N. & Cowland, J.B. Granules of the human neutrophilic polymorphonuclear leukocyte. *Blood* **89**, 3503-3521 (**1997**).
184. Swiecki, M., Gilfillan, S., Vermi, W., Wang, Y. & Colonna, M. Plasmacytoid dendritic cell ablation impacts early interferon responses and antiviral NK and CD8(+) T cell accrual. *Immunity* **33**, 955-966 (**2010**).
185. Paulson, K.E., Zhu, S.N., Chen, M., Nurmohamed, S., Jongstra-Bilen, J. & Cybulsky, M.I. Resident intimal dendritic cells accumulate lipid and contribute to the initiation of atherosclerosis. *Circ Res* **106**, 383-390.
186. Nickel, T., Schmauss, D., Hanssen, H., Sicic, Z., Krebs, B., Jankl, S., Summo, C., Fraunberger, P., Walli, A.K., Pfeiler, S. & Weis, M. oxLDL uptake by dendritic cells induces upregulation of scavenger-receptors, maturation and differentiation. *Atherosclerosis* **205**, 442-450 (**2009**).

187. Mittelbrunn, M., Martinez del Hoyo, G., Lopez-Bravo, M., Martin-Cofreces, N.B., Scholer, A., Hugues, S., Fetler, L., Amigorena, S., Ardavin, C. & Sanchez-Madrid, F. Imaging of plasmacytoid dendritic cell interactions with T cells. *Blood* **113**, 75-84 (**2009**).
188. Ross, R. Atherosclerosis is an inflammatory disease. *Am Heart J* **138**, S419-420 (**1999**).
189. Febbraio, M., Podrez, E.A., Smith, J.D., Hajjar, D.P., Hazen, S.L., Hoff, H.F., Sharma, K. & Silverstein, R.L. Targeted disruption of the class B scavenger receptor CD36 protects against atherosclerotic lesion development in mice. *J Clin Invest* **105**, 1049-1056 (**2000**).
190. Swirski, F.K., Pittet, M.J., Kircher, M.F., Aikawa, E., Jaffer, F.A., Libby, P. & Weissleder, R. Monocyte accumulation in mouse atherogenesis is progressive and proportional to extent of disease. *Proc Natl Acad Sci U S A* **103**, 10340-10345 (**2006**).
191. Stoneman, V., Braganza, D., Figg, N., Mercer, J., Lang, R., Goddard, M. & Bennett, M. Monocyte/macrophage suppression in CD11b diphtheria toxin receptor transgenic mice differentially affects atherogenesis and established plaques. *Circ Res* **100**, 884-893 (**2007**).
192. Landsman, L., Bar-On, L., Zernecke, A., Kim, K.W., Krauthgamer, R., Shagdarsuren, E., Lira, S.A., Weissman, I.L., Weber, C. & Jung, S. CX3CR1 is required for monocyte homeostasis and atherogenesis by promoting cell survival. *Blood* **113**, 963-972 (**2009**).
193. Boring, L., Gosling, J., Cleary, M. & Charo, I.F. Decreased lesion formation in CCR2-/- mice reveals a role for chemokines in the initiation of atherosclerosis. *Nature* **394**, 894-897 (**1998**).
194. Combadiere, C., Potteaux, S., Rodero, M., Simon, T., Pezard, A., Esposito, B., Merval, R., Proudfoot, A., Tedgui, A. & Mallat, Z. Combined inhibition of CCL2, CX3CR1, and CCR5 abrogates Ly6C(hi) and Ly6C(lo) monocytosis and almost abolishes atherosclerosis in hypercholesterolemic mice. *Circulation* **117**, 1649-1657 (**2008**).
195. Nicholls, S.J. & Hazen, S.L. Myeloperoxidase and cardiovascular disease. *Arterioscler Thromb Vasc Biol* **25**, 1102-1111 (**2005**).
196. Sugiyama, S., Kugiyama, K., Aikawa, M., Nakamura, S., Ogawa, H. & Libby, P. Hypochlorous acid, a macrophage product, induces endothelial apoptosis and tissue factor expression: involvement of myeloperoxidase-mediated oxidant in plaque erosion and thrombogenesis. *Arterioscler Thromb Vasc Biol* **24**, 1309-1314 (**2004**).
197. Galis, Z.S. & Khatri, J.J. Matrix metalloproteinases in vascular remodeling and atherogenesis: the good, the bad, and the ugly. *Circ Res* **90**, 251-262 (**2002**).
198. Luttun, A., Lutgens, E., Manderveld, A., Maris, K., Collen, D., Carmeliet, P. & Moons, L. Loss of matrix metalloproteinase-9 or matrix metalloproteinase-12 protects apolipoprotein E-deficient mice against atherosclerotic media destruction but differentially affects plaque

growth. *Circulation* **109**, 1408-1414 (**2004**).

199. Rotzius, P., Soehnlein, O., Kenne, E., Lindbom, L., Nystrom, K., Thams, S. & Eriksson, E.E. ApoE(-/-)/lysozyme M(EGFP/EGFP) mice as a versatile model to study monocyte and neutrophil trafficking in atherosclerosis. *Atherosclerosis* **202**, 111-118 (**2009**).
200. Avanzas, P., Arroyo-Espliguero, R., Cosin-Sales, J., Quiles, J., Zouridakis, E. & Kaski, J.C. Multiple complex stenoses, high neutrophil count and C-reactive protein levels in patients with chronic stable angina. *Atherosclerosis* **175**, 151-157 (**2004**).
201. Turcotte, K., Gauthier, S., Tuite, A., Mullick, A., Malo, D. & Gros, P. A mutation in the Icsbp1 gene causes susceptibility to infection and a chronic myeloid leukemia-like syndrome in BXH-2 mice. *J Exp Med* **201**, 881-890 (**2005**).
202. Schmidt, M., Nagel, S., Proba, J., Thiede, C., Ritter, M., Waring, J.F., Rosenbauer, F., Huhn, D., Wittig, B., Horak, I. & Neubauer, A. Lack of interferon consensus sequence binding protein (ICSBP) transcripts in human myeloid leukemias. *Blood* **91**, 22-29 (**1998**).
203. Diaz-Blanco, E., Bruns, I., Neumann, F., Fischer, J.C., Graef, T., Rosskopf, M., Brors, B., Pechtel, S., Bork, S., Koch, A., Baer, A., Rohr, U.P., Kobbe, G., Haeseler, A., Gattermann, N., Haas, R. & Kronenwett, R. Molecular signature of CD34(+) hematopoietic stem and progenitor cells of patients with CML in chronic phase. *Leukemia* **21**, 494-504 (**2007**).
204. Ganti, A.K., Potti, A., Koka, V.K., Pervez, H. & Mehdi, S.A. Myeloproliferative syndromes and the associated risk of coronary artery disease. *Thromb Res* **110**, 83-86 (**2003**).
205. Lassila, M., Allen, T.J., Cao, Z., Thallas, V., Jandeleit-Dahm, K.A., Candido, R. & Cooper, M.E. Imatinib attenuates diabetes-associated atherosclerosis. *Arterioscler Thromb Vasc Biol* **24**, 935-942 (**2004**).
206. Birnberg, T., Bar-On, L., Sapoznikov, A., Caton, M.L., Cervantes-Barragan, L., Makia, D., Krauthgamer, R., Brenner, O., Ludewig, B., Brockschnieder, D., Riethmacher, D., Reizis, B. & Jung, S. Lack of conventional dendritic cells is compatible with normal development and T cell homeostasis, but causes myeloid proliferative syndrome. *Immunity* **29**, 986-997 (**2008**).
207. Yvan-Charvet, L., Pagler, T., Gautier, E.L., Avagyan, S., Siry, R.L., Han, S., Welch, C.L., Wang, N., Randolph, G.J., Snoeck, H.W. & Tall, A.R. ATP-binding cassette transporters and HDL suppress hematopoietic stem cell proliferation. *Science* **328**, 1689-1693 (**2010**).
208. Levy, Z., Rachmani, R., Trestman, S., Dvir, A., Shaish, A., Ravid, M. & Harats, D. Low-dose interferon-alpha accelerates atherosclerosis in an LDL receptor-deficient mouse model. *Eur J Intern Med* **14**, 479-483 (**2003**).

209. Goossens, P., Gijbels, M.J., Zernecke, A., Eijgelaar, W., Vergouwe, M.N., van der Made, I., Vanderlocht, J., Beckers, L., Buurman, W.A., Daemen, M.J., Kalinke, U., Weber, C., Lutgens, E. & de Winther, M.P. Myeloid type I interferon signaling promotes atherosclerosis by stimulating macrophage recruitment to lesions. *Cell Metab* **12**, 142-153.

210. Van Vre, E.A., Hoymans, V.Y., Bult, H., Lenjou, M., Van Bockstaele, D.R., Vrints, C.J. & Bosmans, J.M. Decreased number of circulating plasmacytoid dendritic cells in patients with atherosclerotic coronary artery disease. *Coron Artery Dis* **17**, 243-248 (**2006**).

211. Decker, T., Muller, M. & Stockinger, S. The yin and yang of type I interferon activity in bacterial infection. *Nat Rev Immunol* **5**, 675-687 (**2005**).

212. Iparraguirre, A., Tobias, J.W., Hensley, S.E., Masek, K.S., Cavanagh, L.L., Rendl, M., Hunter, C.A., Ertl, H.C., von Andrian, U.H. & Weninger, W. Two distinct activation states of plasmacytoid dendritic cells induced by influenza virus and CpG 1826 oligonucleotide. *J Leukoc Biol* **83**, 610-620 (**2008**).

213. Krieg, A.M. CpG motifs in bacterial DNA and their immune effects. *Annu Rev Immunol* **20**, 709-760 (**2002**).

214. Kiechl, S., Egger, G., Mayr, M., Wiedermann, C.J., Bonora, E., Oberhollenzer, F., Muggeo, M., Xu, Q., Wick, G., Poewe, W. & Willeit, J. Chronic infections and the risk of carotid atherosclerosis: prospective results from a large population study. *Circulation* **103**, 1064-1070 (**2001**).

215. Matsuura, E., Kobayashi, K., Matsunami, Y., Shen, L., Quan, N., Makarova, M., Suchkov, S.V., Ayada, K., Oguma, K. & Lopez, L.R. Autoimmunity, infectious immunity, and atherosclerosis. *J Clin Immunol* **29**, 714-721 (**2009**).

216. Shah, P.K. Link between infection and atherosclerosis: who are the culprits: viruses, bacteria, both, or neither? *Circulation* **103**, 5-6 (**2001**).

217. Abou-Raya, A. & Abou-Raya, S. Inflammation: a pivotal link between autoimmune diseases and atherosclerosis. *Autoimmun Rev* **5**, 331-337 (**2006**).

218. Blasi, C. The autoimmune origin of atherosclerosis. *Atherosclerosis* **201**, 17-32 (**2008**).

219. Milner, J.D., Orekov, T., Ward, J.M., Cheng, L., Torres-Velez, F., Junttila, I., Sun, G., Buller, M., Morris, S.C., Finkelman, F.D. & Paul, W.E. Sustained IL-4 exposure leads to a novel pathway for hemophagocytosis, inflammation, and tissue macrophage accumulation. *Blood* **116**, 2476-2483 (**2010**).

220. Kleemann, R., Zadelaar, S. & Kooistra, T. Cytokines and atherosclerosis: a comprehensive review of studies in mice. *Cardiovasc Res* **79**, 360-376 (**2008**).

221. Mattei, F., Schiavoni, G. & Tough, D.F. Regulation of immune cell homeostasis by type I

interferons. *Cytokine Growth Factor Rev* **21**, 227-236 (**2010**).

222. Lienenklaus, S., Cornitescu, M., Zietara, N., Lyszkiewicz, M., Gekara, N., Jablonska, J., Edenhofer, F., Rajewsky, K., Bruder, D., Hafner, M., Staeheli, P. & Weiss, S. Novel reporter mouse reveals constitutive and inflammatory expression of IFN-beta in vivo. *J Immunol* **183**, 3229-3236 (**2009**).
223. Aristimuno, C., de Andres, C., Bartolome, M., de las Heras, V., Martinez-Gines, M.L., Arroyo, R., Fernandez-Cruz, E. & Sanchez-Ramon, S. IFNbeta-1a therapy for multiple sclerosis expands regulatory CD8+ T cells and decreases memory CD8+ subset: a longitudinal 1-year study. *Clin Immunol* **134**, 148-157 (**2010**).
224. Allman, D., Dalod, M., Asselin-Paturel, C., Delale, T., Robbins, S.H., Trinchieri, G., Biron, C.A., Kastner, P. & Chan, S. Ikaros is required for plasmacytoid dendritic cell differentiation. *Blood* **108**, 4025-4034 (**2006**).
225. Albanesi, C., Scarponi, C., Pallotta, S., Daniele, R., Bosisio, D., Madonna, S., Fortugno, P., Gonzalvo-Feo, S., Franssen, J.D., Parmentier, M., De Pita, O., Girolomoni, G. & Sozzani, S. Chemerin expression marks early psoriatic skin lesions and correlates with plasmacytoid dendritic cell recruitment. *J Exp Med* **206**, 249-258 (**2009**).
226. Matsuura, E., Kobayashi, K., Tabuchi, M. & Lopez, L.R. Oxidative modification of low-density lipoprotein and immune regulation of atherosclerosis. *Prog Lipid Res* **45**, 466-486 (**2006**).
227. Coutant, F., Agaugue, S., Perrin-Cocon, L., Andre, P. & Lotteau, V. Sensing environmental lipids by dendritic cell modulates its function. *J Immunol* **172**, 54-60 (**2004**).
228. Perrin-Cocon, L., Coutant, F., Agaugue, S., Deforges, S., Andre, P. & Lotteau, V. Oxidized low-density lipoprotein promotes mature dendritic cell transition from differentiating monocyte. *J Immunol* **167**, 3785-3791 (**2001**).
229. Paulson, K.E., Zhu, S.N., Chen, M., Nurmohamed, S., Jongstra-Bilen, J. & Cybulsky, M.I. Resident intimal dendritic cells accumulate lipid and contribute to the initiation of atherosclerosis. *Circ Res* **106**, 383-390 (**2010**).
230. Alderman, C.J., Bunyard, P.R., Chain, B.M., Foreman, J.C., Leake, D.S. & Katz, D.R. Effects of oxidised low density lipoprotein on dendritic cells: a possible immunoregulatory component of the atherogenic micro-environment? *Cardiovasc Res* **55**, 806-819 (**2002**).
231. Packard, R.R., Maganto-Garcia, E., Gotsman, I., Tabas, I., Libby, P. & Lichtman, A.H. CD11c(+) dendritic cells maintain antigen processing, presentation capabilities, and CD4(+) T-cell priming efficacy under hypercholesterolemic conditions associated with atherosclerosis. *Circ Res* **103**, 965-973 (**2008**).

232. Kanazawa, N. Dendritic cell immunoreceptors: C-type lectin receptors for pattern-recognition and signaling on antigen-presenting cells. *J Dermatol Sci* **45**, 77-86 (**2007**).
233. Blasius, A.L. & Colonna, M. Sampling and signaling in plasmacytoid dendritic cells: the potential roles of Siglec-H. *Trends Immunol* **27**, 255-260 (**2006**).
234. Jaehn, P.S., Zaenker, K.S., Schmitz, J. & Dzionek, A. Functional dichotomy of plasmacytoid dendritic cells: antigen-specific activation of T cells versus production of type I interferon. *Eur J Immunol* **38**, 1822-1832 (**2008**).
235. Meyer-Wentrup, F., Benitez-Ribas, D., Tacken, P.J., Punt, C.J., Figdor, C.G., de Vries, I.J. & Adema, G.J. Targeting DCIR on human plasmacytoid dendritic cells results in antigen presentation and inhibits IFN-alpha production. *Blood* **111**, 4245-4253 (**2008**).
236. Zhang, J., Raper, A., Sugita, N., Hingorani, R., Salio, M., Palmowski, M.J., Cerundolo, V. & Crocker, P.R. Characterization of Siglec-H as a novel endocytic receptor expressed on murine plasmacytoid dendritic cell precursors. *Blood* **107**, 3600-3608 (**2006**).
237. Nilsson, J. & Hansson, G.K. Autoimmunity in atherosclerosis: a protective response losing control? *J Intern Med* **263**, 464-478 (**2008**).
238. Wick, G., Knoflach, M. & Xu, Q. Autoimmune and inflammatory mechanisms in atherosclerosis. *Annu Rev Immunol* **22**, 361-403 (**2004**).
239. Burut, D.F., Karim, Y. & Ferns, G.A. The role of immune complexes in atherogenesis. *Angiology* **61**, 679-689 (**2010**).
240. Gregorio, J., Meller, S., Conrad, C., Di Nardo, A., Homey, B., Lauerma, A., Arai, N., Gallo, R.L., Digiovanni, J. & Gilliet, M. Plasmacytoid dendritic cells sense skin injury and promote wound healing through type I interferons. *J Exp Med* (**2010**).
241. Edfeldt, K., Agerberth, B., Rottenberg, M.E., Gudmundsson, G.H., Wang, X.B., Mandal, K., Xu, Q. & Yan, Z.Q. Involvement of the antimicrobial peptide LL-37 in human atherosclerosis. *Arterioscler Thromb Vasc Biol* **26**, 1551-1557 (**2006**).
242. Alexandroff, A.B., Pauriah, M., Camp, R.D., Lang, C.C., Struthers, A.D. & Armstrong, D.J. More than skin deep: atherosclerosis as a systemic manifestation of psoriasis. *Br J Dermatol* **161**, 1-7 (**2009**).
243. Banchereau, J. & Pascual, V. Type I interferon in systemic lupus erythematosus and other autoimmune diseases. *Immunity* **25**, 383-392 (**2006**).
244. Aprahamian, T., Rifkin, I., Bonegio, R., Hugel, B., Freyssinet, J.M., Sato, K., Castellot, J.J., Jr. & Walsh, K. Impaired clearance of apoptotic cells promotes synergy between atherogenesis and autoimmune disease. *J Exp Med* **199**, 1121-1131 (**2004**).
245. Eloranta, M.L., Lovgren, T., Finke, D., Mathsson, L., Ronnelid, J., Kastner, B., Alm, G.V. & Ronnblom, L. Regulation of the interferon-alpha production induced by RNA-containing

immune complexes in plasmacytoid dendritic cells. *Arthritis Rheum* **60**, 2418-2427 (**2009**).

246. Lovgren, T., Eloranta, M.L., Bave, U., Alm, G.V. & Ronnblom, L. Induction of interferon-alpha production in plasmacytoid dendritic cells by immune complexes containing nucleic acid released by necrotic or late apoptotic cells and lupus IgG. *Arthritis Rheum* **50**, 1861-1872 (**2004**).
247. Pertovaara, M., Kahonen, M., Juonala, M., Laitinen, T., Taittonen, L., Lehtimaki, T., Viikari, J.S., Raitakari, O.T. & Hurme, M. Autoimmunity and atherosclerosis: the presence of antinuclear antibodies is associated with decreased carotid elasticity in young women. The Cardiovascular Risk in Young Finns Study. *Rheumatology (Oxford)* **48**, 1553-1556 (**2009**).
248. Frostegard, J. Systemic lupus erythematosus and cardiovascular disease. *Lupus* **17**, 364-367 (**2008**).
249. Reizis, B., Bunin, A., Ghosh, H.S., Lewis, K.L. & Sisirak, V. Plasmacytoid Dendritic Cells: Recent Progress and Open Questions. *Annu Rev Immunol* (**2010**).
250. Shlomchik, M.J. Activating systemic autoimmunity: B's, T's, and tolls. *Curr Opin Immunol* **21**, 626-633 (**2009**).

8. ACKNOWLEDGEMENTS

Herrn Prof. Dr. Christian Weber danke ich für die Möglichkeit an seinem Institut promovieren zu dürfen und für seine sowohl finanzielle als auch wissenschaftliche Unterstützung meiner Doktorarbeit.

Ganz besonders bedanken möchte ich mich bei PD. Dr. Alma Zernecke für die Betreuung meiner Doktorarbeit, den konstruktiven wissenschaftlichen Austausch und für die Möglichkeit auch eigene Ideen verwirklichen zu können. Desweiteren möchte ich mich auch bei den Mitarbeitern und Mitarbeiterinnen aus der AG Zernecke in Würzburg für die nette Zusammenarbeit bedanken.

Prof. Dr. Martin Zenke danke ich an dieser Stelle für die Übernahme der Zweitkorrektur dieser Arbeit. Weiterhin danke ich ihm für die Möglichkeit ein Teil seiner Arbeitsgruppe sein zu dürfen. Dr. Thomas Hieronymus danke ich für die wissenschaftliche Unterstützung dieser Arbeit. Ausserdem möchte ich der ganzen AG Zenke für die nette Zeit in Aachen danken. Ein ganz besonderer Dank geht hier an Julia Oberblöbaum, für die vielen tollen Gespräche und an Uli, Verena, Julia Pabich und Nadine für die kurzweiligen Unternehmungen.

Ein herzliches Dankeschön auch an meine Bürokollegen Sebastian und Rebekka. Danke für die aufmunternden Gespräche und die vielen lustigen Stunden mit Euch.

An dieser Stelle möchte ich mich ganz herzlich bei allen TAs aus dem IMCAR bedanken. Insbesondere bei Melanie, Steffi, Silvia und Yvonne für die tatkräftige Unterstützung meiner Mausexperimente. Ohne Euch hätte ich das nicht geschafft! Desweiteren möchte ich mich auch bei den Mitarbeitern aus der Tierversuchskunde für die nette Zusammenarbeit bedanken. Ausserdem danke ich Mihail und Susanne für das Sorten meiner Zellen.

Ich danke allen meinen Arbeitskollegen aus dem IMCAR für ihre fachliche Unterstützung und die schöne Zeit in Aachen. Danke ausserdem auch für die vielen und schönen Unternehmungen ausserhalb des Labors und so manchen geselligen Abend. Danke Ake, Ali, Barbara, Delia, Dirk, Heidi, Helene, Holger, Isabella, Jean-Eric, Joana, Jürgen, Klaus, Leon, Martin H., Martin S., Maryam, Michael, Norbert, Remco, Regina, Philip, Santosh und Sebastian, Tessa und Xavier. Weiterhin danke ich Frau Mayer für Ihre Hilfe bei verschiedenen

organisatorischen Problemen und die Korrektur dieser Arbeit.

Ein ganz liebes Dankeschön geht an Svenja für die „Einführung“ in das IMCAR, für die schöne Zeit in Aachen, für die vielen lustigen Abende und die netten Gespräche. Desweiteren möchte ich mich bei Helene, meinem „Hiwi“ bedanken: Ohne Dich gäbe es diese Arbeit nicht! Danke! Ein herzliches Dankeschön auch an Birgit, insbesondere für die vielen bereichernden und interessanten Gespräche und Unternehmungen im letzten Jahr.

Danke auch an meine Freunde ausserhalb des Labors für Eure Unterstützung, Motivation und Geduld. Danke Claudi, Chrisi, Doro, Katrin, Knut und Manu. Ich bin froh, dass es Euch gibt!

Ausserdem möchte ich mich bei den „Dresdenern“ bedanken. Die Besuche bei Euch sind immer erholsam und schön.

Mein ganz besonderer Dank gilt Oli: Danke für den wissenschaftlichen Diskurs und die Unterstützung und Korrektur meiner Arbeit, für die fesselnden Gespräche, die interessanten Unternehmungen, die schönen und lustigen Abende und für Deine Freundschaft.

Ein ganz großes Dankeschön geht an meine Eltern: Danke für Eure Unterstützung, Euren Zuspruch, die vielen aufmunternden Gespräche und Eure Geduld.

Maik - ein riesiges Dankeschön für Deine Unterstützung dieser Arbeit, für Deine Geduld mit mir und meinen Schrulligkeiten, für die vielen erfahrungsreichen, aufregenden, freudigen, intensiven und schönen Momente der letzten 5 Jahre.

9. CURRICULUM VITAE

PERSÖNLICHE DATEN:

Name:	Yvonne Döring
Geburtsdatum:	19.10.1980
Geburtsort:	Lauterbach in Hessen
Nationalität:	Deutsch

BILDUNGSWEG:

Juli 1991	–	Juni 2000	Alexander-von-Humboldt Gymnasium Lauterbach Abschluss: Allgemeine Hochschulreife
Oktober 2000	–	März 2001	Magisterstudium an der Friedrich-Schiller Universität Jena; Fächer: Politik- und Wirtschaftswissenschaften, Psychologie
Oktober 2001	–	September 2004	Universität Osnabrück Studium: Bachelor „Biologie der Zellen“ Abschluss: Bachelor of Science
Oktober 2004	–	Oktober 2006	Johannes Gutenberg Universität Mainz Studium: Master Biomedizin Abschluss: Master of Science
November 2006	–	April 2007	wissenschaftliche Mitarbeiterin am Institut für klinische Chemie und Laboratoriumsmedizin in der Arbeitsgruppe von Prof. von Landenberg, Mainz
Mai 2007	–	Dezember 2010	Doktorandin am Institut für Molekulare Herz-Kreislaufforschung (IMCAR) unter der Leitung von Univ.-Prof. Dr. med. Christian Weber, Aachen

PUPLIKATIONEN:

von Landenberg, P., **Döring, Y.**, Modrow, S., and Lackner, K.J., *Are antiphospholipid antibodies an essential requirement for an effective immune response to infections?* Ann N Y Acad Sci, **2007**. 1108: p. 578-83.

Drechsler, M.D., Obermeier, I., **Döring, Y.**, Lackner, K.J., Modrow, S., and von Landenberg, P., *Generation of multifunctional murine monoclonal antibodies specifically directed to the VP1unique region protein of human parvovirus B19.* Immunobiology, **2008**. 213(6): p. 511-7.

Döring, Y.*, Hurst, J.*, Lorenz, M., Prinz, N., Clemens, N., Drechsler, M.D., Bauer, S., Chapman, J., Shoenfeld, Y., Blank, M., Lackner, K.J., and von Landenberg, P., *Human antiphospholipid antibodies induce TNFalpha in monocytes via Toll-like receptor 8.* Immunobiology, 2**010**. 215(3): p. 230-41.

Döring, Y., Zechner, U., Roos, C., Rosenkranz, D., Zischler, H., and Herlyn, H., *Accelerated evolution of Fetuin-A (FETUA, also AHSG) is driven by positive Darwinian selection, not GC-biased gene conversion.* Gene, **2010**. 463(1-2): p. 49-55.

Weber, C.*, Meiler, S.*, **Döring, Y.***, Koch, M., Drechsler, M., Megens, R.T.A., Rowinska, Z., Bidzhekov, K., Fecher, C., Ribechini, E., van Zandvoort, M.A.M.J., Binder, C.J., Jelinek, I., Hristov, M., Boon, L., Jung, S., Korn, T., Lutz, M.B., Förster, I., Zenke, M., Hieronymus, T., Junt, T., and Zernecke, A.*CCL17-expressing dendritic cells drive atherosclerosis by restraining regulatory T-cell homeostasis in mice.* Journal of Clinical Investigation, **2011** 121(7):p. 2898–2910

Döring, Y.*, Soehnlein, O.*, Drechsler, M., Meiler, S., Shagdarsuren, E., Hartwig, H., Hieronymus, T., Hristov, M., Koenen, R.R., Zenke, M., Weber, C., and Zernecke, A., *Chronic myelogenous leukemia-like disease due to hematopoietic IRF8-deficiency fuels atherosclerosis in mice.* Circulation Research, **2011** (in revision).

Soehnlein, O.*, Wantha, S.*, Simsekyilmaz, S., **Döring, Y.**, Megens, R.T.A., Mause, S., Drechsler, M., Smeets, R., Weinandy, S., Schreiber, F., Gries, T., Vijayan, S., van Zandvoort, M.A.M.J., Agerberth, B., Pham, C.T., Gallo, R.L., Hackeng, T.M., Liehn, E.A., Zernecke, A., Klee, D., and Weber, C., *Neutrophil-derived cathelicidin protects from neointimal hyperplasia.* Science Translational Medicine, **2011** (in revision).

Döring, Y., Manthey, H., Drechsler, M., Lievens, D., Manca, M., Hartwig, H., Busch, M., Koenen, R.R., Soehnlein, O., Zenke, M., Daemen, M.J., Weber, C., Lutgens, E., and Zernecke, A., *Autoantigenic protein-DNA complexes stimulate plasmacytoid dendritic cells to promote atherosclerosis*. Circulation, **2011** (in revision).

Soehnlein, O.*, Drechsler, M.*, **Döring, Y**., Vijayan, S., Lievens, D., Hartwig, H., Projahn, D., Koenen, R.R., Hristov, M., Lutgens, E., Zernecke, A.*, and Weber, C.*, *Sequential contribution of chemokine receptor axes to the prominent proatherogenic function of classical monocytes,* Circulation, **2011** (under review).

MEETINGS:

Keystone Symposia: Dendritic cells; Banff, Alberta, Canada, 28.03.2009 – 02.04.2009.
Posterpräsentation:
Döring Y., Meiler, S., Hieronymus T., Zenke M., Weber C., Zernecke A. **(2009)**.
Plasmacytoid dendritic cells in atherosclerosis

Tag der Medizinischen Forschung, IZKF Aachen, 11.12.2009
Posterpräsentation:
Döring Y., Vijayan S., Bidzhekov, K., Meiler, S. , Drechsler, D., Hieronymus, T., Zenke, M., Weber, C., Zernecke, A.**(2009)**.
Plasmacytoid dendritic cells in atherosclerosis

8th Dutch-German Joint Meeting of the Molecular Cardiology Working Groups, Rotterdam, 18.02.2010-20.02.2010
Posterpräsentation:
Döring, Y., Soehnlein, O., Drechsler, M., Meiler, S., Shagdarsuren, E., Hartwig, H., Hieronymus, T., Hristov, M., Koenen, R.R., Zenke, M., Weber, C., Zernecke, A.**(2010).**
Chronic myelogenous leukemia-like disease due to hematopoietic IRF8-deficiency fuels atherosclerosis in mice.

Tag der Medizinischen Forschung, IZKF Aachen, 26.11.2010
Posterpräsentation:
Döring Y., Vijayan S., Shagdasuren, E., Meiler, S., Drechsler, D., Hieronymus, T., Zenke, M., Weber, C., Zernecke, A.**(2010).**
Plasmacytoid dendritic cells in atherosclerosis

Minerva-Symposium: "Frontiers in Vascular Medicine", Maale Hachmisha, Jerusalem, Israel 28.10.2010 – 31.10.2010

Posterpräsentation:

Meiler, S.*, **Döring, Y.***, Drechsler, M., Koch, M, Fecher, C., Megens, R.T.A.,Bidzhekov, K., van Zandvoort, M.A.M.J, Binder, C.J., Jelinek, I., Hristov, M., Boon, L., Waisman, A., Jung, S., Förster, I., Zenke, M., Hieronymus, T., Junt, T., Weber, C., Zernecke, A. **(2010)**.

CCL17-expressing dendritic cells drive atherosclerosis by restraining regulatory T-cell homeostasis.

* equal contribution